FORCE-GENERATING PROTEINS ASSEMBLE AND POSITION MITOTIC SPINDLES IN *SACCHAROMYCES CEREVISIAE*

A Dissertation

Presented to the Faculty of the Graduate School

of Cornell University

in Partial Fulfillment of the Requirements for the Degree of

Doctor of Philosophy

by

Irene Alexandra Amaro

February 2010

FORCE-GENERATING PROTEINS ASSEMBLE AND POSITION MITOTIC SPINDLES IN *SACCHAROMYCES CEREVISIAE*

Irene Alexandra Amaro, Ph. D.

Cornell University 2010

The mitotic spindle is essential for the segregation of chromosomes during cell division. A combination of microtubule motor and non-motor proteins is involved in generating the forces required for mitotic spindle formation and orientation. Loss of Stu1, the *Saccharomyces cerevisiae* member of the CLASP family of microtubule plus-end-tracking proteins, results in spindle collapse, indicating Stu1 provides an outward spindle-pole-separating force. Similar to *Drosophila* CLASP, I find that Stu1 contributes an outward force by promoting kinetochore microtubule length either through tubulin subunit incorporation or stabilization. In *stu1-5* cells at the restrictive temperature, spindle poles initially separate prior to collapse, indicating that the subsequent establishment of kinetochore-microtubule attachments pulls the poles inward as a result of shortening kinetochore microtubules. Removal of this inward force by disruption of microtubule attachment with the outer kinetochore mutant *ndc80-1* restores pole separation. However, pole separation in *stu1-5 ndc80-1* is unstable and fails to reach separation distances observed in *ndc80-1* alone, indicating that Stu1 may also have a stabilization role at the plus ends of polar microtubules.

A genome-wide screen for gene deletions that are lethal in combination with the temperature-sensitive *stu1-5* allele identified *ldb18Δ*. *ldb18Δ* cells exhibit defects in spindle orientation similar to those caused by a block in the

dynein pathway. I show that Ldb18 is a component of dynactin, a complex required for dynein activity in yeast and mammalian cells. Ldb18 shares modest sequence and structural homology with the mammalian dynactin component p24. It interacts with dynactin proteins in two-hybrid and co-immunoprecipitation assays. In *ldb18Δ* cells, the interaction between Nip100 ($p150^{Glued}$) and Jnm1 (dynamitin) is diminished while the interaction between Jmn1 and Arp1 is not affected. These results indicate that p24 is required for attachment of the $p150^{Glued}$ arm to dynamitin and the remainder of the dynactin complex. A modified Ldb18 species specifically co-migrates with dynactin complex proteins in sucrose gradients, suggesting regulation is involved in final complex assembly. The genetic interaction of *ldb18Δ* with *stu1*-5 also supports the notion that dynein/dynactin helps to generate a spindle pole separating force.

BIOGRAPHICAL SKETCH

Irene Alexandra Amaro was born in Monterey Park, California to parents who had recently immigrated to the United States from Mexico. Alex spent her early years in the Los Angeles area before moving to San Diego where she was intrigued by biology classes in middle school. Alex enjoyed spending extra time after class looking at a wide range of specimens under the microscope. While a student at Rancho Bernardo High School, Alex took a job as an intern at The Scripps Research Institute in La Jolla, CA in the summer of 1997. Here, under the direction of Dr. Steven Mayfield, she realized that a career in science had much to offer. In her first real lab environment, she worked on the green algae *Chlamydomonas reinhardtii* while enjoying a cliffside view of the Pacific Ocean from the lab windows. Alex continued her studies at the University of Notre Dame in northern Indiana, where the biology labs are right next to the famed Notre Dame Stadium where she would cheer on the Fighting Irish. Alex joined the lab of Dr. Crislyn D'Souza-Shorey, where she was first introduced to budding yeast as a model organism, despite the lab's focus on mammalian cell migration. After graduating with a B.S. in Biological Science in 2002, Alex moved farther east to Cornell University in Ithaca, NY where she later joined the lab of Dr. Tim C. Huffaker in the spring of 2003.

Along the way, Alex has been heavily influenced by strong female scientists, specifically Dr. Amy Beth Cohen, Dr. Crislyn D'Souza-Shorey, and especially Dr. Jill Schweitzer. They were instrumental in helping Alex find her place in the science world, and she keeps in close contact with all these women to this day. Alex finds it important to continue mentoring the next

generation of female scientists, and thus volunteered her time as a buddy and an organizing chair for seven years to the Expanding Your Horizons initiative both at Notre Dame and Cornell.

After graduating with her Ph.D. from Cornell in Biochemistry, Molecular, and Cell Biology, Alex plans to remain in the Ithaca area. She intends to join the lab of Dr. John Parker at the James A. Baker Institute for Animal Health to study reovirus pathology.

For Seth

ACKNOWLEDGEMENTS

Many people were involved in my journey through graduate school. Without their help and support, none of this would be possible. I thank my advisor, Tim Huffaker, who always has his door open anytime I want to drop by. His calm demeanor and attention to detail have made graduate school a positive experience. Tim is always supportive, even when experiments are not going well, and he is a true friend as well as mentor. My committee members Tony Bretscher and Volker Vogt have been encouraging and very willing to help with suggestions. I am grateful for the friendships made with members of the "Huffaker Institute for Microtubule Dynamics", including Beth Lalonde, Liru You, Mike Wolyniak, Eric Hwang, Laurie Cook, Baoying Huang, Xue Xia, Zane Bergman, Kristy Blake, Gilda Sheyan, Lily Cao, and Patrick Wu. There are many memories to take with me, including taking lab road trips to meetings, procrastinating on any given afternoon, talking about the latest paper, giving technical advice, or racing to see who will eat the last slice of cake. My early years were shared with my wonderful baymate Xue, while the later years with Zane and Kristy have been filled with lots of laughs that kept me sane.

Completion of this thesis work was aided by technical help and reagents from labs both at Cornell and elsewhere. The SGA screen was completed in collaboration with the Charlie Boone lab from the University of Toronto. Tim Sackton helped me with statistical analysis of Ldb18 and its homologues. I thank to Aster Legesse-Miller, Kelley Tatchell, Mark Rose, Elmar Schiebel, Erica Johnson, and Mark Hochstrasser for graciously providing plasmids, strains, and antibodies. Special thanks to labs throughout Biotech who would let me raid their freezer or chemical shelves when needed,

especially the Vogt, Bretscher, Brown, Tye and Alani labs. A large portion of the microscopy images were captured on the spinning disk confocal maintained by the Brown lab. A portion of this work was funded by the National Institutes of Health pre-doctoral grant GM073576.

I also want to extend my gratitude to my family and friends. There are many ups and downs in research, and it was invaluable to have strong support from so many people. Even though they are on the west coast, my family always came to visit us in all seasons, which made working away from home a bit easier. It was thanks to my husband, Seth, that I was able to accomplish many things. Seth has been by my side providing lots of encouragement, even if he did not know half the time what I was talking about. With good home-cooked food and plenty of laughs, I was able to stay positive doing what I enjoy.

TABLE OF CONTENTS

LIST OF FIGURES

LIST OF TABLES

LIST OF ABBREVIATIONS

aMT	Astral microtubules
CCT	Chaperonin containing TCP-1
ChIP	Chromatin immunoprecipitation
CLASP	CLIP170 associating protein
CSF	Cytostatic Factor
DAPI	4,6 diamidino-2-phenylindole
DNA	Deoxyribonucleic acid
GFP	Green Fluorescent Protein
GDP	Guanosine diphosphate
GST	Gluathione S-transferase
GTP	Guanosine triphosphate
IPTG	Isopropyl β-D-1-thiogalactopyranoside
kMT	Kinetochore microtubles
LB	Luria Broth
MAP	Microtubule associated protein
mRNA	Messenger ribonucleic acid
MT	Microtubules
MTOC	Microtubule organizing center
NEBD	Nuclear envelope breakdown
NEM	N-ethylmaleimide
NPC	Nuclear pore complex
OD	Optical density
ORF	Open Reading Frame
PP2A	Protein phosphatase 2A
SGA	Synthetic genetic array
siRNA	Small interfering RNA
SL	Synthetic lethal
SPB	Spindle pole body
SS	Synthetic sick
SUMO	Small ubiquitin modifier
TCA	Trichloricacidic acid
+TIP	Plus-end tracking protein

CHAPTER ONE

Introduction

GENERAL INTRODUCTION

From unicellular species to multicellular organisms, life is sustained by cell division. This elaborate process culminates in mitosis, which involves segregation of replicated DNA and organelles to each daughter cell. Cells spend only a fraction of their total lifetime undergoing mitosis, yet even minor defects at this stage can be deleterious for the cell. Aneuploidy in cells can affect viability, promote disease, or contribute to cancer. Early scientists studying division in eukaryotic cells observed distinct morphological changes, including the condensation of chromatin into higher order structures and the presence of the spindle fibers (reviewed in Mitchison and Salmon, 2001). Electron microscopy provided the first insights into how these fibers were organized into the spindle structure, the different morphological stages of the spindle, and the interplay with replicated chromatin (Brinkley and Stubblefield, 1966). The mitotic spindle, composed of microtubules and microtubule-associated proteins, is the main vehicle for aligning and separating sister chromatids in each round of cell division.

The spindle is a dynamic structure that changes throughout mitosis. In fact, the stages of mitosis are defined by the morphological state of the spindle and chromosomes (Historical perspective in Rieder and Khodjakov, 2003). Mitosis in higher eukaryotes begins with the disassembly of the nuclear envelope to expose the already condensed and duplicated sister chromatids at the end of prophase. Microtubules emanating from each of the duplicated

centrosomes, which serves as the microtubule organizing center (MTOC), search the cytoplasm to make contact and subsequent attachment with the chromosomes. At metaphase, the spindle poles are oriented opposite each other, while chromosomes attached to microtubule fibers through the kinetochore protein complex are aligned along the metaphase plate. The cohesin joining sister chromatids is then degraded, allowing progression into anaphase where coordinated spindle forces pull the chromatids apart. Surveillance systems monitor each step in this process for any defects. Checkpoint mechanisms ensure that cell cycle progression will not proceed if the DNA is not properly duplicated, chromosomes are not properly attached and bioriented, or chromosomes lag behind during segregation in anaphase. This singular cellular process has captivated scientists since the 1880's, and while advances in imaging, genomics, mathematical modeling, and protein biochemistry have answered some of the original questions, even more continue to be raised. In this thesis, I highlight two processes essential for mitosis: spindle stability and spindle positioning. The formation and maintenance of the spindle is a coordinated effort between microtubules, microtubule-associated proteins, motor proteins, and the chromosomes. In particular, the microtubule plus-end-tracking protein CLASP is involved in spindle maintenance. Following spindle formation in certain cases, namely in early development, in neuronal growth, and in the budding yeast, the minus-end directed motor dynein is involved in positioning the spindle within the cell.

PART I. MICROTUBULE DYNAMICS AND THE +TIP CLASP

Microtubule Structure and Dynamics

Together with actin and intermediate filaments, microtubules comprise the cytoskeleton of eukaryotic cells. Microtubules are composed of α/β tubulin heterodimers arranged in a head-to-tail manner into protofilaments that associate laterally to form a hollow tube (Figure 1.1) (reviewed in Desai and Mitchison, 1997). Following incorporation, tubulin subunits can undergo a number of post-translational modifications, which give the microtubule polymer different functional properties (reviewed in Hammond et al., 2008). As a consequence of the specific orientation of the tubulin heterodimers, the microtubule is a polar structure with rapid polymerization at the plus end and slower polymerization at the minus end.

While both α- and β- tubulin subunits bind GTP, only the β-subunit hydrolyzes the GTP to GDP following incorporation. GDP-tubulin has a curved conformation, which introduces strain in the protofilaments thereby producing a source of stored energy. This strain is contained by a "GTP cap" that arises from hydrolysis lagging behind active polymerization. The GTP-cap promotes polymerization by its conformation, which is suited for subunit binding and can be identified *in vivo* using antibodies (Wang and Nogales, 2005; Dimitrov et al., 2008). As incorporation of subunits slows, the cap is diminished, and the strain from GDP-tubulin curvature is released, leading to rapid deplymerization.

Microtubules both *in vitro* and *in vivo* are inherently dynamic structures with periods of sustained growth (polymerization) and shrinkage (depolymerization). These two states differ structurally, with an open-sheet configuration characteristic of growing microtubules, as opposed to the peeling

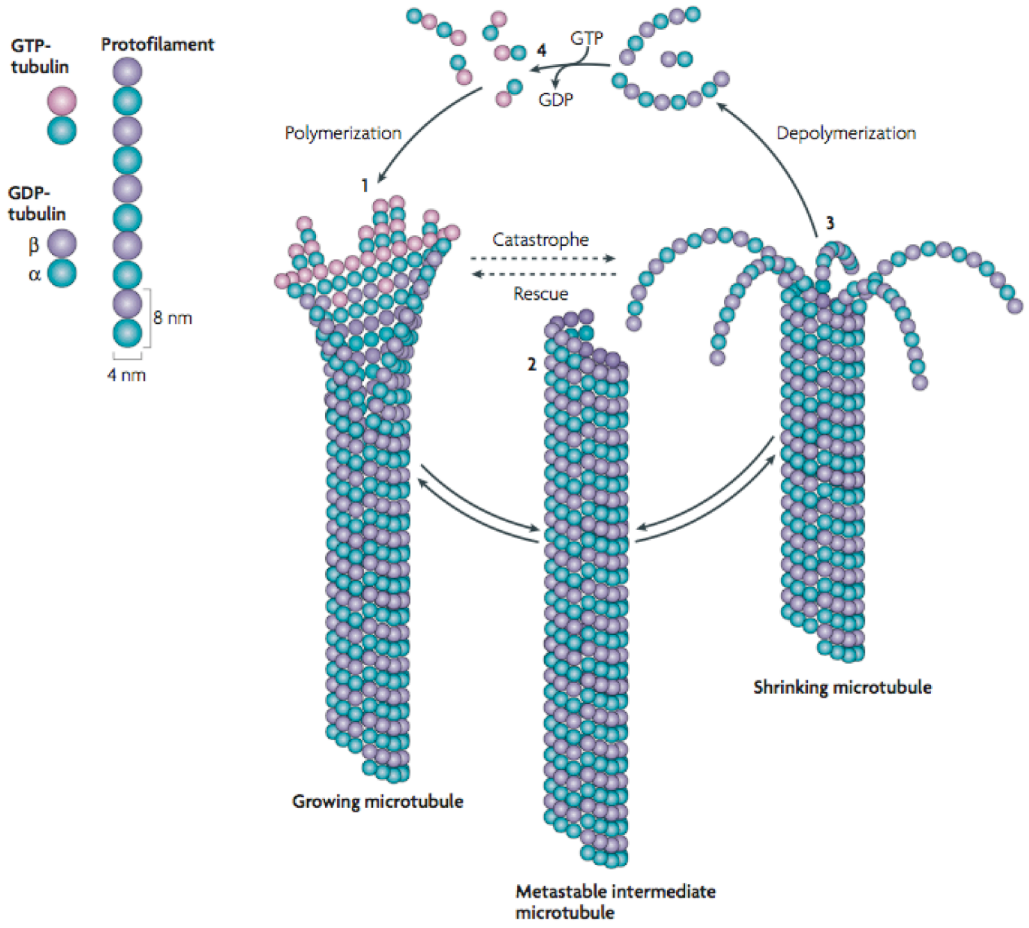

Figure 1.1 Microtubules are dynamic polymers. α/β tubulin heterodimers assemble in a head-to-tail manner to form protofilaments that associate laterally to form a hollow tube. Microtubules are dynamic structures that switch stochastically between periods of growth and shrinkage. GTP hydrolysis occurs on the β-tubulin subunit shortly after incorporation. Adapted from Ahkmanova (2008).

protofilaments observed in shrinking microtubules by electron microscopy. Microtubules transition between these two states, with transitions between polymerization and depolymerization known as a catastrophe, while the opposite is termed a rescue (Figure 1.1) (Walker et al., 1988). Periods of "pause", where no microtubule growth or shrinkage occurs, also can be observed in living cells.

Microtubules have multiple functions in the cell. In mitosis, microtubules comprise the spindle where dynamic microtubules search the cytoplasmic space to capture and later separate chromosomes in mitosis. Microtubules serve as tracks for motor proteins involved in vesicle transport. In migrating cells, stabilized microtubules are reoriented toward the leading edge and associate with cortical proteins and actin filaments to promote movement. Microtubule doublets arranged in a circle around a central pair of microtubules provide the primary structure for cilia and flagella. Flagella are hair-like projections that emanate from eukaryotic and prokaryotic cells that generate force for propulsion. Cilia found on eukaryotic cells, which have a structure similar to flagella, are found on cells in the respiratory, female reproductive, and digestive tract where they aid in fluid movement (Silverman and Leroux, 2009). A specialized organelle termed the primary cilium has been further characterized in eukaryotic cells. This cilium grows out of the older centriole and is organized similar to cilia and flagella, with the exception that the central microtubule pair is absent. It is now clear that the primary cilium is involved in integrating signaling cascades in cells involved in sensory organs (Berbari et al., 2009).

Microtubule Associating Proteins

Microtubules observed *in vivo* are more dynamic than those assembled *in vitro*, with polymerization rates five-ten fold faster in cells (reviewed in Cassimeris, 1993). Microtubules in cells undergo dramatic rearrangements in response to extracellular and cell cycle cues. Migrating cells respond to external stimulus by orienting microtubules toward the leading edge and repositioning the Golgi and MTOC (reviewed in Watanabe et al., 2005). When cells transition from interphase to early mitosis, microtubule turnover and the growth rate increase as the microtubules form the mitotic spindle (Zhai et al., 1996). Microtubules in both mammalian and yeast cells become more stable and dynamics are reduced in response to anaphase signals (Zhai et al., 1995; Higuchi and Uhlmann, 2005). These changes all reflect regulation in space and time of microtubules by cellular factors. Below is a brief overview of proteins that serve to either stabilize or destabilize microtubules.

The classical microtubule-associated proteins (MAPs) were first identified in neuronal cells. MAP1, MAP2, Tau, and MAP4, which is also expressed in non-neuronal cells, bind along the microtubule lattice to promote stabilization and polymerization (reviewed in Desai and Mitchison, 1997). Tau has emerged as an important factor in neuronal diseases such as Alzheimer's Disease, where hyperphosphorylated Tau is a component of the neurofibrillary tangles found in the brain tissue of patients (Robert and Mathuranath, 2007). The severing protein katanin promotes quick turn over of microtubule arrays to increase the amount of short polymers needed for cytoskeletal rearrangements (Baas et al., 2005). Motor proteins from the kinesin-8 and kinesin-13 class exhibit depolymerase activity by destabilizing the GTP-cap (Gupta et al., 2006; Varga et al., 2006; Howard and Hyman, 2007).

Relatively recently, a special class of MAPs that bind preferentially to the growing microtubule end play a major role in influencing dynamics (reviewed in Galjart, 2005; Akhmanova and Steinmetz, 2008). The plus-end tracking proteins (+TIPs) include both motor and non-motor proteins and are conserved throughout eukaryotes. In live-cell imaging, CLIP-170, the founding member, follows the growing end of the microtubules, which gives the appearance of "comets" throughout the cell (Perez et al., 1999). CLIP-170 binds microtubules through an amino-terminal CAP-Gly domain that is only available when protein autoinhibition with the carboxyl terminus is relieved (Lansbergen et al., 2004). End Binding (EB) protein not only binds the plus end, but is required for the plus-end binding of the +TIPs CLASP and CLIP-170 (Tirnauer and Bierer, 2000; Mimori-Kiyosue et al., 2005; Bieling et al., 2008). EB activity in mammalian cells and yeast has been investigated both *in vivo* and *in vitro* with conflicting results concerning the ability of EB family members to promote or suppress MT catastrophes (Komarova et al., 2009; Wolyniak et al., 2006; Bieling et al., 2007; Blake-Hodek, 2009). Purified *S. pombe* Mal3/EB1 binds along the microtubule seam, possibly stabilizing lateral protofilaments to achieve overall stability (Sandblad et al., 2006). The +TIP ch-TOG family promotes microtubule polymerization while binding both growing and shrinking microtubule ends (Gard and Kirschner, 1987; Brouhard et al., 2008). Other +TIPs include APC (reviewed in Nathke, 2004), Lis1, and the dynactin protein $p150^{Glued}$ (reviewed in Akhmanova and Steinmetz, 2008). Understanding the mechanisms for how these different +TIP families alter microtubule dynamics is an area of active study.

Several models describe how +TIPs bind the dynamic microtubule end (reviewed in Carvalho et al., 2003). XMAP215, a member of the ch-TOG

family, “surfs” on the growing end by binding tubulin polymerizing onto microtubules followed by dissociation (Brouhard et al., 2008). The CLIP-170 homologs in both *S. cereviae* and *S. pombe* are physically transported to the ends by kinesins (Busch et al., 2004; Carvalho et al., 2004). Similarly, kinesin II transports APC to the end (Jimbo et al., 2002). As mentioned above, some proteins depend on EB1 for localization even though they have their own microtubule binding domain. EB1 proteins rapidly associate and dissociate from plus ends (Bieling et al., 2008).

Overview of the +TIP CLASP Family

The CLASP family of proteins is involved in a number of diverse cellular processes. CLASP proteins are +TIPs and can be visualized as comets on growing microtubules in eukaryote cells (Maiato et al., 2005; Sousa et al., 2007). Protein homologs exist in a variety of eukaryotes, including the founding member Stu1 in *S. cerevisiae* (Pasqualone and Huffaker, 1994), Cls1/Peg1 in *S. pombe* (Grallert et al., 2006; Bratman and Chang, 2007), Orbit/MAST in *D. melaogaster* (Lemos et al., 2000; Inoue et al., 2000), Cls-2 in *C. elegans* (Cheeseman et al., 2005), XOrbit in *Xenopus laevis* (Hannak and Heald, 2006), CLASP in *Arabidopsis thaliana* (Ambrose et al., 2007; Kirik et al., 2007), and CLASP1 and CLASP2 in mammalian cells (Akhmanova et al., 2001) (Figure 1.2 A). CLASP proteins share distinct protein features. The amino terminus of CLASP proteins contains a TOG domain comprised of a series of HEAT repeats. This motif is also found in the ch-TOG family and is involved in binding tubulin (Al-Bassam et al., 2007) (Figure 1.2 A). CLASP homologs bind microtubules *in vitro* (Lemos et al., 2000; Inoue et al., 2000), and the regions required for binding in the amino terminus of CLASP have

Figure 1.2 The CLASP +TIP family. (A) Phylogenic tree of chTOG containing protein families. XMAP215 and CLASP (circled) proteins are shown from a number of model organisms. Sc=*Saccharomyces cerevisiae*; Hs=*Homo sapiens*; Dm=*Drosophila melanogaster*; Mt=*Medicago truncatula*; At=*Arabidopsis thaliana*; Os=*Oryza sativa*. Image taken from Ambrose (2007). (B and C) CLASP preferentially associates with microtubule plus ends near the cell cortex. (B) CLASP (red) in HeLa cells co-localizes with microtubules (green) at the cortex. Inset is enlargement of cortex. Taken from Mimori-Kiysue (2005). (C) CLASP (green) localizes to EB1 (red) decorated microtubule tips in migrating fibroblasts. Insets highlight microtubule preference for CLASP at the leading edge versus the trailing edge. Taken from Akhmanova (2001). (D-G) Loss of CLASP affects spindle stability in mitosis. Shown are monopolar spindles from CLASP knockout mouse embryonic fibroblasts (D), XOrbit-depleted *Xenopus* extracts (E), *Drosophila* S2 cells following Orbit RNAi knockdown (F), and budding yeast after a shift to the restrictive temperature. Images taken from Pereria (2006), Hannak and Heald (2006), Leycock (2006), and Yin (2002).

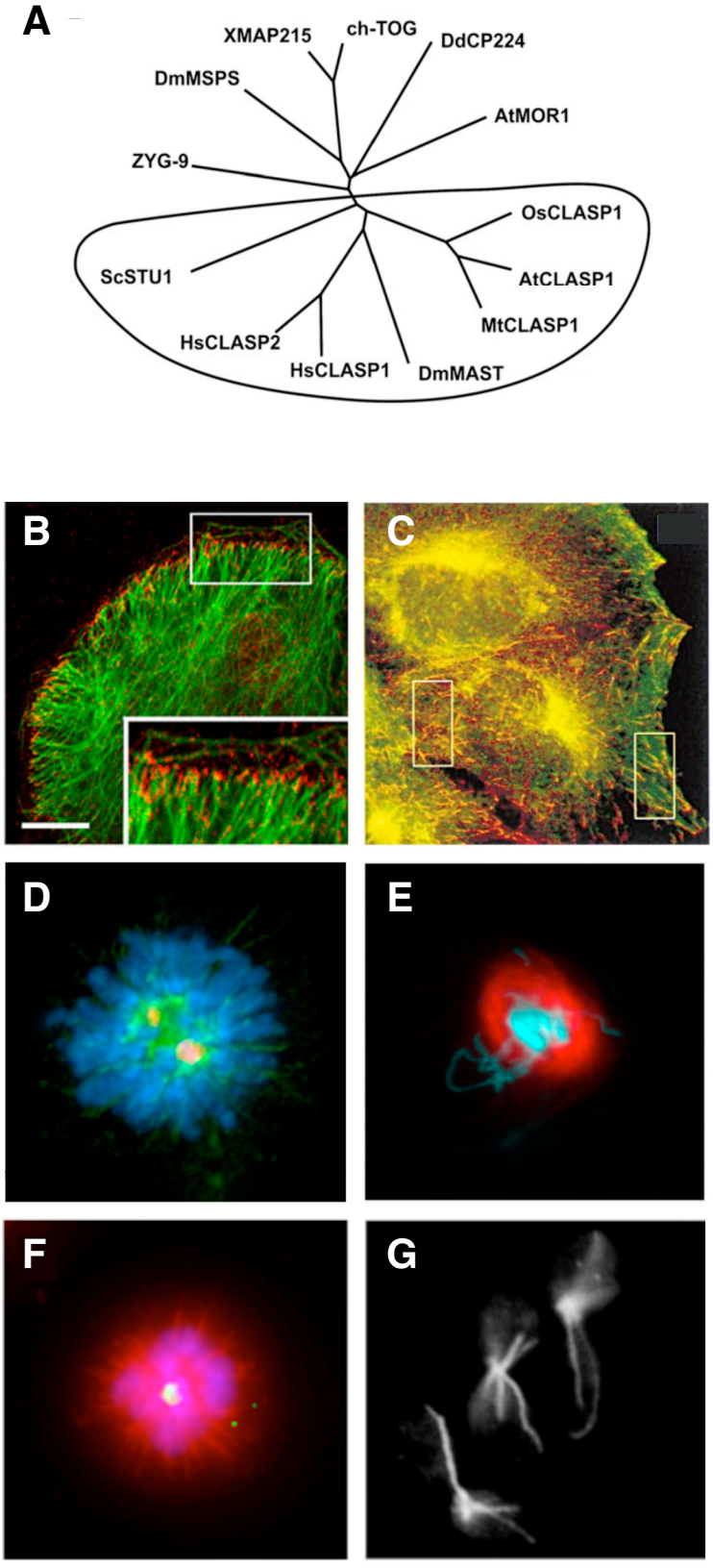
A
XMAP215
ch-TOG
DdCP224
DmMSPS
AtMOR1
ZYG-9
OsCLASP1
ScSTU1
AtCLASP1
MtCLASP1
HsCLASP2
HsCLASP1
DmMAST
B
C
D
E
F
G

been defined through *in vivo* and *in vitro* assays (Mimori-Kiyosue et al., 2005; Bratman and Chang, 2007; Wittmann and Waterman-Storer, 2005; Yin et al., 2002). The carboxyl terminus is involved in kinetochore, cortex, and Golgi association, as well as binding to the +TIP CLIP-170 (Mimori-Kiyosue et al., 2005; Maiato et al., 2005; Akhmanova et al., 2001; Reis et al., 2009). A particular isoform of CLASP2 contains an amino-terminal palmitoylation motif for membrane anchoring (Galjart, 2005). Orbit, XOrbit, and CLASP share significant stretches of homology along the protein length (Galjart, 2005; Hannak and Heald, 2006), while *A. thaliana* CLASP shares 23% identity and 43% similarity with CLASP (Ambrose et al., 2007). Both fungal CLASPs share ~20% homology with mammalian CLASP in three distinct regions, namely the HEAT repeats, microtubule binding domain, and carboxyl terminus (Bratman and Chang, 2007).

Many +TIPs interact physically with each other, and CLASP is no exception. Mammalian CLASP was originally identified in a two-hybrid screen with CLIP-170 (CLIP-170 Associating Protein) (Akhmanova et al., 2001). This interaction is mediated between the carboxyl terminus of CLASP and the coiled-coil region of CLIP-170. CLASP also binds the +TIP EB1 (Mimori-Kiyosue et al., 2005). These specific interactions, and the regions involved, are conserved in a variety of species. For example, *S. pombe* Cls1 binds Tip1 (CLIP-170) and Mal3 (EB1), CLASP in plants binds CLIP-170, Orbit binds CLIP-190, and XOrbit pulls down CLIP-170 (Grallert et al., 2006; Hannak and Heald, 2006; Ambrose et al., 2007; Mathe et al., 2003).

Roles for CLASP in Interphase

CLASP in interphase cells preferentially binds microtubule plus ends near the cell periphery, unlike EB1, which binds all growing microtubule ends (Figure 1.2 B) (Mimori-Kiyosue et al., 2005; Akhmanova et al., 2001). In actively migrating epithelial cells, CLASP localization is biased toward microtubules in the leading edge, especially those near the cortex (Figure 1.2 C). These microtubules are stable and recognized by antibodies against tubulin post-translational modifications that accumulate specifically on stable microtubules (Mimori-Kiyosue et al., 2005; Akhmanova et al., 2001). Knockdown of CLASP hampers directional migration and alters the organization of microtubules at the leading edge (Akhmanova et al., 2001; Drabek et al., 2006). Specifically, the dwell times of microtubule ends at the cortex are decreased and angles are altered in the absence of CLASP (Mimori-Kiyosue et al., 2005). CLASP is linked to the cortex via direct interaction with the proteins LL5β and ELKS that localize near focal adhesions (Lansbergen et al., 2006). Microtubule binding at the cortex is regulated by factors downstream of Rac1 and the GSK3β kinase (Akhmanova et al., 2001; Wittmann and Waterman-Storer, 2005). Activated Rac1 promotes CLASP microtubule binding in addition to actin polymerization at the leading edge. GSK3β can phosphorylate CLASP *in vitro* and *in vivo* resulting in loss of microtubule lattice binding. In migrating cells, the activity of GSK3β is inactivated in the leading edge, and this allows CLASP to stabilize microtubules (Wittmann and Waterman-Storer, 2005).

CLASP cortex localization is in part dependent on the spectraplakin protein ACF7 (Drabek et al., 2006). ACF7 acts as a cross-linking protein between actin and microtubule filaments. There is evidence to suggest that

CLASP can mediate interactions between these cytoskeletal structures. CLASP1 and CLASP2 in epithelial and neuronal cells co-localize with actin fibers, exhibit treadmilling at the cortex, and immunoprecipitate with actin. The TOG and microtubule-binding domain of CLASP are required for actin association (Tsvetkov et al., 2007). CLASP also co-localizes and interacts with the actin protein IQGAP (Watanabe et al., 2009). Current work is focused on understanding the interplay between different cytoskeletal components at focal adhesions.

CLASP in mammalian epithelial cells is required for promoting and stabilizing *de novo* nucleation of microtubules from the Golgi. This microtubule population, which requires γ-tubulin for nucleation, is asymmetrically directed toward the leading edge and contributes to cell motility. RNAi knockdown of CLASP affects the number of Golgi-nucleated microtubules, but not microtubules emanating from traditional centrosomes (Akhmanova et al., 2001; Efimov et al., 2007). CLASP localizes to the Golgi via an interaction with the TGN protein GCC185 (Akhmanova et al., 2001; Efimov et al., 2007). The CLASP binding to the Golgi TGN, which orients in the direction of migration, sets up the asymmetry of the microtubule array. CLASP protein levels measured on plus ends are higher on microtubules nucleated from the Golgi than from centrosomes (Efimov et al., 2007). This is an additional example of CLASP binding a subset of microtubules in migrating cells. CLASP-stabilized microtubules are also implicated in normal Golgi organization and maintenance (Miller et al., 2009).

In fungi, no interphase role has come to light for *S. cerevisiae* Stu1 as it has not been localized to astral microtubule plus ends (Yin et al., 2002). Cls1 in *S. pombe*, however, does have a role in stabilization of the interphase

microtubule bundle. Cls1 localizes to the bundle, but not to the plus ends of microtubules emanating from the bundle. When Cls1 is disrupted, microtubules shrink back to the bundle and do not grow again. Conversely, when Cls1 is overexpressed, microtubules rarely undergo catastrophe or shrink back to the interphase bundle. Overall, Cls1 prevents disassembly of interphase microtubules by promoting rescues (Bratman and Chang, 2007).

CLASP Proteins in Mitosis

CLASP proteins are involved in multiple aspects of mitosis. CLASP protein localization is dynamic and highly conserved across eukaryotes. CLASP binds kinetochores early in metaphase where it remains until anaphase onset, when CLASP concentrates on the region of polar microtubule overlap in the spindle, also referred to as the midzone (Bratman and Chang, 2007; Lemos et al., 2000; Cheeseman et al., 2005; Hannak and Heald, 2006; Yin et al., 2002; Maiato et al., 2003). In higher eukaryotes, CLASP remains associated with the midbody during cytokinesis (Lemos et al., 2000; Maiato et al., 2003). Less intense centrosome staining can also be observed in flies, mammalian cells, worms, and frog extracts (Lemos et al., 2000; Cheeseman et al., 2005; Hannak and Heald, 2006; Maiato et al., 2003).

CLASP affects kinetochore-microtubule attachment to varying degrees in different organisms. One report from *Drosophila* S2 cells reports that kinetochore-microtubule attachments are intact and bipolarity is established following RNAi knockdown of Orbit (Reis et al., 2009). However, other reports show that chromosomes are unable to congress to the metaphase plate when CLASP is disrupted, indicating defects in the microtubule-kinetochore attachment (Cheeseman et al., 2005; Hannak and Heald, 2006; Mimori-

Kiyosue et al., 2006; Maiato et al., 2002). The checkpoint protein BubRI and the kinetochore proteins Zw10 and dynein normally leave the kinetochore when attachment is established. However, after Orbit knockdown, protein localization persists (Maiato et al., 2002). Biorientation defects are also observed in *C. elegans*, where chromosome pairs are both near one spindle pole (Cheeseman et al., 2005). In addition, the distance between centromeres in CLASP1/CLASP2 depleted cells is shorter than in controls, indicating a lack of tension across the spindle (Mimori-Kiyosue et al., 2006). Defects in congression are likely due to the influence of CLASP on microtubule properties. Disrupting CLASP by antibody injection in mammalian cells results in kinetochore microtubule fibers (kFibers) that are no longer dynamic (Maiato et al., 2003).

Mitotic spindle structure is compromised when cells lack functional CLASP. Spindles are shorter on average, can contain multiple poles, or are disorganized (Inoue et al., 2000; Hannak and Heald, 2006; Mimori-Kiyosue et al., 2006; Maiato et al., 2002; Pereira et al., 2006). Noticeably, CLASP defects result in monopolar spindles in many organisms (Figure 1.2 D-G) (Pasqualone and Huffaker, 1994; Bratman and Chang, 2007; Lemos et al., 2000; Inoue et al., 2000; Hannak and Heald, 2006; Maiato et al., 2003). A similar monopolar phenotype is observed when cells are treated with monastrol, an inhibitor of the kinesin-5 motor protein that generates an outward force on spindle poles by sliding microtubules past each other (Mayer et al., 1999). Real-time imaging of CLASP-depleted cells reveals that monopolar spindles arise from spindle collapse after initial pole separation (Maiato et al., 2005; Reis et al., 2009). kFibers, composed of a bundle of microtubules, control their overall length through a process known as “flux”, where tubulin subunits are

incorporated at the plus end of the microtubules while concurrently subunits are removed from the minus end (Buster et al., 2007). Changes to kFiber length are accomplished by regulating the proteins responsible for the addition or removal of subunits. In Orbit-depleted S2 cells, kFibers shorten after initial pole separation and flux is not observed, leading ultimately to spindle collapse. This indicates that CLASP is needed for subunit incorporation at the plus end to counter the removal of minus end subunits. Spindle bipolarity can be restored by co-depletion of minus-end depolymerizing kinases Klp10A, Klp59C, and Klp69A to stop subunit removal (Buster et al., 2007; Laycock et al., 2006). A recent report shows that co-depletion of the minus-end directed motor dynein with Orbit restores not only bipolar spindles, but flux as well (Reis et al., 2009). Loss of dynein does not affect the localization of the minus-end depolymerases, and dynein itself does not have depolymerase activity, so bipolarity is not restored due to canceling antagonizing factors (Reis et al., 2009). From this, it appears that dynein and CLASP have antagonizing roles at the kinetochore.

Later in anaphase, CLASP is positioned at the midzone where an outward force is generated by motor proteins and elongating microtubules to separate spindle poles. Spindles in XOrbit-depleted *Xenopus* extracts quickly depolymerize their microtubules upon entry into anaphase (Hannak and Heald, 2006). Spindle measurements in early embryos with a hypomorphic Orbit allele demonstrated a dramatic decrease in spindle length as cells progressed through anaphase (Maiato et al., 2002). These results indicate that CLASP is involved in anaphase, likely by affecting the dynamic properties of microtubules at the midzone by either promoting stability or increased polymerization.

CLASP Promotes Microtubule Stabilization and Attachment

Phenotypic data suggests that CLASP is a microtubule stabilizer. Loss of CLASP often results in less stable microtubules and less microtubule polymer in cells (Bratman and Chang, 2007; Akhmanova et al., 2001; Drabek et al., 2006). Disruption of CLASP in *A. thaliana* results in dwarf plants with defects in specific cell types known to be heavily dependent on microtubules (Ambrose et al., 2007; Kirik et al., 2007). Microtubules are absent in certain plant tissues and plants are susceptible to microtubule destabilizing drugs (Ambrose et al., 2007). In contrast, overexpression of CLASP readily results in microtubule bundling and an increase in stabilized microtubules (Bratman and Chang, 2007; Kirik et al., 2007; Akhmanova et al., 2001; Aonuma et al., 2005). CLASP has been implicated as a stabilizer in neuronal growth cones where it is a downstream effector of Abl kinase. In response to a repellent factor in axon guidance during early development, CLASP is hypothesized to stabilize microtubules, causing the neuronal growth cone to orient toward a positive signal (Lee et al., 2004). One recent study suggests that CLASP achieves microtubule stabilization *in vivo* by promoting the pause state (Sousa et al., 2007). Microtubules in S2 cells depleted of Orbit are very dynamic and as a consequence spend less time pausing. These microtubules spend over half the total time shrinking as opposed to growing, while the frequency of rescues and catastrophes is unchanged. It is unclear how CLASP can promote pausing while tracking growing microtubules. Similar results were obtained after examining cortex microtubules in HeLa cells (Mimori-Kiyosue et al., 2005). Xenopus CSF extracts depleted of XOrbit do not have an effect on the number or length of microtubule asters as seen for other +TIPs like XMAP215 (Hannak and Heald, 2006). Hence, CLASP is not a global

regulator, but rather is targeted to specific microtubule populations for stabilization.

In addition to modulation of microtubule dynamics, a role in mediating microtubule attachment is beginning to take shape for the CLASP family. Roles for CLASP in eukaryotes in maintaining the microtubule-kinetochore association in metaphase spindles (Maiato et al., 2003) and forming contacts at the cortex of migrating cells have been discussed above (Lansbergen et al., 2006). Microtubule-cortex interactions are not only disrupted in migrating cells, but in S2 and HeLa cells as well where microtubules in knockdown cells run parallel to the cortex (Mimori-Kiyosue et al., 2005; Sousa et al., 2007). In *S. pombe*, mitochondria positioning is dependent on microtubule dynamics rather than on motors. A screen looking for mutants unable to position mitochondria yielded a mutant of Cls1 with a single amino acid change. While overall interphase microtubule morphology looked normal, the mitochondria were distributed on the cell edge in the mutant, similar to when cells are treated with microtubule-depolymerizing drugs (Chiron et al., 2008). Hence, CLASP here could be involved in mediating attachment between the mitochondria and the plus end of the dynamic microtubule. Another example can be found in higher plants. In root and cotyledon leaf cells from *A. thaliana* with a T-DNA insertion disrupting CLASP expression, microtubules at the cell cortex partially detach. Rather than maintain a relatively perpendicular orientation in relation to the cortex, the microtubules in a mutant cell are bundled parallel to the cortex. Time-lapse movies show that microtubule detachment is more frequent and longer in duration than in wild type (Ambrose and Wasteneys, 2008). CLASP mediating microtubule-cortex interactions is a

common theme. These roles may be a result of CLASP primarily stabilizing microtubule plus ends at these interfaces.

PART II. THE MITOTIC SPINDLE

Spindle Formation Pathways

Microtubules, microtubule motor and non-motor proteins, and chromosomes are involved in generating forces required for mitotic spindle formation (Rogers et al., 2005; Sharp et al., 2000). While variations exist among organisms, many key processes are conserved. Establishment of bipolar spindles occurs by two pathways: one utilizing centrosomes, and a second that relies on chromatin independent of centrosomes (Figure 1.3 A) (reviewed in Walczak and Heald, 2008). The contribution of each pathway differs based on the cell type, but both utilize motor proteins and microtubule stabilizers.

Spindle formation in cell types where centrosomes function as the spindle poles begins just prior to nuclear envelope breakdown (NEBD) (reviewed in Rosenblatt, 2005). Duplicated microtubule-emanating centrosomes use the nuclear envelope as a track for initial separation. This separation is dependent on the minus-end-directed microtubule motor dynein found on the nuclear envelope (Vaisberg et al., 1993). Following NEBD, dynein at the cell cortex continues to aid in centrosome separation by pulling on astral microtubules. Dynein is not solely responsible for separation, since some separation is observed in cells lacking functional dynein. In addition, the homotetrameric kinesin-5 proteins are major contributors to centrosome separation (Goshima and Vale, 2003; Enos and Morris, 1990; Heck et al., 1993). Kinesin-5 proteins cross-link antiparallel polar microtubules and slide

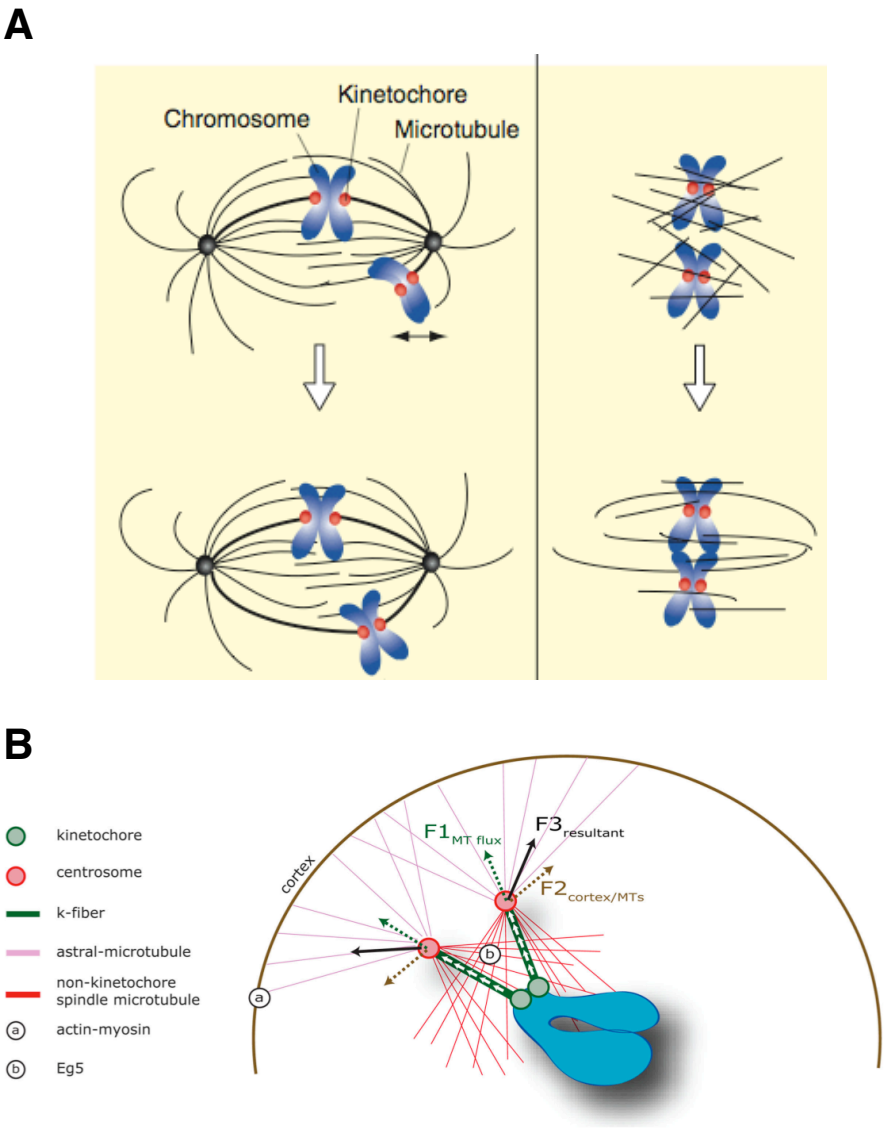

Figure 1.3 Modes of spindle assembly. (A) Illustration of spindle assembly with and without centrosomes. Microtubules emanating from centrosomes search the cytoplasm for kinetochores. In the absence of centrosomes, microtubules are organized and stabilized from chromosomes. (B) Diagram of the forces generated in centrosome separation. Cortical dynein and myosin motors pull the centrosomes apart (a). The kinesin-5 proteins, represented in the diagram by Eg5, crosslink antiparallel microtubules and slide them past each other to generate a pushing force on centrosomes (b). Growth and flux from kinetochore microtubules (kFibers) nucleated from centromeres also can exert a separating force. Images taken from Biggins (2006) and Toso (2009).

them past one another to generate a spindle-pole-separating force (Sharp et al., 1999). Disruption of kinesin-5 proteins, either by depletion or drug treatment, results in monopolar spindles with the centrosomes located near each other (Mayer et al., 1999). This mechanism is conserved in systems that undergo a closed mitosis where NEBD does not occur. In the budding yeast *S. cerevisiae*, spindle formation relies on the kinesin-5 proteins, Cin8 and Kip1, and on Stu1, a member of the CLASP family of microtubule plus-end tracking proteins (Yin et al., 2002; Hoyt et al., 1992; Roof et al., 1992). In temperature-sensitive *cin8-3 kip1Δ* and *stu1-5* strains, spindle pole separation is blocked, and metaphase spindles collapse with their previously separated spindle poles being drawn together, similar to what is observed in other organisms. This process is regulated by the Aurora B and Polo-like kinases, which modulate kinesin-5 activity (Barr et al., 2004; Barr and Gergely, 2007; Kotwaliwale et al., 2007). The bundling protein Ase1 in budding yeast contributes to spindle pole separation in the absence of Cin8 (Kotwaliwale et al., 2007). Spindle poles can also be separated by a pushing force generated by kinetochores. If centrosomes are not separated at NEBD in cells depleted of the kinetochore protein Mcm21R, monopolar spindles arise. Live-cell imaging shows that pushing forces from elongating kFibers nucleated at centromeres contribute to spindle pole separation (Figure 1.3 B) (Maiato et al., 2004; Toso et al., 2009).

Spindles can form in cell types that do not have centrosomes, including certain plant species and female germ cells undergoing meiosis (reviewed in Walczak and Heald, 2008). The centrosome-independent pathway can contribute to spindle formation even in somatic cells that contain centrosomes, as laser ablation of centrosomes does not affect assembly (Khodjakov et al.,

2000). Elegant work in *Xenopus* extracts stems from the initial observation that spindles form without the addition of centrosomes (Karsenti et al., 1984). Instead, microtubules are nucleated, stabilized, and organized from the chromosomes themselves. This process is regulated largely by the GTPase Ran, which is also involved in nuclear transport (Carazo-Salas et al., 2001). A gradient of Ran-GTP has been visualized both in extracts and in live cells (Kalab et al., 2002; Kalab et al., 2006). This gradient is established by the guanine-nucleotide exchange factor (GEF) RCC1 that resides on chromosomes, while the RanGAP is in the cytoplasm. Activated Ran has many downstream targets and effectors, which ultimately influence motor proteins, including the kinesin-5 proteins, and microtubule stabilizers (reviewed in Walczak and Heald, 2008). CLASP may be one of the microtubule stabilizers required for this process as XOrbit-depleted *Xenopus* extracts are unable to form spindles off of DNA coated beads (Hannak and Heald, 2006).

Chromosome-Microtubule Attachment

Following initial spindle pole separation, microtubules from each pole establish contact with chromosomes. The microtubule interacts with chromosomes via the multi-protein kinetochore complex (Figure 1.4) (reviewed in Cheeseman and Desai, 2008; Westermann et al., 2007). Kinetochore complexes assemble at centromeric regions of the chromosome that are distinguished by an alternate histone composition in the nucleosome. On this site, multiple sub-complexes assemble in a step-wise manner. In budding yeast, more than 60 proteins have been identified through a combination of genetic screens and biochemical purification (Cheeseman et al., 2001). The

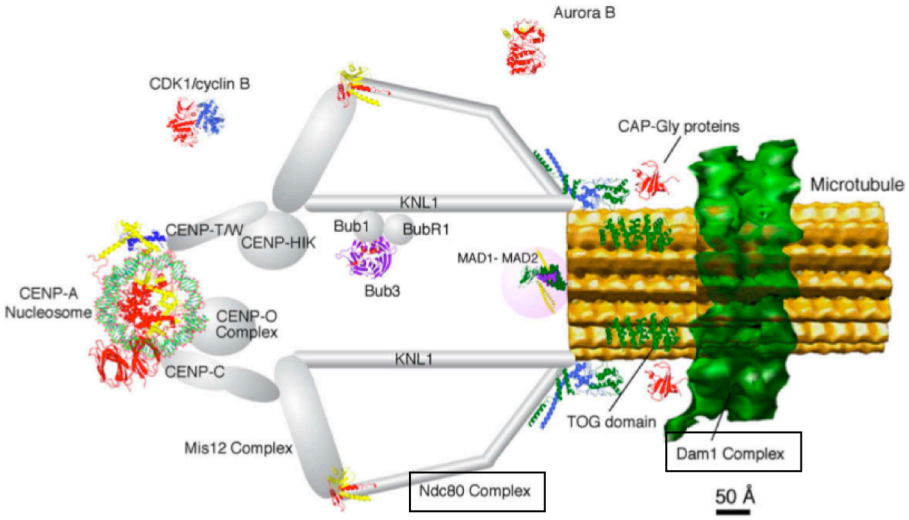

Figure 1.4 Kinetochore Structure. Illustration highlighting protein complexes found at the kinetochore-microtubule interface with available solved protein structures included. Boxed complexes (the Ndc80 and Dam1 complexes) are the outer-most protein complexes, and are involved in mediating attachment. Note the ring complex of Dam1. Image taken form Welburn (2008).

Dam/DASH and Ndc80/HEC1 sub-complexes are of particular interest as they are outer kinetochore complexes involved in mediating microtubule attachment. The ten proteins of the Dam/DASH complex can be purified as an intact complex, and the complete complex can further oligomerize into a ring structure that assembles onto microtubules (Westermann et al., 2005; Miranda et al., 2005). The ring complex can move laterally along microtubules, making it an excellent candidate to couple dynamic microtubule ends with the kinetochore. To date, no homologs of the Dam/DASH ring complex have been found in higher eukaryotes, although all ten proteins do exist in *S. pombe*. The Ndc80/HEC1 complex is comprised of four proteins and is conserved throughout eukaryotes (reviewed in Walczak and Heald, 2008). RNAi knockdown of Ndc80 affects chromosome attachment, but not assembly of other kinetochore complexes (DeLuca et al., 2005). Structure studies have elucidated that the complex forms a heterotetrameric elongated coiled-coil with Ndc80/Nuf2 globular heads at one end and Spc24/Spc25 on the other. Ndc80/Nuf2 binds microtubules, while Spc24/Spc25 associates with the kinetochore, making the complex an ideal bridge to mediate attachment (Ciferri et al., 2008; Cheeseman et al., 2006). The kinetochore is also the site for the spindle assembly checkpoint (SAC) protein localization, which delays anaphase entry if any microtubule attachment defects are detected (reviewed in Musacchio and Salmon, 2007).

Chromosome capture is based on a “search and capture” model where microtubules extend into the cytoplasm to make chromosome contact (Kirschner and Mitchison, 1986). Chromosome kinetochores often initially interact laterally with microtubules. Following initial contact, the chromosome is translocated towards one pole (Rieder and Alexander, 1990). An elegant

study in budding yeast looking at capture of individual kinetochores found that a number of +TIPs and the kinesin-14 Kar3 are involved in kinetochore capture by microtubules (Tanaka et al., 2005a). Eventually, this lateral association matures into an end-on attachment with the microtubule plus end (reviewed in Tanaka et al., 2005b; Tanaka et al., 2007). The +TIP CLASP is involved in maintaining end-on attachment possibly by stabilizing microtubules (Maiato et al., 2003). For mammalian cells, chromosome alignment along the metaphase plate is mediated by motors and +TIPs. In particular, the kinesin-7 CENP-E translocates kinetochores toward the center of the spindle by tracking along existing kFibers (Kapoor et al., 2006). Many +TIPs localize to the kinetochore where they can stabilize microtubule attachment as well as modulate kFiber length. As described above, chromosomes are distributed along the spindle instead of near the equator after knockdown of CLASP.

Spindle Pole Separation in Anaphase

After establishing kinetochore attachments and aligning the chromosomes, the spindle ultimately separates the sister chromatids from each other. The chromatids are first pulled toward the poles by motor proteins, as well as by coupling kinetochore movement with depolymerizing kinetochore microtubules (reviewed in Walczak and Heald, 2008). Kinetochore microtubule length decreases due to the depolymerase activity at the plus end, as well as from the minus end (Brust-Mascher and Scholey, 2002). Elongation of the spindle itself further contributes to chromosome segregation. Motor and non-motor proteins at the spindle midzone, the region of polar microtubule overlap, generate an outward force to further distance spindle poles. The kinesin-5 proteins again use their anti-parallel sliding

activity to push the poles out, while at the same time the interpolar microtubules themselves elongate (reviewed in Walczak and Heald, 2008). Microtubules sliding against each other can be observed in cells where one end of an elongating spindle is severed by laser ablation near the pole (Khodjakov et al., 2004).

There are questions as to whether cortical dynein can also contribute a pulling force to separate spindle poles. Effects on anaphase pole separation due to dynein loss are difficult to interpret since dynein is involved early in spindle pole separation (Vaisberg et al., 1993) and is involved in localizing numerous spindle proteins. In yeast, dynein motor activity pulls the spindle through the bud neck (Yeh et al., 1995), and there are some indications that it may be involved in spindle pole separation as well. First, deletions of a number of genes encoding dynein/dynactin proteins (*dynΔ*, *jnm1Δ*, *ldb18Δ*, and *nip100Δ*) are synthetic lethal with loss of Cin8, a kinesin-5 protein (Geiser et al., 1997; Tong et al., 2001). In addition, anaphase spindle pole separation depends on both Cin8 and Dyn1 (Saunders et al., 1995). Specifically, a *cin8-3 dyn1Δ* strain at the restrictive temperature is unable to complete the slow phase of anaphase (Gerson-Gurwitz et al., 2009).

PART III. SPINDLE ORIENTATION AND DYNEIN/DYNACTIN

Asymmetric Cell Division Requires Spindle Positioning

Asymmetric cell division is an important means to generate differentiated cells (Figure 1.5 A and B) (reviewed in Siller and Doe, 2009). To achieve this, cell fate determinants are specifically distributed to opposing regions of the cell, such that after division, the resulting cells have different protein compositions. The central spindle influences the plane of cytokinesis,

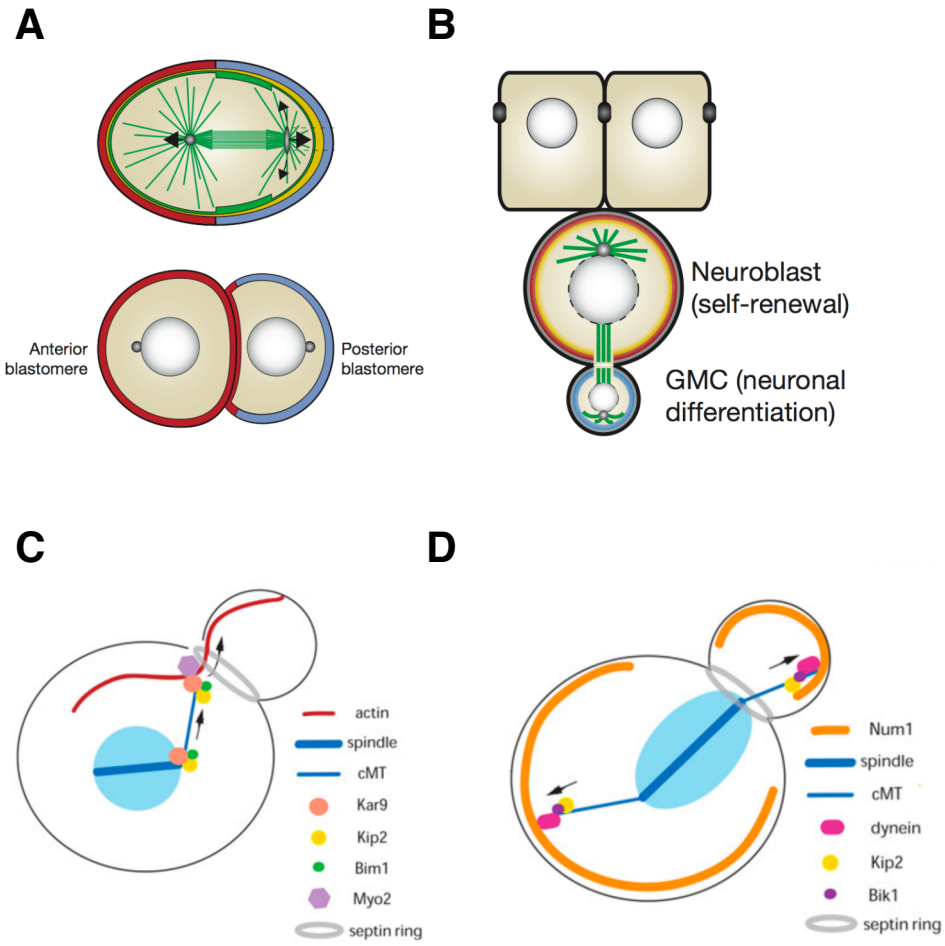

Figure 1.5 Asymmetric cell division. Examples of asymmetric cell division in the *C. elegans* early embryo (A) and *Drosophila* neuroblast (B). Arrow in (A) denotes spindle movement to the posterior. Colors at cell cortex denote different cellular factors, which differentiate the cells after cell division. (C-D) Asymmetric cell division in the budding yeast. Spindles are positioned at the neck by a pathway involving Myo2-directed movement of microtubules along actin cables followed by cytoplasmic microtubule (cMT) depolymerization by Kip3. Microtubules are coupled to Myo2 via Bim1 and Kar9, which are transported to the plus end by Kip2 (C). After anaphase onset, the minus-end directed motor dynein anchored at the cortex pulls the spindle through the bud neck (B). Images taken from Fraschini (2008) and Siller (2009).

hence positioning and orientation of the mitotic spindle along the polarity axis is key to this process. In the *C. elegans* early embryo, centrosomes oriented perpendicular to the cell axis move to the cell center and then rotate 90° following fertilization. Shortly after anaphase onset, the spindle shifts laterally to the posterior, which results in a larger anterior cell following the first division. Each of these movements is coordinated by dynein at the cortex along with actin and myosin. The localization and activities of these motor proteins are regulated by cortical cues, including the PAR proteins (reviewed in Siller and Doe, 2009). Stem cells rely on asymmetric cell division to generate one daughter cell with differentiation potential while the original cell maintains its ability for future regeneration. Disruptions to stem cell asymmetric division can lead to excessive self-renewal, which results in cancer (Yamashita and Fuller, 2008). *Drosophila* embryonic neuroblasts are similar to stem cells in that they undergo asymmetric cell division to "bud off" small cells that are the progenitors to the central nervous system (reviewed in Doe, 2008).

In the budding yeast *S. cerevisiae*, the site of cytokinesis is predetermined at the mother-daughter neck rather than influenced by the spindle. Hence, it is necessary to physically move and orient the spindle to the neck to ensure proper segregation of chromosomes to each cell. The astral microtubules extending out into the cytoplasm are required to position the spindle (Huffaker et al., 1987). In yeast, the spindle is oriented via two sequential pathways (Figure 1.5 C and D). Prior to anaphase, the spindle moves to the bud neck and becomes aligned along the mother-bud axis. This process involves a complex of the microtubule plus-end-binding protein Bim1, Kar9, the myosin V motor Myo2 that transports microtubule tips along actin filaments towards the bud neck, and the kinesin-8 protein Kip3 that promotes

microtubule depolymerization (Gupta et al., 2006; Hwang et al., 2003; Yin et al., 2000). Shortly after the onset of anaphase, the elongating spindle is pulled through the mother-bud neck. In this process, complexes of Bik1-Kip2 or Pac1-Ndl1 load dynein onto the plus end of an astral microtubule (Lee et al., 2003; Li et al., 2005; Sheeman et al., 2003). When dynein contacts the bud cortex at Num1 cortical sites, the minus-end directed motor reels in the microtubule, pulling the spindle pole through the bud neck (Adames and Cooper, 2000; Eshel et al., 1993; Heil-Chapdelaine et al., 2000; Lee et al., 2005). Although both Kar9 and dynein pathway mutants show defects in spindle orientation, they are viable; however, loss of both pathways is lethal (Miller and Rose, 1998).

In order to ensure that the spindle positioning machinery acts only on one pole, Kar9 is asymmetrically localized to the older spindle pole. The +TIP Bik1 and the mitotic regulators Cdc28/Cdk and Clb4/Clb5 prevent Kar9 association with the mother-directed pole through phosphorylation (Moore et al., 2006; Moore and Miller, 2007). Dynein loads onto the daughter-bound spindle pole body following Kar9. Unlike Kar9, dynein localization is restricted by Cdc28/Cdk and the cyclins Clb1/Clb2 (Grava et al., 2006). The specific downstream effectors that localize dynein are not known. Protein asymmetry at centrosomes is observed in other cells that orient and position their spindle to varying degrees (reviewed in Fraschini et al., 2008).

Dynein and Dynactin

Dynein is a minus-end directed microtubule motor that is involved in many cellular processes (reviewed in Hook and Vallee, 2006). As illustrated in previous sections, dynein is involved in spindle pole separation and spindle

positioning, localizes and translocates kinetochore proteins, focuses spindle poles in centrosome-independent spindle formation, and may contribute to anaphase. Dynein is also involved in vesicle movement, especially retrograde transport in neuronal cells (reviewed in Levy and Holzbaur, 2006). Maintenance of cilia and flagella is largely based on dynein function (reviewed in Ross et al., 2008). In budding yeast, the only role for dynein is to pull the spindle through the bud neck during anaphase.

Dynein activity requires the dynactin complex (Figure 1.6). Dynactin was originally isolated as a multi-subunit complex required for dynein function *in vitro* (Gill et al., 1991; Schroer and Sheetz, 1991). Dynactin contains a 40 nm rod composed of the actin-related protein Arp1. One end of the rod is capped by the actin capping protein CapZ, while the other end contains a second actin-related protein, Arp11. Proteins p25, p27, and p62 are localized at the pointed end of the Arp1 filament. A shoulder-sidearm projection, consisting of $p150^{Glued}$, dynamitin, and p24, binds the rod and projects away from the filament (Schroer, 2004). When the dynactin complex is disrupted, these proteins can be isolated together as a subcomplex with a $p150^{Glued}$:dynamitin:p24 stoichiometry of 2:4:2 (Eckley et al., 1999). $p150^{Glued}$ is the subunit responsible for binding dynein and contains a CAP-Gly motif for microtubule binding.

Homologs for key dynactin subunits in budding yeast have been identified, including Nip100 ($p150^{Glued}$), Jnm1 (dynamitin), Arp1 (Arp1), and Arp10 (Arp11) (Clark and Rose, 2006; Kahana et al., 1998; McMillan and Tatchell, 1994; Muhua et al., 1994). Loss of any one of these proteins results in a spindle orientation defect similar to that observed for dynein mutants. The dynactin complex in yeast is proposed to mediate dynein off-loading from the

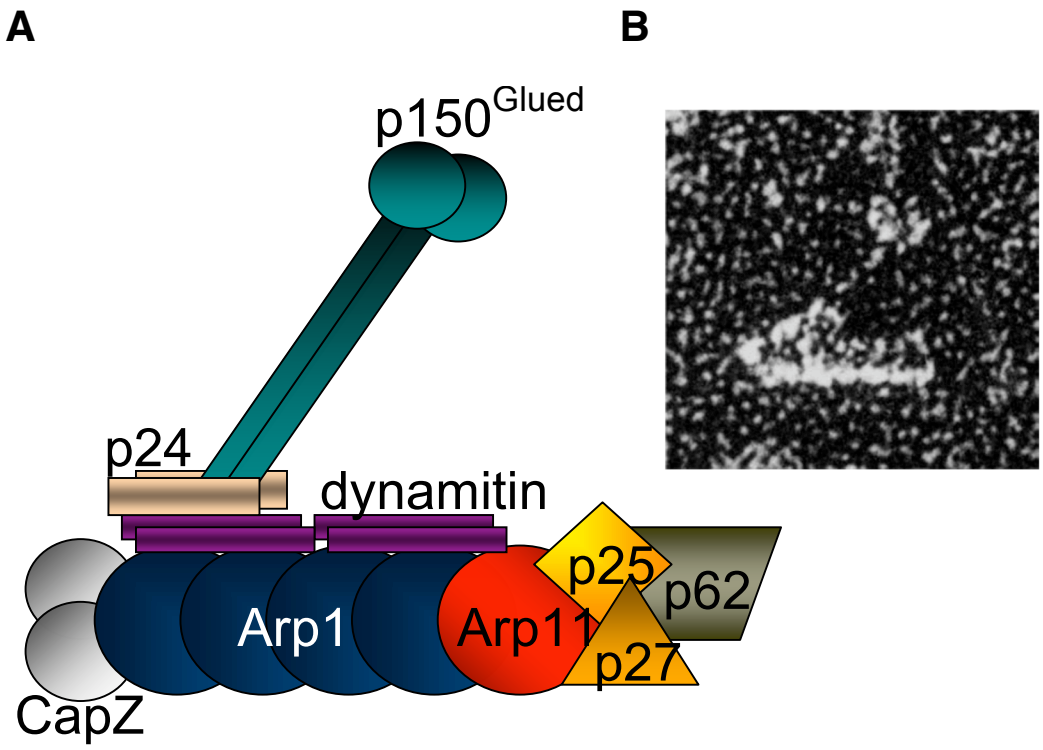

Figure 1.6 Dynactin complex architecture. (A) Schematic of mammalian dynactin complex. Arp1 forms a filament, while dynamitin, $p150^{glued}$, and p24 comprise the shoulder-sidearm complex. (B) Electron micrograph of a purified dynactin complex. Images taken and adapted from Schroer (2004).

microtubule plus end to Num1 cortical patches in anaphase. Dynein fails to localize to the cell cortex in the absence of any of the dynactin proteins and instead accumulates on the plus end (Moore et al., 2008; Markus et al., 2009). All of the dynactin proteins, except for Nip100 which contains its own microtubule binding domain, depend on dynein and Nip100 to localize to microtubule plus ends (Moore et al., 2008). Evidence is emerging that the protein She1 inhibits premature dynein activity by restricting the localization of dynactin proteins to the microtubule plus end until anaphase rather than regulate the localization of dynein itself (Woodruff et al., 2009).

PART IV. THESIS SIGNIFICANCE AND OVERVIEW

Health Implications

Defects in either microtubules or their associated proteins can contribute to the manifestation of a variety of diseases. Mutations in proteins that affect the ability of microtubules to form functional spindles can ultimately lead to chromosome instability. Aneuploidy resulting from chromosome missegregation is a leading cause of cancer. A form of colon cancer can be traced back to mutations or truncations of the +TIP APC, a tumor suppressor gene (Aoki and Taketo, 2007). Abnormal EB1 expression has been identified in glial cell tumors (Suarez-Merino et al., 2005). Currently, Paciltaxol is a major cancer therapeutic agent, which acts by stabilization of microtubule filaments. New cancer drugs are aggressively being targeted against microtubule-associated proteins that affect the dynamic properties of microtubules (Bhat and Setaluri, 2007).

Microtubule associated protein function is especially important in neuronal cells. Neuronal lissencephaly disorders, which result in decreased

motor function and epilepsy, arise from mutations in the +TIP LIS1, a gene important for migration of neurons (reviewed in Jaworski et al., 2008). LIS1 associates with dynein and localizes to kinetochores, yet the significance of these interactions is an area of active investigation. Amyotrophic lateral sclerosis (ALS), a disease where patients suffer from motor neuron loss, has been attributed to mutations in $p150^{Glued}$ (reviewed in Jaworski et al., 2008). Defects in CLIP-115 have been linked to Williams Syndrome, a disease characterized by facial abnormalities, cardiovascular difficulties, loss of motor skills, and mild retardation (Hoogenraad et al., 2004). The MAP Tau is hyperphosphorylated and a component of neurofibrillary tangles in brains from Alzheimer's Disease patients (Robert and Mathuranath, 2007).

Additionally, in early development, the motor protein dynein is crucial for orientation and positioning of the spindle. Failure to correctly divide the early embryo asymmetrically leads to developmental defects since the cellular cues for cell fate do not properly segregate.

Thesis Overview

A great effort has been made to understand the organization of microtubules as well as the regulation of their dynamics for proper spindle function. Moving microtubules and directing their properties is critical for spindle formation, chromosome alignment and separation, and spindle positioning. The discovery of MAPs, +TIPs, and depolymerizing motor proteins has yielded insights into how microtubule dynamic regulation is accomplished; yet the precise mechanism of how and when these proteins alter dynamics is an area of intense investigation. +TIPs provide a way to

regulate dynamics in response to cell cycle or external cues, while motor proteins organize microtubule arrays by crosslinking and sliding microtubules.

In this thesis, I provide insight into the role of Stu1, the CLASP homolog in the budding yeast *Saccharomyces cerevisiae*, in spindle function. Stu1 is required for spindle stability, yet the details are not clear. I demonstrate that Stu1 acts primarily at the plus ends of kinetochore microtubule populations to stabilize the short metaphase spindle. Through a genetic screen with Stu1 to identify additional proteins that are involved in spindle function, I identified Ldb18. My work provides evidence that Ldb18 is the yeast homolog of the mammalian protein p24 that is involved in the dynactin complex, which is required for dynein function. In yeast, dynein is important for movement of the spindle through the bud neck.

CHAPTER TWO

The Microtubule-Binding Protein Stu1 Acts at Kinetochores to Stabilize the Metaphase Mitotic Spindle.

INTRODUCTION

Stu1 is the sole homolog of the CLASP family of +TIPs in yeast. Stu1 was originally identified as a suppressor of a cold-sensitive β-tubulin mutation (Pasqualone and Huffaker, 1994). Stu1 binds microtubules directly through a region that is highly basic. Detailed interaction studies revealed that a β-tubulin patch facing outward on the microtubule binds Stu1 (Yin et al., 2002). Stu1 on metaphase spindles localizes inside the SPBs in a bilobed pattern consistent with microtubule plus-end binding at kinetochores (Yin et al., 2002). Kinetochore association was further demonstrated by chromatin immunoprecipitation (ChIP) (Ma et al., 2007). Stu1 is also found at the region of polar microtubule overlap in the elongating spindle known as the midzone. Unlike the +TIPs Stu2, Bik1, and Bim1, Stu1 does not localize to astral microtubule ends at any point in the cell cycle (Yin et al., 2002).

Characterization of the temperature-sensitive *stu1-5* strain revealed that Stu1 contributes an outward spindle force to maintain spindle pole body (SPB) separation. At the restrictive temperature, cells not only arrest as large-budded cells with replicated SPBs situated near each other, but also contain abnormally long and numerous astral microtubules (Pasqualone and Huffaker, 1994; Yin et al., 2002). Yeast without the kinesin-5 proteins Cin8 and Kip1 yield a similar phenotype. These motor proteins localize to the midzone and are responsible for sliding anti-parallel microtubules, thus generating an

outward force (Hoyt et al., 1992). When *stu1-5* cells arrested with short spindles are shifted to the restrictive temperature, spindles collapse and SPBs are pulled in together (Yin et al., 2002). Minor overexpression of the spindle kinesin Cin8 can rescue *stu1-5* at 35°, possibly by exerting additional outward forces to compensate for partial Stu1 loss.

Stu1 is important for maintaining spindle stability, yet a mechanism explaining Stu1 involvement is not known. Members of the CLASP family are considered microtubule stabilizers that act by directly adding tubulin subunits, promoting pause events, or increasing rescue events (Mimori-Kiyosue et al., 2005; Maiato et al., 2005; Sousa et al., 2007). The effect of Stu1 on microtubule dynamics has been difficult to investigate *in vivo* since individual nuclear microtubules are indiscernible and no Stu1 is observed on astral microtubules in the cytoplasm. The spindle collapse phenotype suggests that Stu1 function as a microtubule stabilizer similar to CLASP. Within the nucleus, there are two populations of microtubules. The polar microtubules extend across the spindle, while kinetochore microtubules mediate chromosome attachment. Stu1 can potentially influence the plus end dynamics of either of these two populations. To date, the activity of Stu1 on each of these microtubule populations, and how this activity in turn contributes to spindle stability has not been explored. This chapter further explores the localization of Stu1 throughout the cell cycle, and attempts to determine which population of microtubules is affected by Stu1 activity.

MATERIALS AND METHODS

Yeast strains and plasmids: Strains used in this study are listed in Table 2.1. Yeast strains were cultured in standard media (Sherman, 1991). Standard

Table 2.1 Yeast Strains

Strain	Genotype
AHY19	*MATα his3-Δ200 leu2-3,112 ura3-52 Stu1-3GFP::HIS5 Spc42-mRFP::KanMX*
AHY157	*MATa his3-Δ200 leu2-3,112, ura3 lys2Δ stu1-5::ClonNat ndc80-1::KanMX Spc42-GFP::HIS5*
AHY164	*MATa his3-Δ200 leu2-3,112 ura 3-52 trp1-Δ1 bik1Δ::TRP1 stu1-5::KanMX Spc42-GFP::HIS5*
AHY165	*MATa his3-Δ200 leu2-3,112 ura 3-52 trp1-Δ1 bik1Δ::TRP1 stu1-5::KanMX GFP-Tub1::HIS5*
AHY166	*MATa his3-Δ200 ura3-52 leu2 stu1-5::KanMX stu2-13::URA3 Spc42-GFP::HIS5*
AHY171	*MATα his3-Δ200 leu2-3,112, ura3-52 trp1-Δ1 stu1-5::ClonNat GFP-TUB1::HIS5*
AHY173	*MATα his3-Δ200 leu2-3,112 ura3-52 trp1-Δ1 stu1-5::ClonNat Mtw1-3GFP::HIS3 Spc42-mRFP::KanMX*
AHY181	*MATa his3-Δ200 leu2-3,112 lys2Δ ura3 trp1-1::256LacO::TRP1 ndc80-1::KanMX Spc42-GFP::HIS5*
AHY186	*MATa his3Δ0 leu2Δ0 ura3Δ0 stu1-5::ClonNat kip3Δ::KanMX GFP-Tub1::HIS5*
AHY187	*MATa his3Δ0 leu2Δ0 ura3Δ0 stu1-5::ClonNat kip3Δ::KanMX Spc42-GFP::HIS5*
CUY1139	*MATa ade2-1 trp1-1 can1-100 leu2-3,112 his3-11,15 ura3 ssd1-Δ2(cla1) spc42Δ1::LEU2 TRP1::Spc42-GFP (x3) Gal+*
CUY1158	*MATa stu1-5 TRP::Spc42-GFP (x3) spc42Δ1::LEU2 his3 ura3-52*
CUY1846	*MATa ade2 his3-Δ200 leu2-3,112 ura3-52 Mtw1-3GFP::HIS3 Spc42-mRFP::KanMX6*
Y190	*MATa ade2-101 leu2-3,112 ura3-52 trp1-901 his3 gal4 gal80 cyhR URA3::GAL-LacZ LYS2::GAL(UAS)-His3*

protocols for cloning and yeast lithium acetate transformation were utilized. To observe Stu1 in relation to spindle pole bodies, the carboxyl-terminus of Spc42-mRFP and the Kanamycin marker were amplified from CUY1562 genomic DNA (Primers from Baoying Huang) and transformed into CUY1539 (*Stu1-3GFP*) to generate AHY19 by homologous recombination into the genome. To examine Mtw1 localization in a *stu1-5* background, AHY173 was made by transforming the integrating plasmid pCU1205 (*Mtw1-3GFP*) cut with SnaBI into AHY134 (*stu1-5*), followed by addition of the Spc42-mRFP PCR fragment. Strains with *ndc80-1* alone or in combination with *stu1-5* were generated by crossing AHY134 (*stu1-5*) with AHY126 (*ndc80-1*) or BLY56 (*ndc80-1*) respectively. Selected spores were transformed with a PCR fragment generated with primers AHP146/147 on pCU730 (pFA6a-GFP-TRP) to tag Spc42 with GFP in the genome. The *stu1-5 bik1Δ* double mutant strain was selected from a cross of CUY413 (*bik1Δ*) and CUY1537 (*stu1-5*). The *stu1-5 kip3Δ* strain was isolated after sporulation and dissection of double mutant diploids obtained from a SGA screen (Tong et al., 2001, Chapter 3). The selected spores were transformed with either the integrating plasmid pCU1210 (P_{Tub1}-GFP-TUB1) linearized with XbaI (AHY164; AHY186) or PCR from AHP146/147 (AHY165; AHY187).

Two-hybrid assays were performed as described previously (Wolyniak et al., 2006). Vectors used are summarized in Table 2.2. Ase1 two-hybrid plasmids were constructed by digesting PCR amplified regions of Ase1 with BamHI/SacI or NcoI/BamHI followed by ligation with T4 ligase (Invitrogen, Carlsbad, CA) into pACTII (pCU370) or pASII (pCU369). Following lithium acetate transformation of plasmids into Y190, β-galactosidase activity was determined by the filter assay and scored for blue color.

Table 2.2 Plasmids

Plasmid	Markers
pACTII	*ampR, 2μ, LEU2, P_{ADH}-GAL4AD*
pAH42	*ampR, 2μ, LEU2, P_{ADH}-GAL4AD-Ase1*
pAH53	*ampR, 2μ, TRP1, P_{ADH}-GAL4BD-Ase1*
pAH68	*ampR, 2μ, LEU2, P_{ADH}-GAL4AD-Ase1 (650-885)*
pAH69	*ampR, 2μ, TRP1, P_{ADH}-GAL4BD-Ase1 (443-885)*
pAH70	*ampR, 2μ, LEU2, P_{ADH}-GAL4AD-Ase1 (443-885)*
pAH71	*ampR, 2μ, TRP1, P_{ADH}-GAL4BD-Ase1 (300-885)*
pAH72	*ampR, 2μ, LEU2, P_{ADH}-GAL4AD-Ase1 (300-885)*
pAH75	*ampR, 2μ, LEU2, P_{ADH}-GAL4AD-Ase1 (1-600)*
pAH76	*ampR, 2μ, TRP1, P_{ADH}-GAL4BD-Ase1 (1-600)*
pAH77	*ampR, 2μ, LEU2, P_{ADH}-GAL4AD-Ase1 (1-442)*
pAH78	*ampR, 2μ, TRP1, P_{ADH}-GAL4BD-Ase1 (1-442)*
pAH80	*ampR, 2μ, LEU2, P_{ADH}-GAL4AD-Ase1 (785-885)*
pAH87	*ampR, 2μ, TRP1, P_{ADH}-GAL4BD-Ase1 (1-786)*
pAH88	*ampR, 2μ, LEU2, P_{ADH}-GAL4AD-Ase1 (1-786)*
pAH89	*ampR, 2μ, TRP1, P_{ADH}-GAL4BD-Ase1 (1-836)*
pAH90	*ampR, 2μ, LEU2, P_{ADH}-GAL4AD-Ase1 (1-836)*
pAH91	*ampR, 2μ, TRP1, P_{ADH}-GAL4BD-Ase1 (1-861)*
pAH92	*ampR, 2μ, LEU2, P_{ADH}-GAL4AD-Ase1 (1-861)*
pASII	*ampR, 2μ, TRP1, P_{ADH}-GAL4BD*
pCU1161	*ampR, 2μ, TRP1, P_{ADH}-GAL4BD-Stu1 (1-1000)*
pLY11	*ampR, 2μ, TRP1, P_{ADH}-GAL4BD-Stu1*
pLY12	*ampR, 2μ, LEU2, P_{ADH}-GAL4AD-Stu1*
pLY62	*ampR, 2μ, LEU2, P_{ADH}-GAL4AD-Stu1 (307-718)*
pLY185	*ampR, 2μ, LEU2, P_{ADH}-GAL4AD-Stu1 (1-718)*
pLY188	*ampR, 2μ, LEU2, P_{ADH}-GAL4AD-Stu1 (308-1000)*
pLY190	*ampR, 2μ, LEU2, P_{ADH}-GAL4AD-Stu1 (996-1514)*

Microscopy: Live-cell imaging was done on a spinning disk confocal imaging system (UltraVIEW, Perkin-Elmer, Wellesley, MA). Microtubules were depolymerized using nocodazole (20 μg/ml final with 1% DMSO) for 30 min. Log phase cultures involved in time-course experiments were diluted to an OD=0.2 and arrested in α-factor (12.5 uM final) (Zymo Research, Orange, CA) for 2.5-3 hours at permissive temperature in appropriate minimal media. The culture was washed three times with 1 ml minimal media, resuspended in 50 μl YPD, and 5 μl placed on a media pad (synthetic complete media in 0.8% agarose) and immediately moved into a pre-warmed chamber (26° or 37°) assembled on the microscope. Time post-release starts once slide is in chamber. Distance between SPBs was calculated by using the measure function on Image J (NIH, Bethesda, MD). This was used with the distance in the Z-direction to calculate total distance using the Pythagorean theorem.

RESULTS

Stu1 Localizes to Unattached Kinetochores Before Translocation to the Spindle Midzone

Similar to other members of the CLASP family, Stu1 associates with kinetochores during metaphase. Interestingly, kinetochore localization for CLASP1 and CLASP2 is microtubule independent (Maiato et al., 2003; Mimori-Kiyosue et al., 2006; Pereira et al., 2006). In collaboration with Beth Lalonde, I questioned whether the same was true for Stu1. We examined the localization of Stu1-3GFP in cells expressing the SPB protein Spc42-mRFP after treatment with the microtubule-depolymerizing drug nocodazole. In treated cells, SPBs are unable to maintain separation as the microtubule shortens, resulting in close SPBs. The unattached kinetochores are clustered proximal

to the SPBs, while kinetochores that maintain attachment even after nocodozole treatment, colocalize with the SPBs. Following treatment, Stu1 localizes as a single group adjacent to the collapsed SPBs, indicating preference for uattached kinetochores. This localization is similar to Mtw1-GFP, a known kinetochore structural protein, (Figure 2.1 A, B) which is clustered in two groups, representing both attached and unattached kinetochores. Hence, kinetochore localization in metaphase in the absence of microtubules is conserved throughout the CLASP family.

Once cells enter anaphase, Stu1 no longer associates with kinetochores. Rather, Stu1 localizes to the region of polar microtubule overlap in elongating spindles known as the midzone (Yin et al., 2002). To observe the transition of Stu1 from kinetochores to the midzone in elongating spindles, we followed the Stu1-3GFP signal in relation to spindle poles marked with Spc42-mRFP (Figure 2.1 C). Stu1 is observed along the short metaphase spindle and remains near the center of the spindle as SPBs begin to separate. The Stu1 signal becomes increasingly more focused at the midzone throughout anaphase, corresponding to the diminishing region of polar microtubule overlap. For the duration of anaphase, the kinetochores are localized adjacent to the SPBs. Stu1 is not observed near the SPBs during anaphase, indicating Stu1 translocates from the kinetochore to the spindle midzone. Stu1 is not distributed across the entire anaphase spindle.

Stu1 localization to the midzone requires the non-motor protein Ase1 (Khmelinskii et al., 2007). To see if this recruitment requires direct protein-protein contact, I tested whether Stu1 and Ase1 interact using a yeast two-

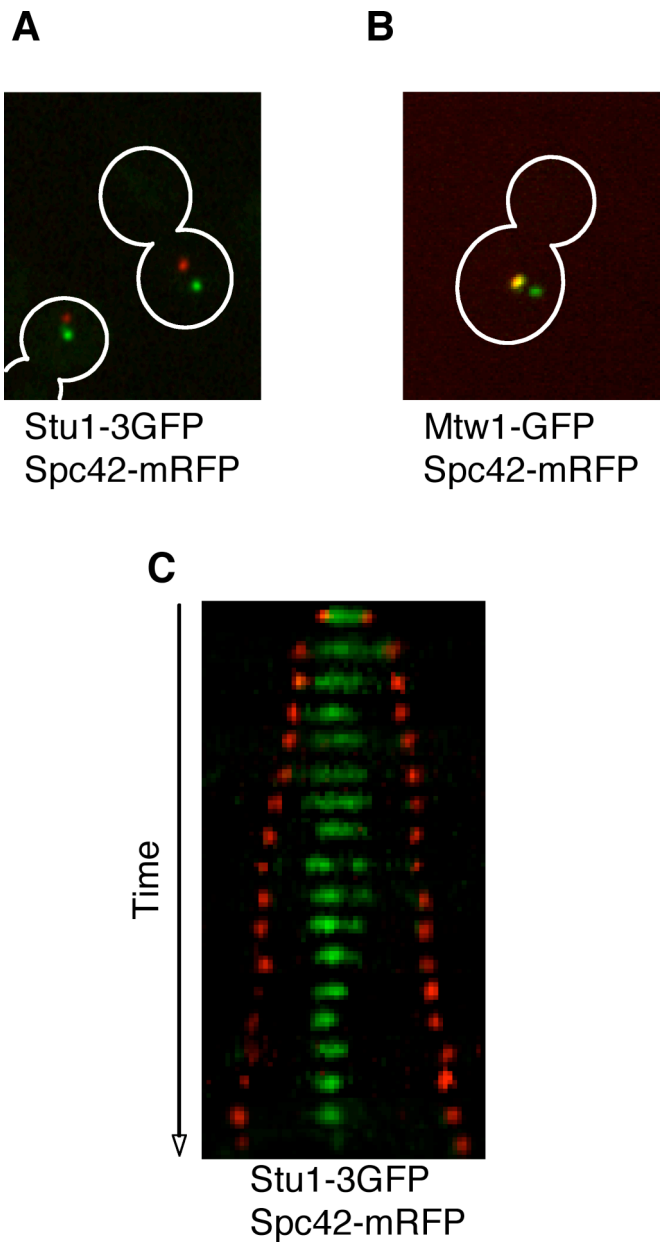

Figure 2.1 Stu1 localization throughout the cell cycle. (A and B) Stu1 associates with unattached kinetochores. After treatment with nocadozole (AHY19) for 30 minutes to depolymerize microtubules, Stu1 (green) localizes near unseparated spindle pole bodies (Spc42, red) as a single cluster, indicative of unattached kinetochores (A). Similar localization is observed for the kinetochore protein Mtw1 (CUY1846; green) (B). (C) Time-lapse microscopy (AHY19) of Stu1 (green) in relation to spindle poles (Spc42, red). Stu1 localizes along the metaphase spindle before translocating to the midzone during anaphase. Total time is 80 minutes with variable time intervals. Images acquired and processed by Beth Lalonde.

hybrid assay. A positive interaction, as indicated by a blue color change in a β-galactosidase filter assay, can be detected between full length Stu1 fused to the Gal4 binding domain and full length Ase1 (Figure 2.2 A). A number of available Stu1 truncations were used to narrow down the interaction domain. An amino-terminal fragment containing Stu1 amino acids 307-718, which spans much of the microtubule-binding domain, is the smallest fragment to interact with Ase1. Attempts to further narrow down the interaction domain within this fragment were not successful (data not shown). Using nested truncations of Ase1, I determined that Stu1 interacts with the carboxyl terminus of Ase1, particularly the region between amino acids 600-650 (Figure 2.2 B and C). Co-immunoprecipitation experiments with Stu1-13Myc were unable to detect either epitope-tagged Ase1 or native Ase1 *in vivo* (data not shown). It is possible that this interaction is transient and cell cycle specific. As the Ase1-binding region is near the amino terminus of Stu1, I do not expect that the epitope tag at the carboxyl terminus of Stu1 interferes with binding. In support of this, immunostaining can detect Stu1-13Myc at the spindle midzone (Yin et al., 2002), indicating it is recognized and targeted properly by Ase1.

Stu1 Function at Kinetochores is Critical to Maintain Spindle Pole Body Separation

Preformed spindles collapse in *stu1-5* cells at the restrictive temperature. However, it is unknown whether loss of Stu1 precludes the formation of spindles in the first place. To investigate if Stu1 has a role in initial spindle formation, I arrested cells with α-factor, then released the culture at the restrictive temperature and monitored SPB separation by imaging Spc42-GFP. At 60-75 minutes post-release, wild-type cells (n=6) separate

Figure 2.2 Yeast two-hybrid analysis of the Stu1-Ase1 interaction. (A) Full length and nested truncations of Stu1 fused to the either the binding or activation domain of GAL4 were tested for interaction with full length Ase1. The red box represents the microtubule-binding domain, while the blue box on Stu1 denotes the region homologous to the *S. pombe* Ase1 interaction domain. (B) Nested truncations of Ase1 fused to either the binding or activation domain of GAL4. Constructs were tested with either Stu1 307-718 (Binding domain) or Stu1 1-1000 (Activation Domain). All interactions were assayed with a colony filter β-galactosidase color assay. Positive interactions were scored by appearance of blue colonies by visual inspection. +, interaction/blue; +/-, weak interaction/light blue; -, no interaction; N/A, construct did not transform into yeast; MTBD, Microtubule binding domain; AD, Activation Domain; BD, Binding Domain

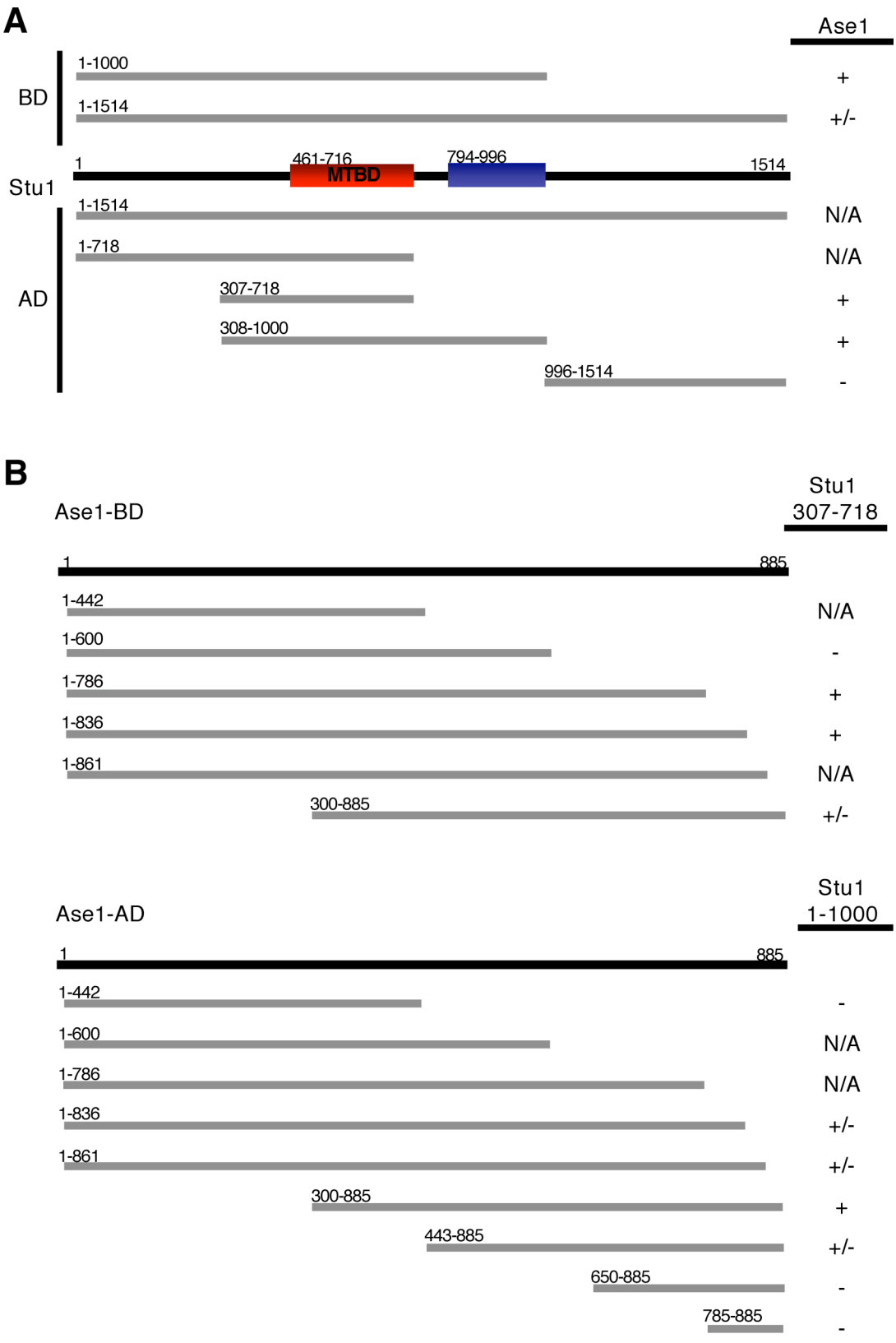
A
Ase1
BD
1-1000
+
1-1514
+/-
Stu1
1
461-716
MTBD
794-996
1514
1-1514
N/A
AD
1-718
N/A
307-718
+
308-1000
+
996-1514
-
B
Ase1-BD
Stu1
307-718
1
885
1-442
N/A
1-600
-
1-786
+
1-836
+
1-861
N/A
300-885
+/-
Ase1-AD
Stu1
1-1000
1
885
1-442
-
1-600
N/A
1-786
N/A
1-836
+/-
1-861
+/-
300-885
+
443-885
+/-
650-885
-
785-885
-

their SPBs to form a short spindle of approximately 2 μm. The short spindle remains relatively stable until anaphase onset (Figure 2.3 A, C). In *stu1-5* (n=7), SPBs can separate up to ~1 μm, but often this is followed by immediate collapse. Half of the observed cells (4 out of 7) undergo continuous rounds of minimal SPB separation and collapse, while other cells make only a few attempts. Regardless, spindle pole separation is no more than 1.5 μm (Figure 2.3 B ,D, E). Overall, initial SPB separation is not completely blocked in the absence of Stu1, but separation is minimal and unstable.

Spindle collapse suggests that Stu1 is needed to provide an outward force on the spindle poles. Motor proteins push SPBs by sliding anti-parallel polar microtubules, but the kinetochore microtubules can also exert forces on the poles. Kinetochore-attached microtubules restrict outward spindle pole movement, thus producing an inward force (Figure 2.3 F). In addition, kFibers in mammalian cells contribute an outward force based on a "flux" mechanism to control fiber length (see introduction). CLASP is essential for promoting flux through the incorporation of tubulin subunits at the microtubule plus end. When incorporation stops, the kinetochore microtubule decreases in length while still maintaining attachment at the kinetochore, thereby pulling the poles inward. Yeast kinetochore microtubules do not exhibit flux (Maddox et al., 2000), but the plus ends of kinetochore microtubules are still dynamic as observed by oscillation of GFP labeled centromeres between spindle poles at metaphase (He et al., 2001). Similar to CLASP, Stu1 at kinetochores may add tubulin subunits to promote microtubule growth, countering microtubule depolymerases that shorten the microtubule and restrict spindle pole outward movement (Figure 2.3 G). Kinetochore attachment occurs shortly after initial pole separation; hence the observation that newly duplicated spindle poles

Figure 2.3 Initial SPB separation in *stu1-5*. (A and B) Wild type and *stu1-5* cells (CUY1139, CUY1158) were arrested in α-factor for three hours at 26°. Cultures were released from arrest on agarose pads at 37°. Spindle poles (Spc42-GFP) were imaged every 30 seconds. Shown are still frames with time in minutes after release noted. (C and D) Graphs of spindle pole distance measured over time from individual cells. Lines in red correspond to still images. (E) Graphs of pole separation in two independent *stu1-5* cells later in time course. (F) Spindle formation in budding yeast. Chromosomes are initially attached via the kinetochore complex in G1. Following SPB duplication, the chromosomes are captured by microtubules resulting in many sister chromatid pairs having both kinetochores attached to the same pole. Motor proteins slide the polar microtubules past each other to push the SPB outward. Once the SPB are separated, the microtubules from the opposite pole can begin to establish bipolar kinetochore attachment, which provides an inward force. Note that bipolarity is established after SPB separation. (G) Model for *stu1-5* mediated spindle collapse. In wild-type cells, tubulin subunit incorporation is balanced with subunit removal. Stu1 may promote subunit incorporation at the kinetochore microtubule plus end shortly after initial pole separation. Without Stu1 present in the cell, microtubule-depolymerizing proteins are no longer antagonized, leading to an ultimate shortening of the microtubule. Spindle poles are “reeled in” as the kinetochore remains attached to the shrinking microtubule. SPB, Spindle Pole Body; MT, microtubule

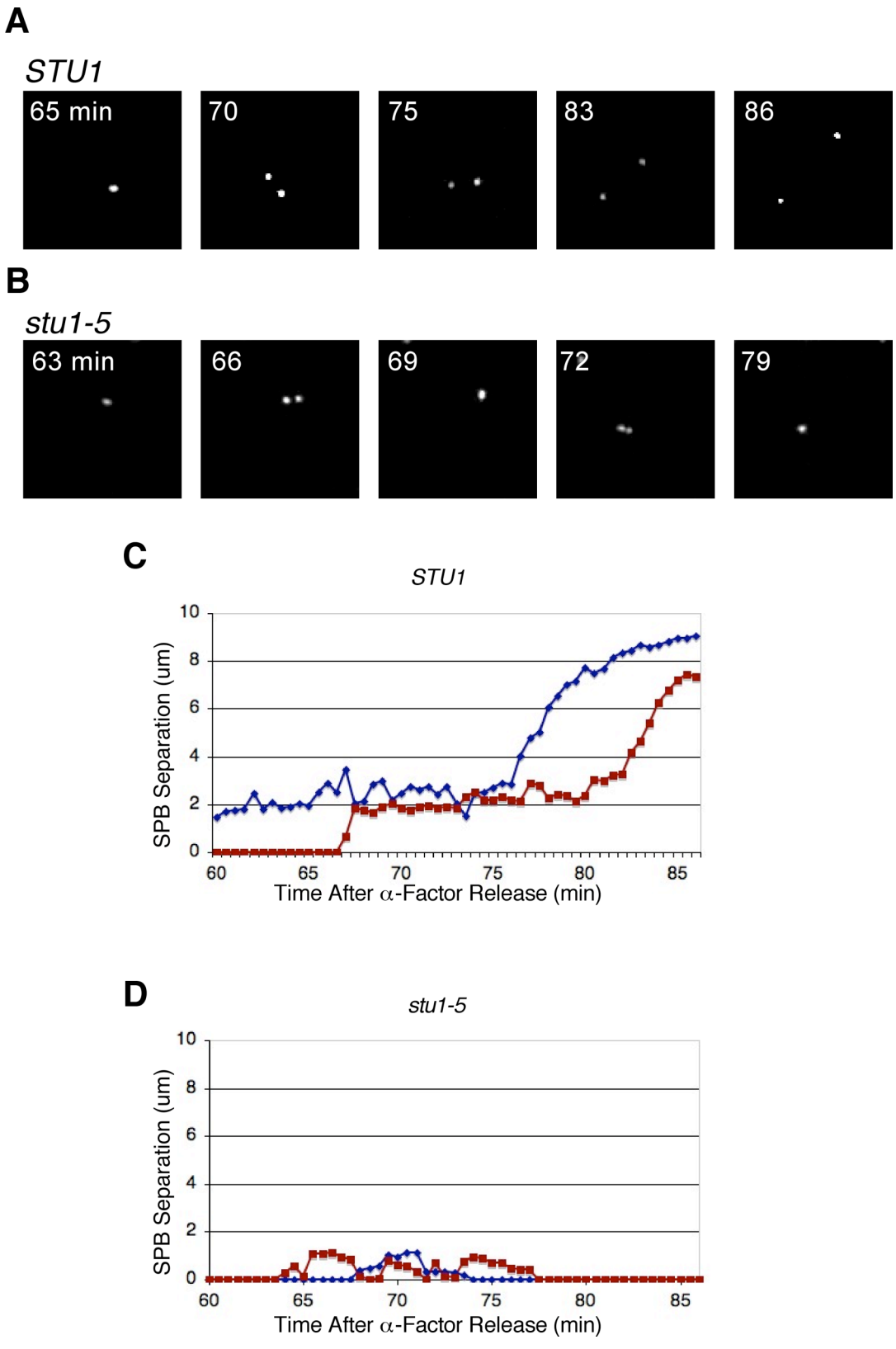
A
STU1
65 min
70
75
83
86
B
stu1-5
63 min
66
69
72
79
C
STU1
SPB Separation (um)
0
2
4
6
8
10
60
65
70
75
80
85
Time After α-Factor Release (min)
D
stu1-5
SPB Separation (um)
0
2
4
6
8
10
60
65
70
75
80
85
Time After α-Factor Release (min)

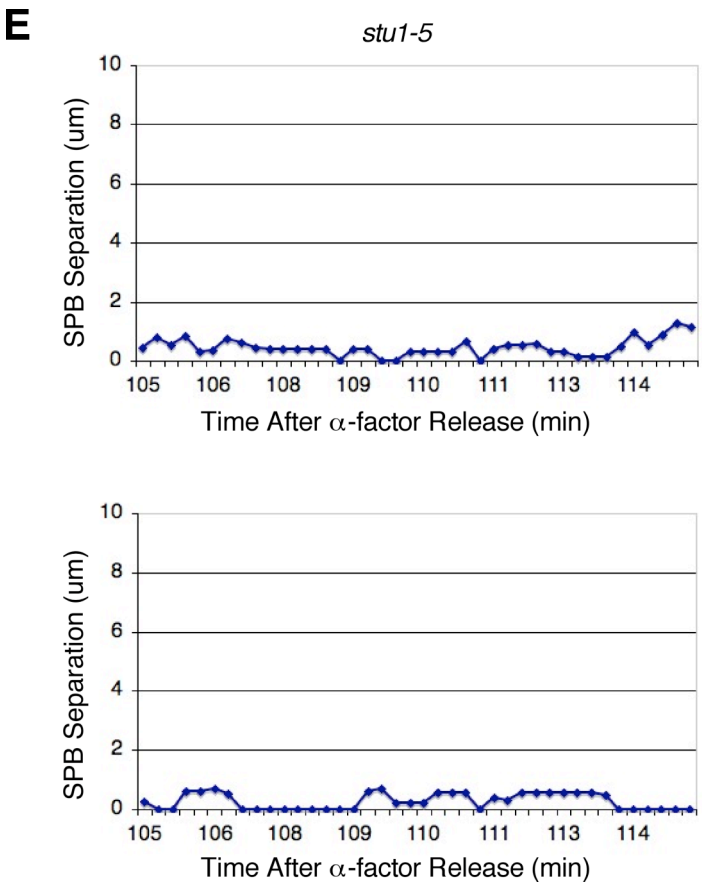
E
stu1-5
SPB Separation (um)
10
8
6
4
2
0
105
106
108
109
110
111
113
114
Time After α-factor Release (min)
SPB Separation (um)
10
8
6
4
2
0
105
106
108
109
110
111
113
114
Time After α-factor Release (min)

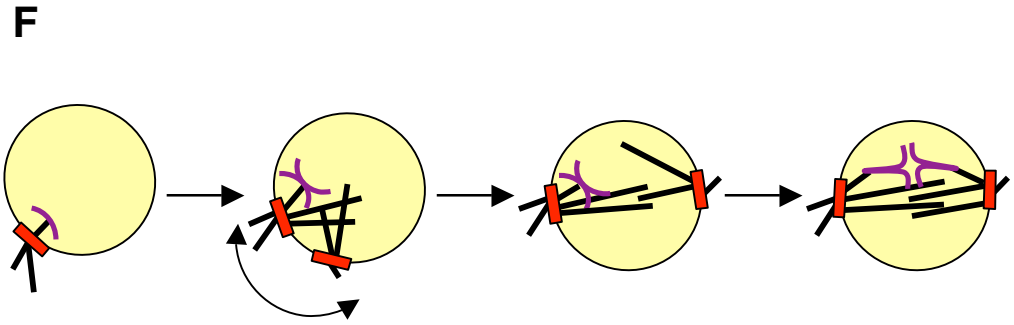
F

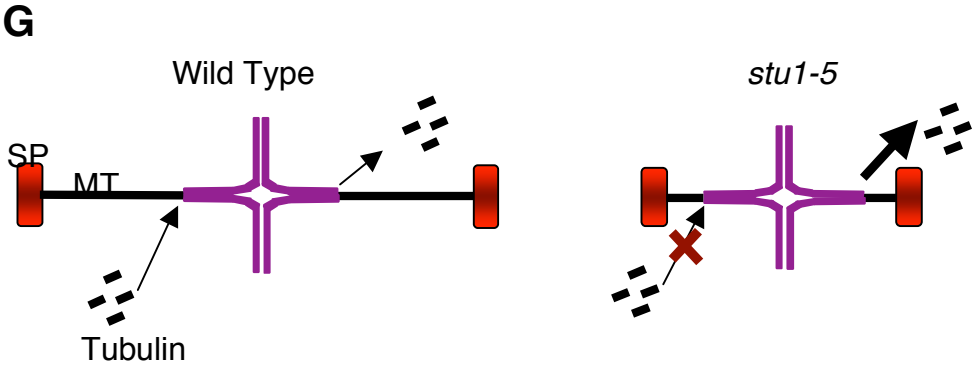
G
Wild Type
stu1-5
SP
MT
Tubulin

initially separate before collapsing in *stu1-5* suggests that the inward force generated by kinetochore-attached microtubules drives collapse.

To test this model, I relieved the inward force by disrupting kinetochore-microtubule attachment with a temperature-sensitive allele of the outer-kinetochore protein Ndc80. When kinetochores cannot maintain attachment in *ndc80-1* (n=10), the spindle poles separate continuously without pausing at two microns, illustrating the need for an inward force to restrict spindle length (Figure 2.4 A and C). In *stu1-5 ndc80-1* mutants (n=9) at the restrictive temperature, spindle pole separation between 1.5 and 5 μm is observed, although this separation is not stable (Figure 2.4 B and D). From this I conclude that Stu1 does contribute an outward force on the spindle by promoting microtubule stability at the kinetochore. It also is clear that Stu1 may have a role at the plus ends of polar microtubules since spindle pole elongation does not mirror that of *ndc80-1* alone.

If the role of Stu1 at kinetochore microtubules is to stabilize or add tubulin subunits, then loss of this activity would favor counteracting proteins that remove subunits or destabilize kinetochore microtubules, leading to shorter microtubules overall. In *Drosophila*, bipolar spindles are restored when Orbit and the kinesin depolymerase Klp10A are co-depleted in cells, illustrating the need to maintain balance between the two activities (Laycock et al., 2006). The yeast kinesin-8 Kip3 and kinesin-14 Kar3 exhibit depolymerase activity (Gupta et al., 2006; Varga et al., 2006; Sproul et al., 2005), while purified Bik1 *in vitro* increases the incidence of catastrophe events (Blake-Hodek, 2009). I deleted each of these microtubule destabilizers in combination with *stu1-5* to test if spindle collapse could be suppressed. Kar3 was not tested as *kar3Δ* is synthetic lethal with *stu1-5* (Liru You, personal

Figure 2.4 Disruption of kinetochore-microtubule attachment restores spindle pole separation. (A and B) *ndc80-1* and *stu1-5 ndc80-1* cells (AHY181, AHY157) were arrested in α-factor for three hours at 26°. Cultures were released from arrest on agarose pads at 37°. Spindle poles (Spc42-GFP) were imaged every 60 seconds. Shown are still frames with time in minutes after release noted. (C and D) Graphs of spindle pole distance measured over time. Lines in red correspond to still images. SPB, Spindle Pole Body

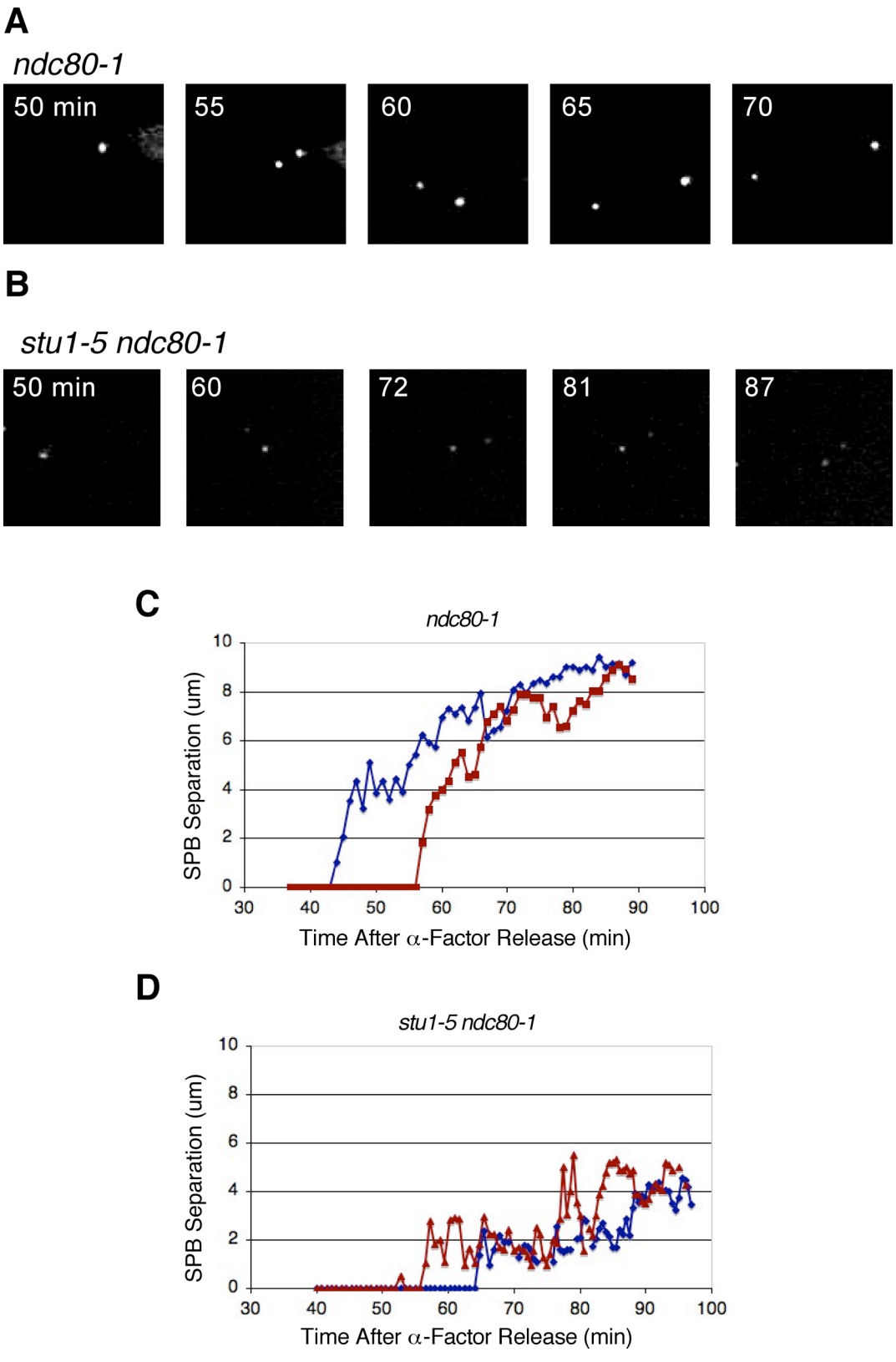
A
ndc80-1
50 min
55
60
65
70
B
stu1-5 ndc80-1
50 min
60
72
81
87
C
ndc80-1
SPB Separation (um)
Time After α-Factor Release (min)
D
stu1-5 ndc80-1
SPB Separation (um)
Time After α-Factor Release (min)

communication). After α-factor arrest and release at the restrictive temperature, SPB separation in *bik1Δ stu1-5* (n=20) and *kip3Δ stu1-5* (n=9) was identical to *stu1-5* alone (Figure 2.5). *kip3Δ* and *bik1Δ* alone were not tested. Interestingly, the long astral microtubules found in *stu1-5* require Bik1, as they are no longer present in *bik1Δ stu1-5* (Figure 2.6). The +TIP Stu2 is also found at the kinetochore and may work in concert with Stu1 to regulate kMT dynamics (He et al., 2001). A *stu2-13 stu1-5* double mutant is not capable of maintaining separation of the SPBs at the restrictive temperature after α-factor release (AHY166; data not shown). Attempts here to identify the counteracting protein to Stu1 stabilization activity were not successful.

Determining the Nature of *stu1-5* Arrest

Cells without Stu1 arrest as large-budded cells with the nucleus positioned at the bud neck. This arrest is dependent on the spindle assembly checkpoint (SAC), as *mad2Δ stu1-5* cells do not arrest, but rather re-bud at the restrictive temperature when the checkpoint is inactivated (data not shown). To test if loss of Stu1 affects stable microtubule-kinetochore attachments, which in turn activates SAC, I observed individual kinetochores in *stu1-5* with the kinetochore protein Mtw1-GFP at the restrictive temperature. After shifting an asynchronous culture to 37° for three hours, Mtw1-GFP staining in the wild-type and *stu1-5* was indistinguishable (Figure 2.7). Kinetochores in wild-type cells localized between spindle poles, with some localizing in a bilobed manner, indicative of establishment of bipolar attachment. Due to spindle collapse in *stu1-5*, many spindle poles are detected as a single foci. Kinetochores co-localize with these foci and are not distributed randomly in the nucleus, indicating they are still attached to microtubules. In cases where

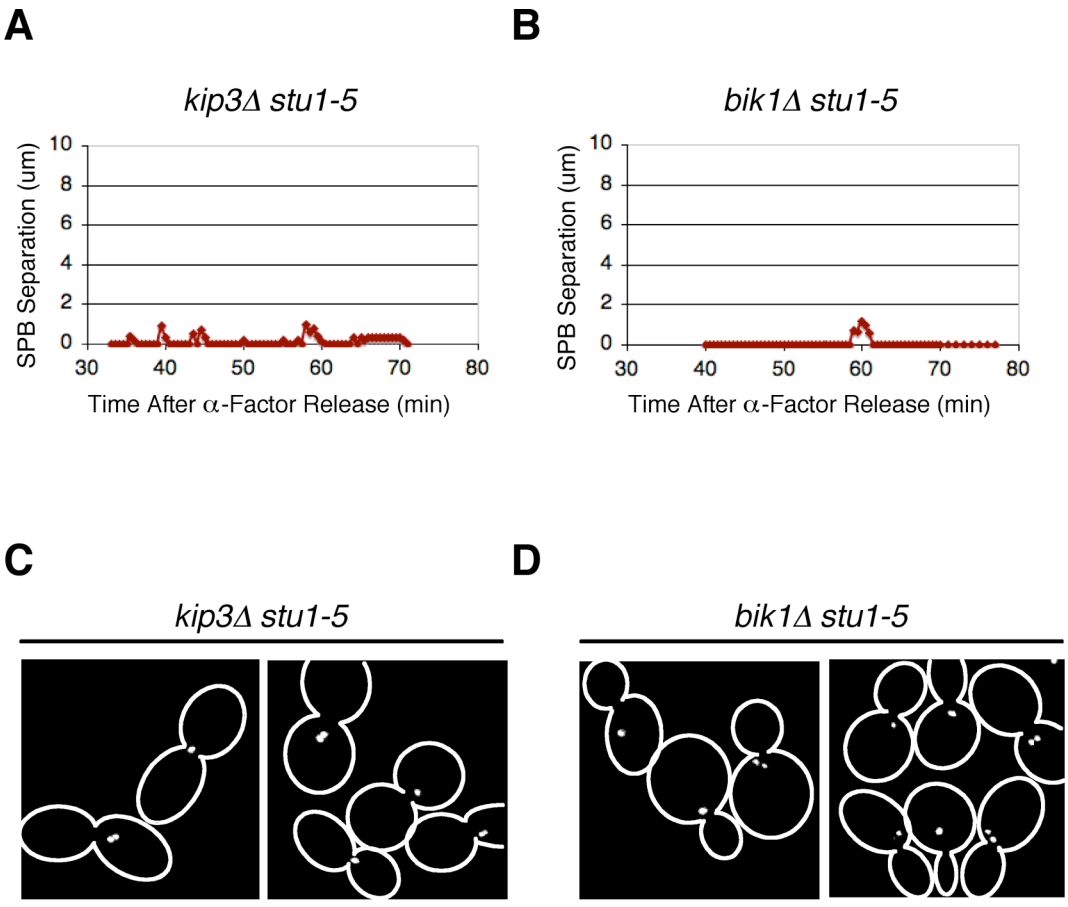

Figure 2.5 Spindle collapse is not suppressed by inactivating microtubule depolymerases. (A and B) Graphs depicting spindle pole body (Spc42-GFP) separation over time in *kip3Δ stu1-5* and *bik1Δ stu1-5* double mutants (AHY164, AHY187) at the restrictive temperature 37° following release from α-factor arrest at 26°. Spindle poles are unable to maintain separation and collapse similar to *stu1-5*. (C and D) Still frames of spindle pole bodies (Spc42-GFP) in *kip3Δ stu1-5* and *bik1Δ stu1-5* double mutants (AHY164, AHY187) after two hours post-α-factor release resemble *stu1-5* alone.

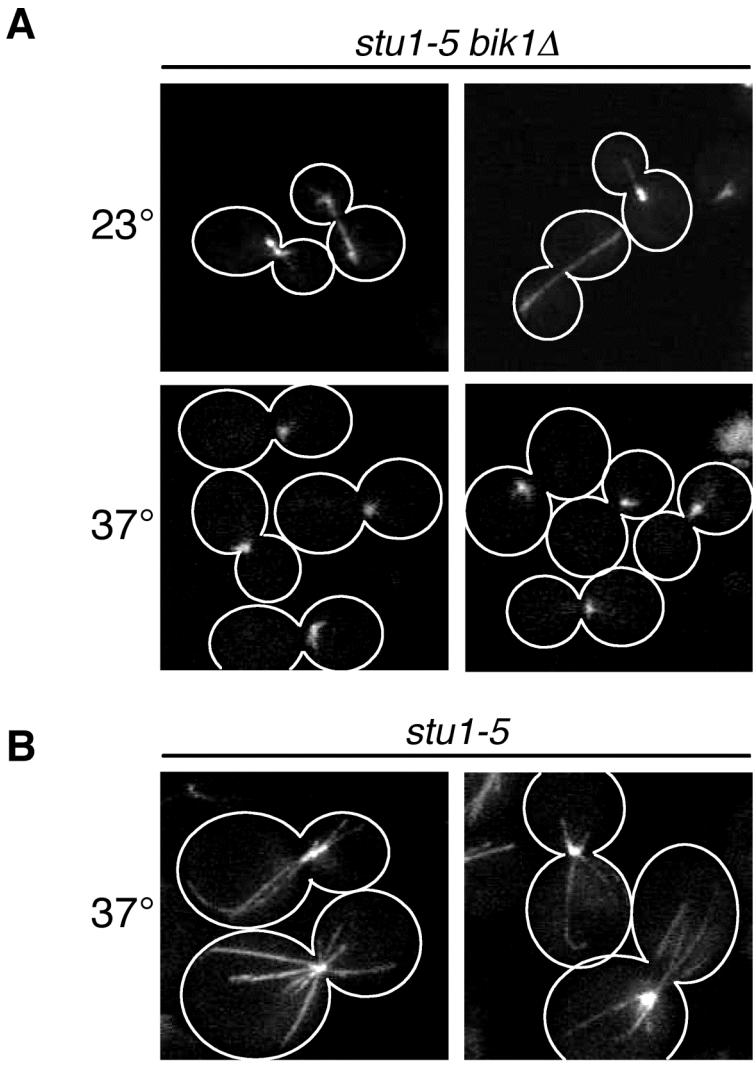

Figure 2.6 Loss of Bik1 affects the long astral microtubules in *stu1-5*. (A) Asynchronous culture of *bikΔ stu1-5* (AHY165) at permissive and restrictive temperature. Microtubules and spindles appear normal at permissive temperature. At the restrictive temperature spindle poles collapse, yet no microtubules extend outward. (B) Typical *stu1-5* phenotype (AHY171) at restrictive temperature with many long astral microtubules.

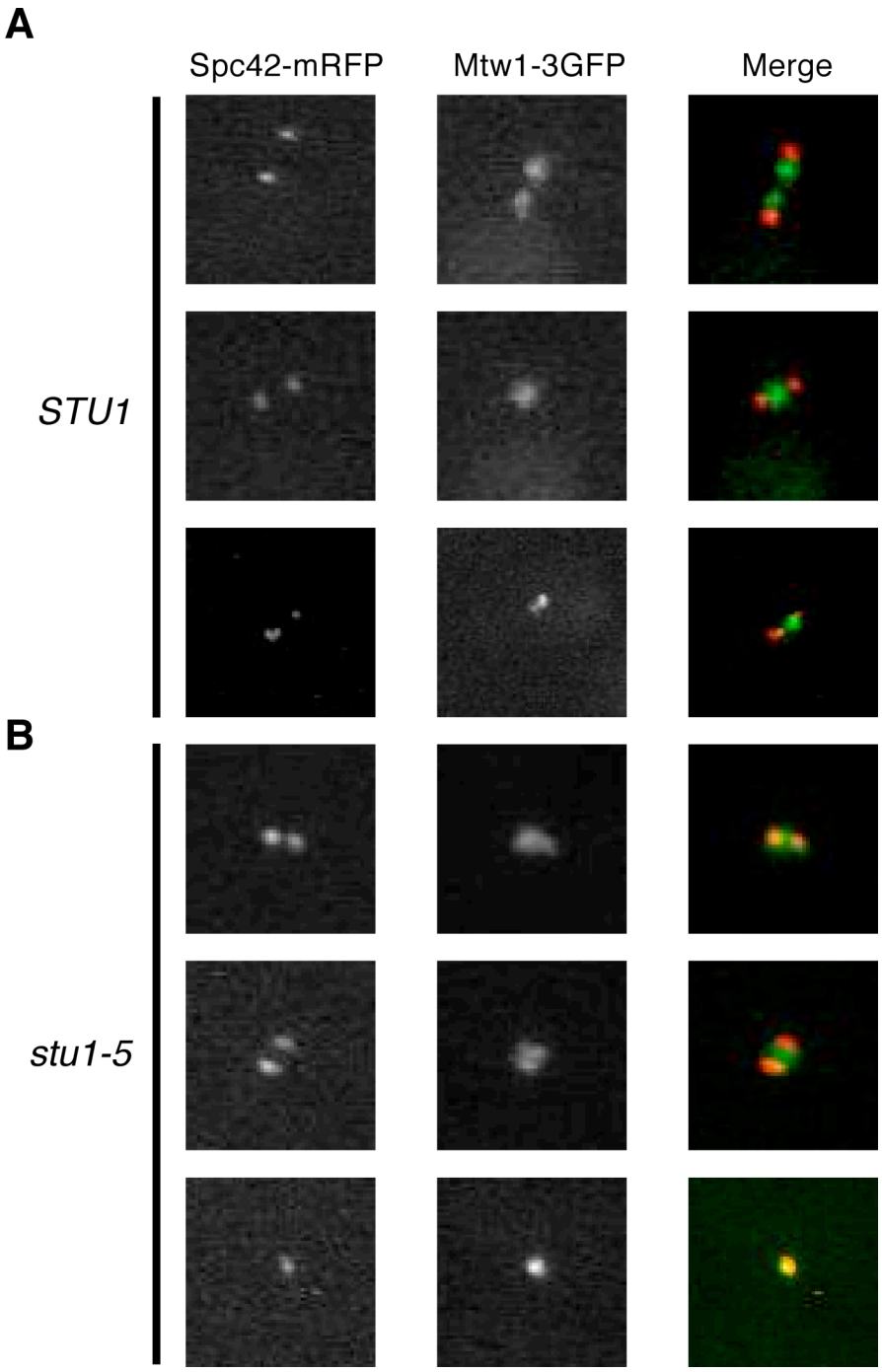

Figure 2.7 Examination of kinetochore attachment in *stu1-5*. Images of kinetochores (Mtw1-GFP, green) in relation to spindle pole bodies (Spc42-mRFP, red) in wild-type (A, CUY1846) and *stu1-5* (B, AHY173) asynchronous cultures after a three hour shift at 37°.

stu1-5 cells demonstrate minimal pole separation, the kinetochores reside mostly between the poles. While more sensitive methods for determining kinetochore attachment may detect more subtle defects, there is no gross defect in kinetochore-microtubule attachment in a Stu1 mutant.

SAC activation can also arise indirectly from lack of tension across the kinetochore microtubules, which is normally generated when each kinetochore of a sister chromatid pair is attached to opposite poles. Lack of tension signals the kinase Ipl1 to phosphorylate outer kinetochore proteins leading to disruption of kinetochore-microtubule attachments, which in turn activates the checkpoint (Pinsky et al., 2006). I introduced a temperature-sensitive allele of Ipl1 to see if arrest in *stu1-5* could be bypassed. The *ipl1-321* allele alone does not produce multi-budded cells (data not shown, Norden et al., 2006). In preliminary experiments, *stu1-5 ipl1-321* cells remain arrested as large-budded cells after five hours at 37° (AHY208, data not shown). It appears that loss of Stu1 does not result in gross defects in kinetochore-microtubule attachments or tension, but attachments may be weak.

DISCUSSION

Dynamic Stu1 localization

Stu1 localization in the absence of microtubules is consistent with that of kinetochores. CLASP protein homologs also bind kinetochores in a microtubule-independent fashion. *S. pombe* Cls1, *Drosophila* Orbit, and both CLASP1 and CLASP2 in HeLa cells localize to the kinetochore when microtubules are absent (Maiato et al., 2003; Mimori-Kiyosue et al., 2006; Pereira et al., 2006, Bratman and Chang, 2007; Lemos et al., 2000) while XOrbit can be co-purfied with kinetochore complexes isolated from *Xenopus*

extracts treated with nocodazole (Emanuele et al., 2005). Other +TIPs, such as *S. cerevisiae* Bik1 (Lin et al., 2001) and *Drosophila* CLIP-190 (Dzhindzhev et al., 2005), can bind the kinetochore independent of microtubules.

The carboxyl terminus of CLASP is sufficient for kinetochore targeting, which is independent of the microtubule-binding domain in the amino terminus (Hannak and Heald, 2006; Maiato et al., 2003; Mimori-Kiyosue et al., 2006). Although the carboxyl terminus also interacts with CLIP-170, which localizes to the kinetochore, CLIP-170 is not required for CLASP localization (Mimori-Kiyosue et al., 2006). It is not known at this point if a similar region of Stu1 is required for kinetochore binding, or if this binding is dependent on Bik1.

It is not currently clear exactly which of the various kinetochore subcomplexes bind CLASP; however, a few individual interactions have emerged from pull-down experiments in several systems. Mass spectroscopy analysis from *Xenopus* extracts identified CENP-E, a kinetochore kinesin (Hannak and Heald, 2006), while HCP1 and HCP2, homologs of CENP-F, are both required for localization of CLASP to kinetochores in worms (Cheeseman et al., 2005). In yeast, Stu1 kinetochore association is still detected by ChIP in a *spc24-9* background, which disrupts the outer kinetochore Ndc80 complex (Ma et al., 2007). An interaction between the outer kinetochore ring complex Dam1 and Stu1 has been identified (Hwang, 2005), yet in an exhaustive step-wise purification of the kinetochore subcomplexes in yeast, Stu1 was curiously not identified (Cheeseman et al., 2002).

In yeast, kinetochore-microtubule attachments are maintained even in G1. Stu1 may associate with kinetochores at this stage as well, even though microtubules are short. Initial localization studies with Stu1-GFP identified distinct foci within the nucleus near the SPB in G1 cells (Yin, 2001). ChIP

analysis could provide additional insights on the conditions for Stu1-kinetochore association. Arrest with α-factor and subsequent release could illustrate the temporal dynamics of Stu1 localization. Importantly, ChIP can assay Stu1 association in specific kinetochore mutants to determine the protein complexes required for binding. Stu1 is only one of several +TIPs that are represented at the kinetochore, but as discussed below, it serves an important function.

As mitosis progresses, Stu1 transitions from the kinetochore to the spindle midzone. CLASP proteins in a variety of organisms also localize to the midzone (Bratman and Chang, 2007; Lemos et al., 2000; Cheeseman et al., 2005; Maiato et al., 2003; Pereira et al., 2006; Inoue et al., 2004). This specific migration is observed in both yeast and mammalian cells for several proteins collectively termed the Chromosomal Passenger proteins. Aurora B (Ipl1 in *S.c.*), Borealin, INCENP (Sli15), Survivin (Bir1), and TD60 form a regulatory complex that acts throughout mitosis and meiosis (Ruchaud et al., 2007). In addition to Ipl1, Sli15, and Bir1 in yeast, the kinetochore proteins Ndc10 and Slk19 also move to the midzone, as well as along the spindle (Bouck and Bloom, 2005). The Stu1 localization change appears to be coordinated with the onset of anaphase, indicating this process is likely to be regulated. Stu1 localization is dependent on dephosphorylation of Ase1 by Cdc14 (Khmelinskii et al., 2007), however Stu1 itself can also be a target for regulation.

I demonstrated evidence to suggest that the recruitment of Stu1 to the midzone by Ase1 is through direct protein-protein interaction. A positive protein interaction between Ase1 homologs and CLASP has been documented for *S. pombe* and mammalian cells (Bratman and Chang, 2007; Liu et al.,

2009). In both systems, the Ase1 carboxyl terminus is sufficient for CLASP binding. The *S. pombe* Cls1 region encompassing amino acids 607-812 is needed for Ase1 binding activity (Bratman and Chang, 2007). When the two yeast CLASP proteins are aligned, this Ase1 binding region corresponds to amino acids 791-996 in Stu1 (Figure 2.2 A). Data presented here varies, as a yeast two-hybrid Stu1 construct that excludes this predicted region yields a positive result. While the specific region may ultimately vary, it is clear that the amino terminus of Stu1 is required for binding similar to CLASP and Cls1 (Bratman and Chang, 2007; Liu et al., 2009).

Stu1 Stabilizes Spindles by Promoting a Kinetochore Outward Force

I propose that Stu1 is essential for maintaining a kinetochore microtubule outward pushing force on spindle poles, similar to what has been found in higher eukaryotes. Normally in wild-type cells, tubulin subunit incorporation at the kinetochore microtubule plus end is in balance with subunit removal. Like CLASP, Stu1 may promote subunit incorporation at the kinetochore microtubule plus end. After Stu1 loss, microtubule-depolymerizing proteins are no longer antagonized, and this leads to ultimate shortening of the microtubule. Spindle poles are “reeled in” as the kinetochore remains attached to the shrinking microtubule. A few lines of evidence support this model. First, spindle poles in *stu1-5* initially separate prior to collapsing. This timing corresponds to the establishment of bipolar kinetochore-microtubule attachments, which would contribute an inward force. A similar temporal phenotype is observed in cells lacking functional CLASP in other species (Bratman and Chang, 2007; Maiato et al., 2005; Reis et al., 2009). Second, disrupting the inward force on spindle poles by preventing microtubule-

kinetochore attachment allows for pole separation. Stu1 appears to also provide an outward force via the polar microtubules. In *stu1-5 ndc80-1*, SPB separation occurs, yet it is unstable and takes significant time to reach distances greater than ~2-4 μm. This is in contrast to the continuous and quick separation observed in *ndc80-1*. The instability suggests that Stu1 may stabilize or promote elongation of the polar microtubules. It is possible that Stu1 stabilizes the microtubules that serve as tracks for kinesin-5 motor protein activity. The precise activity of Stu1 on microtubule ends is not known, but its overall stabilization activity is essential for viability in budding yeast. In plants, CLASP is not detected at kinetochores, which may explain why plant cells with disrupted CLASP are not affected as much as fungal or mammalian species (Ambrose et al., 2007). However, some +TIPs and motors are not found in higher plants, and these may be essential to mediate spindle collapse.

Loss of functional CLASP activates the spindle assembly checkpoint, resulting in arrest and an increased mitotic index. Strong accumulation of the checkpoint proteins Bub1 and BubRI is detected at centromeres in cells without CLASP (Lemos et al., 2000; Maiato et al., 2002). The cell cycle arrest in *stu1-5* is dependent on the spindle assembly checkpoint protein Mad2. Hence, arrest in *stu1-5* cells could potentially arise due to lack of either kinetochore attachment or tension, both of which signal to SAC. Visualizing individual kinetochores with Mtw1-3GFP in *stu1-5* cells suggests that they are not completely unattached at the restrictive temperature. This is predicted by the model for spindle collapse, which relies on maintenance of the kinetochore attachment to pull in the SPBs. There are conflicting results as to the extent CLASP directly or indirectly affects kinetochore attachment (see introduction).

If the kinetochores are attached in *stu1-5* cells, the chances are low they are properly bioriented to satisfy the tension-sensing mechanisms in the cell. Surprisingly, removal of the tension-monitoring kinase Ipl1 did not relieve the *stu1-5* arrest. The mechanism behind the *stu1-5* arrest remains unclear.

Microtubule length and dynamics are influenced by a wide variety of +TIPs and motor proteins, many of which can bind microtubules at the same time. A steady-state balance between antagonistic microtubule stabilizers and destabilizers is important for maintaining microtubule function. In *Xenopus* extracts, depletion of the +TIP XMAP215 results in shorter microtubules nucleated from asters. This phenotype is due to overactivity of the destabilizer XKCM1, as co-depletion of both in extracts restores microtubule aster length (Tournebize et al., 2000). Co-depletion of Klp10A with Orbit restores the balance, as incidences of monopolar spindles and apoptosis are nearly eliminated (Laycock et al., 2006). Based on experiments above, Stu1 may be the major, if not only, +TIP involved in kinetochore microtubule stabilization or growth, despite the presence of other +TIPs at the kinetochore. While the possibility exists that other +TIPs play a role, the absence of none of them results in drastic spindle instability. The shortening kinetochore microtubules in *stu1-5* suggest a scenario where microtubule-destabilizing factors are no longer antagonized. Attempts to deplete yeast kinetochore depolymerases to prevent excess microtubule shrinkage or instability, and therefore restore SPB separation were unsuccessful. It is possible that multiple proteins can function as depolymerases at the kinetochore, meaning rescue will only be observed if all are depleted at the same time. I would expect that any mutant that restores SPB separation could suppress *stu1-5* lethality at 37°. None of the double mutants I tested are viable at 37° (data not shown). Prior non-systematic

second-site suppression screens have not identified genes other than the tubulin genes *TUB1* and *TUB3*. A similar result was observed in *S. pombe*, where deletion of both kinesin-8 proteins did not rescue spindle collapse in a temperature-sensitive *cls1* allele (Bratman and Chang, 2007). As both kinetochore and polar microtubules are affected by *stu1-5,* a single mutation may not be sufficient to rescue cells.

While loss of Bik1 did not affect SPB separation in *stu1-5* cells, it did have an effect on the astral microtubules that normally emanate into the cytoplasm. While *in vitro* data suggests that Bik1 promotes catastrophes, the opposite appears to be true *in vivo* where microtubules are short in a *bik1Δ* background (Blake-Hodek, 2009, Berlin et al., 1990). Here, the double mutant exhibits the same phenotype. Given that the activity of Bik1 appears to differ, it may not be surprising that removing Bik1 did not rescue spindle collapse.

Stu1 Midzone Function During Anaphase

Stu1 may play an important, yet not essential, role in anaphase spindle elongation. Midzone localization depends on proper localization of Ase1, yet an *ase1Δ* strain is viable. In *ase1Δ*, elongating spindles only reach a maximum length of 4 μm versus the 8 μm typical of wild-type cells (Schuyler et al., 2003). This distance can result from the motor proteins Cin8 and Kip1 sliding the ~2 μm ipMTs past each other (Yeh et al., 1995; Kahana et al., 1998). It is tempting to speculate that Stu1 is required for addition of tubulin subunits on polar microtubule plus ends to elongate microtubules. However, many other proteins, particularly other +TIPs such as Bim1 and Bik1, also localize to the midzone in an Ase1 dependent fashion. It is likely that redundant pathways exist to execute the critical function of chromosome

segregation. To dissect the individual role of Stu1 at the midzone, a *stu1*^{Ase1} allele that could no longer bind Ase1 directly, yet still localize to kinetochore, could prove beneficial. Further narrowing of the Ase1-binding domain of Stu1 could provide a target for site-directed mutagenesis. It may be possible to observe anaphase at the restrictive temperature in *stu1-5* cells after first arresting at metaphase at the permissive temperature. This would allow observation of spindles by bypassing the phase of stu1-5-mediated spindle collapse. One observation from the *ndc80-1 stu1-5* strain is that the spindle does not elongate past 5 μm. Interestingly, these cells re-bud, giving an indication that these cells bypass the checkpoint and continue into anaphase. Initial studies to monitor the Pds1 levels in this strain to show that they were in anaphase were inconclusive, but bear repeating. The localization of Ase1, which normally appears at the midzone only after anaphase onset, would also indicate if the cells were in anaphase, and if the major midzone protein could still localize properly. It would be beneficial if this strain is in anaphase, yet cannot extend the spindle to give insight into Stu1's role at the midzone.

Anaphase defects in other systems lacking CLASP have been observed. Spindles assembled in *Xenopus* extracts depleted of XOrbit rapidly disassemble upon entry into anaphase (Hannak and Heald, 2006). In *Drosophila* primary spermatocytes, interior microtubules in the spindle breakdown after entry into anaphase and consequently, lead to defects in effective cleavage furrow ingression during cytokinesis (Inoue et al., 2004). The stability of the midzone in *S. pombe* is maintained by Cls1 (Bratman and Chang, 2007).

CHAPTER THREE

Synthetic Genetic Array (SGA) Analysis for *stu1-5* and *stu1-8*

INTRODUCTION

The budding yeast *Saccharomyces cerevisiae* is a powerful model organism for dissecting eukaryotic cell processes. The genetically tractable system provides a significant advantage for investigators, with the ability to carry out genetic screens as a means to identify genes involved in various cellular pathways. Use of mutagenesis screens, overexpression studies, and suppressor screens has been invaluable not only in identification of genes in a wide range of essential processes, but also in providing insights as to how these processes interact with each other (Boone et al., 2007).

Geneticists identified instances where two independent genes each on its own is viable when deleted or mutated, but the combination results in inviability. This interaction is termed synthetic lethality, and is a genetic tool used in many organisms to show a functional link between genes (Guarente, 1993). This is not surprising, as a large number of eukaryotic genes can be individually compromised, yet not have a drastic enough phenotype to affect viability. For example, nearly 5,000 of the estimated 6,000 genes in budding yeast are non-essential, which implies built-in redundancy in biological systems (Hartman et al., 2001). Synthetic-lethal relationships can arise when gene products are involved in parallel or redundant pathways for an essential cellular function. It is also possible that two genetically interacting genes act in the same pathway if both mutations compromise a pathway below a functional threshold. Genetic screens looking for genes that are synthetic lethal with a

given starting gene have proven effective, particularly in budding yeast, yielding clues for gene products that act in similar pathways (Boone et al., 2007; Bender and Pringle, 1991). Synthetic-lethal screens have been instrumental in identifying genetic relationships in the areas of DNA repair (Pan et al., 2006), cell polarity (Bender and Pringle, 1991), the cytoskeleton (Holtzman et al., 1993), and chromosome segregation (Montpetit et al., 2005), to name a few.

Prior synthetic-lethal screens in yeast relied on random mutagenesis, which does not ensure complete genomic coverage. The completion of the yeast genome sequence, as well as an available collection of non-essential gene deletions, has made it possible to systematically screen for genetic interactions. Synthetic genetic array (SGA) analysis individually tests all non-essential genes in combination with a given gene deletion or conditional allele relatively quickly and effectively. An additional benefit of testing each double-mutant combination individually is the elimination of having to clone candidate genes.

Spindle formation requires a major rearrangement of microtubules by motor and non-motor proteins. As described in the previous chapter, the microtubule-associated protein Stu1 is important for spindle integrity, providing an outward spindle force by stabilizing kinetochore and polar microtubule ends. To further understand the forces acting on spindles, we set out to identify proteins that interact genetically with Stu1.

MATERIALS AND METHODS

Synthetic Genetic Array (SGA) was performed by the Boone lab (U. of Toronto) as described previously (Tong et al., 2001; Tong and Boone, 2006).

Briefly, the temperature-sensitive strain CUY1977 (MATα stu1-5::NatR can1Δ::STE2pr-Sp_HIS5 lyp1Δ::STE3pr-LEU2 his3Δ1 leu2Δ0 ura3Δ0) or CUY1978 (MATα stu1-8::NatR can1Δ::STE2pr-Sp_HIS5 lyp1Δ::STE3pr-LEU2 his3Δ1 leu2Δ0 ura3Δ0) was crossed to ~4700 nonessential gene deletion strains. The resulting double mutants were sporulated and plated on media to select for haploid cells. Double mutants were selected and screened for viability in triplicate at 26° and 30° for *stu1-5* and 30° and 35° for *stu1-8*. Candidates were determined by comparing the colony size between the single and double mutant. Select genes were verified by manual tetrad dissection at 26°, 30°, 33°, 35°, and 37°.

RESULTS

To identify genes involved in spindle stability, we carried out a SGA screen in collaboration with Dr. Charlie Boone, looking for gene deletions that are lethal in combination with the temperature-sensitive *stu1-5* allele. Candidate genes were identified by comparing the colony size of the individual single mutants with that of the double mutant at the permissive temperatures 26° and 30°. Using this metric, we singled out both synthetic-lethal and synthetic-sick interactions. The screen was done in triplicate to ensure reproducibility. At 26°, 130 unique open reading frames (ORFs) showed decreased cell growth or death when in combination with *stu1-5*. At 30°, 152 ORFs demonstrate a genetic interaction, with 87 of those ORFs also identified at 26°. Many of the genes are involved in a relatively small number of processes including tubulin folding, dynein/dynactin activity, microtubule and spindle function, spindle checkpoint activity, kinetochore structure, chromosome cohesion, and nuclear transport (Table 3.1).

Table 3.1 Major classes of select genes identified through SGA with *stu1-5* and *stu1-8*

Open Reading Frame	Gene Name	Function	*stu1-5* *stu1-8*
Tubulin Folding			
YOR349W	CIN1	Tubulin folding factor D	*1-5/1-8*
YPL241C	CIN2	Tubulin folding factor C	*1-5/1-8*
YMR138W	CIN4	Tubulin folding	*1-8*
YNL153C	GIM3	Prefoldin complex subunit	*1-5/1-8*
YEL003W	GIM4	Prefoldin complex subunit	*1-5/1-8*
YML094W	GIM5	Prefoldin complex subunit	*1-5*
YER007W	PAC2	Tubulin folding factor E	*1-5/1-8*
YGR078C	PAC10	Prefoldin complex subunit	*1-5/1-8*
YDR183W	PLP1	CCT interactor	*1-8*
YLR200W	YKE2	Prefoldin complex subunit	*1-5/1-8*
Dynein/Dynactin			
YHR129C	ARP1	Dynactin complex	*1-5/1-8*
YKR054C	DYN1	Dynein heavy chain	*1-5/1-8*
YDR424C	DYN2	Dynein light chain	*1-5/1-8*
YMR299C	DYN3	Dynein light intermediate chain	*1-5/1-8*
YMR294W	JNM1	Dynactin complex/p50 dynamitin	*1-5/1-8*
YPL174C	NIP100	Dynactin complex/p150^{glued}	*1-5/1-8*
YDR150W	NUM1	Mediates dynein-cortex interaction	*1-8*
YOR269W	PAC1	Nuclear migration/targets dynein	*1-5/1-8*
YDR488C	PAC11	Dynein intermediate chain	*1-5/1-8*
Microtubule and Spindle Function			
YOR058C	ASE1	Spindle midzone establishment	*1-5/1-8*
YER016W	BIM1	Microtubule associated protein	*1-5/1-8*
YMR198W	CIK1	Kar3 binding partner	*1-8*
YPR141C	KAR3	Kinesin	*1-8*
YPL269W	KAR9	Spindle positioning	*1-5/1-8*
YGL216W	KIP3	Kinesin, spindle positioning	*1-5/1-8*
YML124C	TUB3	Alpha-tubulin subunit	*1-5/1-8*
YPL253C	VIK1	Kar3 binding partner	*1-5/1-8*

Table 3.1 (continued)

Open Reading Frame	Gene Name	Function	*stu1-5* *stu1-8*
Spindle-Assembly Checkpoint Activity			
YGR188C	BUB1	Kinase, Checkpoint complex	*1-5*
YOR026W	BUB3	Kinetochore Protein in metaphase	*1-5/1-8*
YGL086W	MAD1	Checkpoint complex	*1-5/1-8*
YJL030W	MAD2	Checkpoint complex	*1-5/1-8*
YJL013C	MAD3	Checkpoint complex	*1-5/1-8*
Kinetochore Structure			
YDR254W	CHL4	Outer kinetochore	*1-5/1-8*
YLR381W	CTF3	Outer kinetochore	*1-5/1-8*
YPL018W	CTF19	COMA complex	*1-5/1-8*
YBR107C	IML3	Outer kinetochore	*1-5*
YPR046W	MCM16	Inner kinetochore	*1-8*
YDR318W	MCM21	COMA complex	*1-5/1-8*
YJR135C	MCM22	Inner kinetochore	*1-5/1-8*
Chromosome Cohesion			
YPL008W	CHL1	DNA helicase	*1-5/1-8*
YPR135W	CTF4	Binds DNA polα	*1-8*
YHR191C	CTF8	Binds Replication Factor C	*1-5/1-8*
YMR078C	CTF18	Binds Replication Factor C	*1-5/1-8*
YMR048W	CSM3	DNA repair	*1-8*
YCL016C	DCC1	Binds Replication Factor C/telomere	*1-5/1-8*
Nuclear Transport			
YBR194W	AIM4	Nuclear pore complex	*1-5*
YIL040W	APQ12	mRNA nucleocytoplasmic transport	*1-5/1-8*
YJR074W	MOG1	Stimulates Ran GSP1 GTP release	*1-5*
YDR432W	NPL3	mRNA nucleocytoplasmic transport	*1-5*
YBL079W	NUP170	Nuclear pore complex	*1-5*
YML103C	NUP188	Nuclear pore complex	*1-5/1-8*
YDR159W	SAC3	mRNA nucleocytoplasmic transport	*1-5/1-8*
YNL253W	TEX1	mRNA nucleocytoplasmic transport	*1-5*

Table 3.1 (Continued)

Open Reading Frame	Gene Name	Function	*stu1-5* *stu1-8*
Regulation Pathways			
YER167W	BCK2	Involved in Protein kinase C signaling	*1-5*
YNL298W	CLA4	Kinase, involved in cytokinesis	*1-5/1-8*
YLR210W	CLB4	Cyclin G2/M transition, activates CDC28	*1-5/1-8*
YPL256C	CLN2	Cyclin G1/S transition	*1-8*
YNL307C	MCK1	Homology to GSK-3 kinase	*1-8*
YPL152W	RRD2	Activator of Phosphatase 2A	*1-8*
YOR014W	RTS1	Phosphatase 2A subunit	*1-5/1-8*
Miscellaneous			
YER177W	BMH1	14-3-3, Pull down Stu1 in screen[1]	*1-8*
YCR047C	BUD23	Bud site selection	*1-5*
YGL173C	KEM1	Exonuclease, known Stu1 SL interactor	*1-5*
YLL049W	LDB18	Low Dye Binding, unknown function	*1-5/1-8*
YBR095C	RXT2	Cellular fusion, SL with Bim1	*1-5*

1- Ho et al., 2002

As this was a high-throughput genomic screen, I verified the SGA results of select candidates using manual tetrad dissection over a range of temperatures (Figure 3.1). Loss of genes involved in cell cycle transitions (*CLA4, CLB4*) and nuclear pore composition (*NUP170, NUP188*) did not result in slow growth or death with *stu1-5* at any temperature tested. Most double-mutants tested were dead at 33°, slightly higher than the temperature tested in the initial screen. Two genes that demonstrated the strongest phenotype were *BUB3 and CTF18*, whose double-mutant strains were dead at 26°. The ORF which scored as having the highest probability of a genetic interaction, as determined by t-test analysis by the Boone lab, was *LDB18*, a gene with no known function. When tested individually, *ldb18Δ* was synthetic-sick with *stu1-5* at 26° and 30°, and synthetic-lethal at 33° (Figure 3.2).

For comparison, an additional SGA analysis was conducted using *stu1-8* at 30° and 35°. This screen at 30° yielded 134 hits, while 202 genes were identified at 35°. When compared to results from *stu1-5*, 94 of the genes overlapped between the two independent screens and belonged mostly to the groups enriched and identified above.

DISCUSSION

Synthetic Genetic Array with Temperature-Sensitive *stu1* Alleles

Genes involved in various cellular processes have a genetic interaction with *stu1* temperature-sensitive alleles (*stu1^{ts}*). Genes previously isolated in an earlier nonsystematic synthetic-lethal analysis with *stu1-5* (*PAC10, GIM3, and KEM1*) (Brew and Huffaker, 2002) emerged in this SGA, demonstrating the effectiveness of identification of *stu1-5* synthetic-lethal interactions. A higher number of genes was found through the *stu1-8* screen, most likely a

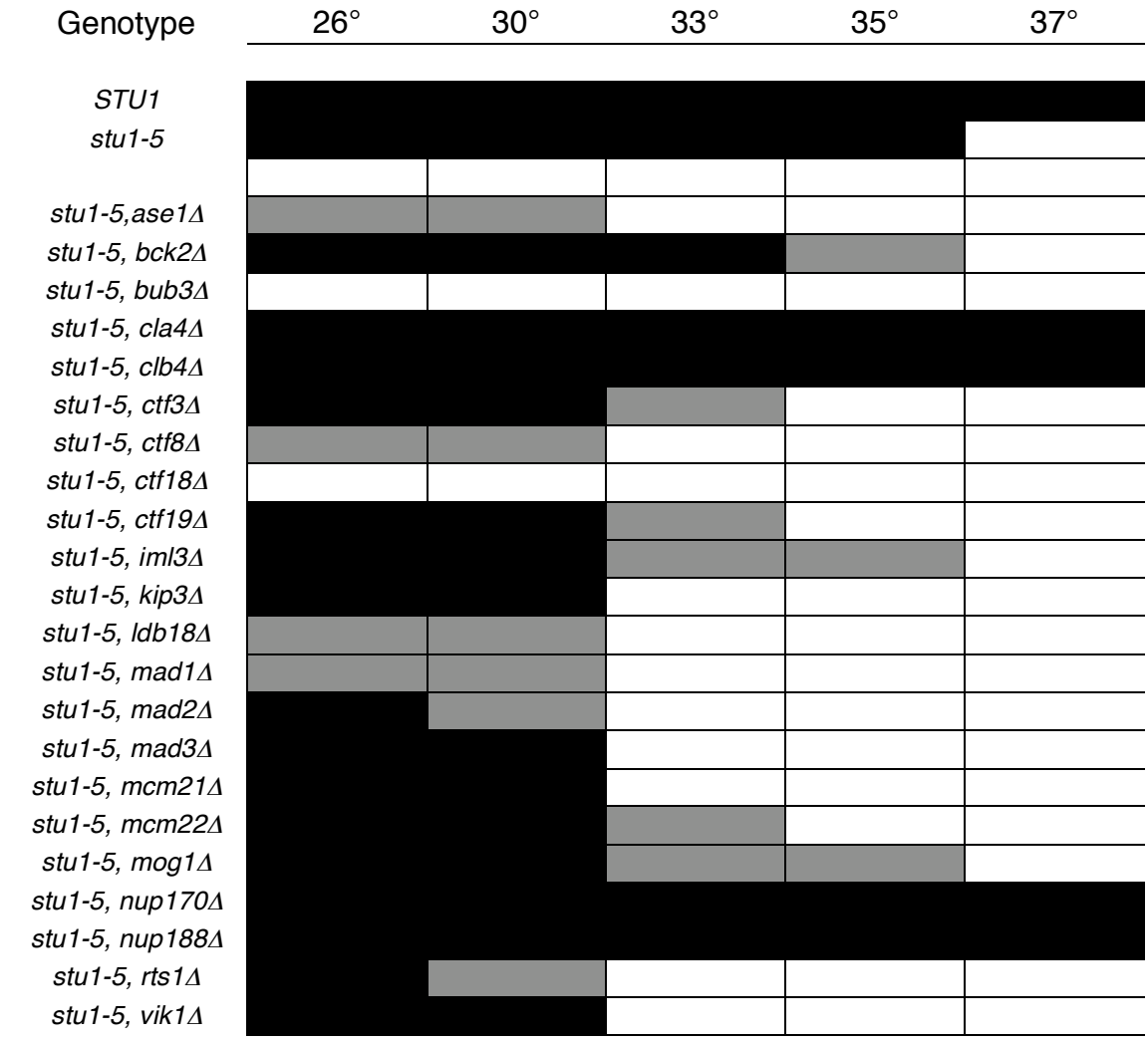

	Normal growth
	Slow growth (Synthetic-sick)
	No growth (Synthetic-lethal)

Figure 3.1 Manual Dissection of *stu1-5* SGA candidates. Individual double mutant spores isolated by tetrad dissection were incubated at a range of temperatures to verify SGA results.

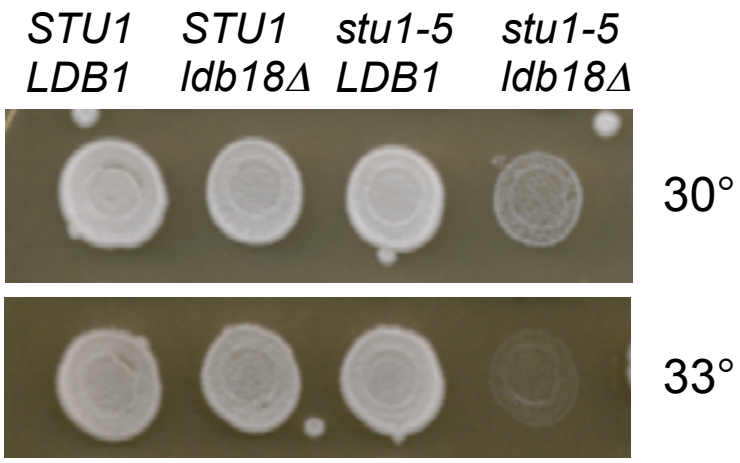

Figure 3.2 Ldb18 demonstrates a genetic relationship with Stu1. Shown are spores from a single tetrad on YPD. Genotypes of individual spores are indicated. Loss of Ldb18, a gene with a previously unknown function, is synthetic-sick with *stu1-5* at 30°, and synthetic-lethal at 33°. Single mutant spores do not have growth defects at the indicated temperatures.

result of the screen being conducted at higher temperatures compared to *stu1-5*. Already at the permissive temperature of 26°, the Stu1 protein levels in a *stu1-5* strain are reduced 3-fold compared to wild type. As the temperature increases to 33°, Stu1 protein is reduced 5-fold, although the strain is still viable (Brew and Huffaker, 2002). Spindle length likewise is shorter at 26° compared to wild type and progressively worsens as the temperature increases (Yin, 2001). It is possible that *stu1-8* similarly affects protein levels and spindle length, and this compromised function of the single mutant at higher semi-permissive temperatures makes it easier to identify double mutants that affect viability.

In comparing the two screens directly, a high degree of overlap exists, especially among genes identified with a high degree of confidence or in groups likely to be involved with microtubules or in microtubule-dependent processes. These genes likely have true genetic interactions with $stu1^{ts}$. The overlap may be due to both *stu1-5* and *stu1-8* containing mutations in the amino terminus of the protein. It would be interesting to compare SGA results from an allele with mutations in a different region of the protein.

Not all of the candidate genes individually tested by tetrad dissection were verified. With the amount of data generated from this and many other genomic screens, the need to have methods to identify relevant results is becoming apparent. Recently, labs have been combining data from multiple screens relating to a query gene to find interactions that are likely to be informative and correct. For example, synthetic-lethal screens are integrated with reciprocal synthetic-lethal screens, protein level studies, transcriptional analysis, phenotypic screens, large-scale mass spectrometry, and yeast two-

hybrid analysis to statistically determine functional groups (Schoner et al., 2008; Leidel et al., 2009).

Analysis of Individual Functional Groups from SGA

Many of the genes identified as having a high probability of interaction with *stu1*^{ts} can be grouped in specific cellular processes. One group includes genes involved in formation of stable tubulin heterodimers (reviewed in (Lopez-Fanarraga et al., 2001). Nascent α- and β-tubulin polypeptides first encounter proteins in the Prefoldin/GimC complex, which serves to escort the polypeptide to the chaperonin containing TCP-1 (CCT). Subsequently, additional cofactors bind each individual tubulin subunit (Cofactors A and D bind β-tubulin; Cofactors B and E bind α-tubulin) resulting in heterodimer formation following GTP hydrolysis of β-tubulin (Tian et al., 1996; Tian et al., 1999). Genes involved at each of these steps were identified in the SGA. Abnormalities in tubulin folding are believed to alter cellular tubulin concentrations, which in turn affect microtubule polymerization rates (Hoyt et al., 1990). Altered dynamics could adversely affect microtubule-dependent processes when combined with the effects of *stu1-5*. Tubulin-folding genes in yeast were largely first identified through screens looking at chromosome loss or microtubule drug sensitivity (Hoyt et al., 1990; Hoyt et al., 1997). The CCT is also the chaperone for actin and other proteins, particularly those involved in cell cycle progression (Cdc20, Polo kinase, Cdh1, cyclins) (reviewed in Brackley and Grantham, 2009). This could lead to lethality with *stu1-5* through a secondary mechanism.

Genes involved in nuclear migration were identified in this screen, particularly many of the dynein and dynactin components. In the last chapter,

I discussed a role for Stu1 in providing an outward force on spindle pole body (SPB) separation in early spindle formation and possibly in anaphase. Dynein/dynactin exerts force on astral microtubules at the cell cortex to pull the daughter-bound SPB through the mother-bud neck. Assuming the mother-bound SPB is somehow tethered in the mother cell, dynein/dynactin activity could also provide a SPB-separating activity. Previous evidence indicates that dynein plays a role in SPB separation. First, deletions of a number of genes encoding dynein/dynactin proteins (*dynΔ*, *jnm1Δ*, and *nip100Δ*) are synthetic lethal with loss of Cin8, a kinesin-5 protein that is also required for SPB separation (Geiser et al., 1997; Tong et al., 2001). In addition, anaphase SPB separation depends on both Cin8 and Dyn1 (Saunders et al., 1995). Thus, the synthetic lethality between *stu1-5* and loss of dynein activity is possibly due to their overlapping roles in SPB separation.

It is not surprising to identify genes involved in microtubule function. These motor and non-motor proteins act both on microtubule dynamics and organization. These genes likely genetically interact with Stu1 because they are in similar pathways with redundant function or within a singular pathway.

In the preceding chapter, I identified a critical role for Stu1 at the kinetochore. While microtubule attachment is mediated by the outer kinetochore components, proteins located throughout the kinetochore structure were identified in the SGA. Similar to kinetochore mutants, cells without CLASP in mammalian cells exhibit lagging chromosomes that are unable to congress at the metaphase plate (Maiato et al., 2003), hence these proteins could be involved in an overlapping function that contributes to a synthetic-lethal phenotype. It is not clear if Stu1 is involved in attachment, although if it is, it is likely minor. The spindle assembly checkpoint proteins also localize to

the kinetochore. Stu1 interacts with the checkpoint proteins Mad1 and Mad3 in yeast two-hybrid analysis (Hwang, 2005), but a role for Stu1 in the spindle assembly checkpoint has not come to light.

Sister chromatids are tethered together by the cohesin protein complex until the onset of anaphase when proteases are activated to degrade cohesin to allow chromosome segregation. While a number of essential genes prevent premature chromatid separation, a number of non-essential genes also contribute to cohesion. Many of these genes were originally identified in screens scoring for chromosome loss (Spencer et al., 1990), and can genetically be grouped in one of two seemingly parallel pathways: one involving Ctf8, Ctf18, Mrc1, and Dcc1 and another involving Csm1, Tof1, Ctf4, and Chl1 (Mayer et al., 2001; Mayer et al., 2004; Xu et al., 2007). These genes contribute to cohesin function, yet are primarily involved in DNA replication, DNA repair, and telomere maintenance. Many of these non-essential genes were identified in the Stu1 SGA, with Ctf18 showing a tight synthetic-lethal phenotype at 26° when individually tested. Reduction of cohesion results in less tension across the kinetochore microtubule, which may trigger a cell cycle arrest when in combination with *stu1-5*.

One group to emerge from the screen includes components of the nuclear pore complex (NPC). Yeast undergo a closed mitosis where the nuclear envelope does not break down as it does in higher eukaryotes. Recent studies suggest a connection between the nuclear pore and kinetochore proteins. Mutations in Nup170 lead to chromosome segregation defects and possible defects in kinetochore structure, yet Nup170 itself is not a kinetochore protein (Kerscher et al., 2001). Nup170 specifically binds checkpoint proteins Mad1 and Mad2 throughout the cell cycle, with a small

subset redistributing to kinetochores until the checkpoint is satisfied (Iouk et al., 2002). Not only are kinetochore proteins found at the NPC, but in human cells, subcomplexes of the NPC can be found at kinetochore shortly after nuclear envelope breakdown (Belgareh et al., 2001). *S. pombe* also has nuclear envelope genes that when deleted or mutated lead to chromosome or even microtubule defects (Pardo and Nurse, 2005; Tange et al., 2002). While the connection to kinetochores is intriguing, the genetic interactions with Nup170 and Nup188, another NPC protein, were not verified when individually tested with *stu1-5*. Proteins involved in mRNA transport across the membrane were identified in the SGA. Apq12, a mRNA transport protein, was identified in SGA screens with temperature-sensitive alleles of outer kinetochore proteins and found to cause a delay in anaphase, premature entry into the next cell cycle, and resistance to benomyl (Montpetit et al., 2005). The transport protein Sac3 was identified in a screen looking for suppressors of cold-sensitive actin alleles, and SGA analysis using Sac1 as a query gene identified several inner kinetochore proteins (Novick et al., 1989; Measday et al., 2005). It is possible these genetic interactions are indirect, as defects in translocation of mRNA and protein through the nuclear envelope affect cell cycle and checkpoint proteins known to make such translocations.

Stu1 localization transitions from the kinetochore in metaphase to the spindle midzone in anaphase. This movement is likely highly regulated to correspond with cell cycle progression cues. CLASP localization itself is influenced by GSK3β and Rac1 in the leading edge of migrating cells (Wittmann and Waterman-Storer, 2005; Watanabe et al., 2009). I identified various signaling proteins in the SGA, including a homolog of the GSK3 kinase, which may regulate Stu1 localization or activity. Rts1 is a regulatory

subunit of the protein phosphatase 2A (PP2A). Rts1-PP2A has a role in the spindle position checkpoint by regulating the localization of the kinase Kin4, which in turn influences mitotic exit (Chan and Amon, 2009). Loss of Rts1 affects the mitotic exit checkpoint, and this in combination with diminished spindles in *stu1* temperature-sensitive alleles could lead to diminished cell growth. Additional candidates identified in the SGA were Clb4, a B-type cyclin involved at the G2/M transition and in the asymmetric SPB localization of Kar9 (Grava et al., 2006), and Cla4, a kinase involved in cytokinesis. Neither of these genes could be confirmed to be synthetic-lethal with *stu1-5*. Bck2 is an activator of cell cycle dependent genes (Ferrezuelo et al., 2009), but the double mutant only manifested a synthetic-sick phenotype at higher temperatures.

Both screens yielded unidentified ORFs, some of which are designated as dubious because they are unlikely to produce functional protein (data not shown). Many of these dubious ORFs can be explained by the fact that they overlap with genes from the opposite strand that were also hit in the screen. One ORF with unknown function, Ldb18, was found in both screens and verified by manual tetrad dissection. Further investigation of this gene is explored in the subsequent chapter.

CHAPTER FOUR

Ldb18, the *S. cerevisiae* Homolog of p24, Is Essential for Maintaining the Association of p150^{Glued} With the Dynactin Complex

INTRODUCTION

The relatively uncharacterized gene Ldb18 was found through SGA analysis to be synthetic lethal with both *stu1-5* and *stu1-8*. Ldb18 was originally identified in a screen for mutants with defective oligosaccharide modifications on cell wall proteins. The cationic dye alcian blue, which binds negative charges on the cell wall primarily from the mannosyl phosphate groups found on oligosaccharides, was used to screen the non-essential gene deletion collection. Any disruptions in the oligosaccharide modification process result in a low dye binding, or Ldb, phenotype (Corbacho et al., 2005). Additionally, *ldb18Δ* had previously been shown to be synthetic lethal with a variety of genes involved in spindle elongation, nuclear migration, and tubulin folding (Tong et al., 2001; Ye et al., 2005). Based on the genetic data, I further investigated whether Ldb18 has a role in microtubule or spindle function.

MATERIALS AND METHODS

Yeast strains and sequence analysis: The yeast strains and plasmids used in this study are listed in Table 4.1 and Table 4.2. Yeast strains were grown in standard media (Sherman, 1991). Gene deletion strains were obtained from the Genomic Deletion Collection (Winzeler et al., 1999).

Table 4.1 Yeast Strains

Strain	Genotype
AHY191	*MATa, ura3Δ0, leu2Δ0, his3Δ1, met15Δ0 uba4Δ::KanMX Ldb18-13Myc::HIS5*
BY4741	*MATa, ura3Δ0, leu2Δ0, his3Δ1, met15Δ0*
CUY26	*MATα, his3Δ200, leu2-3,112, ura3-52*
CUY1816	*MATa, ura3Δ0, leu2Δ0, his3Δ1, met15Δ0, ldb18Δ::KanMX*
CUY1823	*MATa, ura3Δ0, leu2Δ0, his3Δ1, met15Δ0, dyn1Δ::KanMX*
CUY1928	*MATa, ura3Δ0, leu2Δ0, his3Δ1, met15Δ0, GFP-TUB1::LEU2*
CUY1929	*MATa, ura3Δ0, leu2Δ0, his3Δ1, met15Δ0, ldb18Δ::KanMX, GFP-TUB1::LEU2*
CUY1930	*MATa, ura3Δ0, leu2Δ0, his3Δ1, met15Δ0, dyn1Δ::KanMX, GFP-TUB1::LEU2*
CUY1931	*MATα, his3Δ1, leu2Δ0, ura3Δ0, met15Δ0, lys1Δ, can1Δ::STRpr-SPHIS5, Ldb18-3GFP::URA3, Spc42-mRFP:KanMX*
CUY1932	*MATα, his3Δ200, leu2-3,112, ura3-52, LDB18-13Myc::HIS5*
CUY1933	*MATα, his3Δ200, leu2Δ, ura3-52 ade2Δ, LDB18-13Myc::HIS5, NIP100-3HA::KanMX*
CUY1934	*MATα, his3Δ200, leu2Δ, ura3-52, ade2Δ, ade3Δ, lys2-801, LDB18-13Myc::HIS5, ARP10-3HA::KanMX*
CUY1935	*MATa, ura3, leu2, his3, ade2Δ, ade3Δ, JNM1-3HA::KanMX, ARP1-13Myc::KanMX, ldb18Δ::HIS5*
CUY1935	*MATa, ura3, leu2, his3, ade2Δ, lys2-801, met15Δ0, JNM1-3HA::KanMX, ARP1-13Myc::KanMX*

Table 4.1 (Continued)

Strain	Genotype
CUY1936	*MATa, ura3, leu2, his3, ade2Δ, met15Δ0, JNM1-3HA::KanMX, NIP100-13Myc::KanMX, ldb18Δ::HIS5*
CUY1994	*MATa, ura3Δ0, leu2Δ0, his3Δ1, met15Δ0 urm1Δ::KanMX*
CUY1995	*MATa, ura3Δ0, leu2Δ0, his3Δ1, met15Δ0 uba4Δ::KanMX*
CUY2005	*MATa, ura3Δ0, leu2Δ0, his3Δ1, met15Δ0 elp2Δ::KanMX*

Table 4.2 Plasmids

Plasmid	Markers
pAH34	*ampR, 2μ, TRP1 P_{ADH}-Gal4BD-Ldb18*
pAH35	*ampR, 2μ, LEU2 P_{ADH}-Gal4AD-Ldb18*
pAH44	*ampR, HIS3, Ldb18 (C-term)-13Myc*
pAH49	*KanR, GST-Ldb18*
pAH50	*ampR, 2μ, LEU2 P_{ADH}-GAL4AD-Nip100*
pAH51	*ampR, 2μ, LEU2 P_{ADH}-GAL4AD-Nip100 400-600*
pALM79	*ampR, URA3, Ldb18(C-term)-3GFP*
MR4187	*ampR, 2μ, LEU2 P_{ADH}-GAL4AD-Arp1*
MR4212	*ampR, 2μ, LEU2 P_{ADH}-GAL4AD-Jnm1*
MR5393	*ampR, 2μ, LEU2 P_{ADH}-GAL4AD-Arp10*

Epitope-tagging of Ldb18 was accomplished by integrating plasmids pAH44 and pALM79 into wild-type strains; pAH44 and pALM79 contain a C-terminal segment of Ldb18 fused to 13Myc and 3GFP, respectively. Epitope-tagged versions of Ldb18 were deemed functional because they did not increase the percentage of binucleate cells and were not synthetic lethal with *kar9Δ*. Strains containing epitope-tagged versions of Nip100, Jnm1, and Arp100 (MY8895, MY8896, MY8912, MY8913, MY8938) were provided by Mark Rose (Princeton, NJ). A strain expressing mCherry-Tub1 (Khmelinskii et al., 2007) was provided by Elmar Schiebel (Universität Heidelberg, Germany).

The AlignX module of VectorNTI suite (Invitrogen, Carlsbad, CA) was used to align sequences Ldb18 and human dynactin 3 (NP_009165) using the Clustal W algorithm. To determine the statistical significance of the observed prevent identity between p24 and Ldb18, we performed a permutation test by randomly shuffling the p24 sequence 10,000 times and determining the identity between each of the shuffled p24 sequences and Ldb18. The (one-tailed) P-value was calculated as the number of shuffled sequences with percent identity equal to or greater than the observed percent identity, divided by the number of permutations done. Secondary structures were predicted using PHD (Rost and Sander, 1993). Coiled-coil domains were predicted using the MTIDK matrix and 2.5 fold weighing function of the COILS algorithm (Lupas et al., 1991).

Two-hybrid assays: Two hybrid assays were performed as described previously (Wolyniak et al., 2006) and in chapter two. Vectors containing Jnm1 (MR4212), Arp1 (MR4187), and Arp10 (MR5393) fused the Gal4 activation-domain were a gift from Mark Rose (Princeton, NJ). pAH34 (Gal4-

BD LDB18), pAH35 (Gal4-AD LDB18), pAH50 (Gal4AD-NIP100) and pAH51 (Gal4AD-NIP100 (400-600)) were constructed in this study by cloning fragments into pASII and pACTII vectors with NcoI and BamHI. Vectors are summarized in Table 4.2.

Coimmunoprecipitation: Coimmunoprecipitation experiments were performed as described previously (Wolyniak et al., 2006). Yeast cultures were harvested at an OD of 0.8, washed with water and resuspended in breakage buffer (30 mM $NaPO_4$ pH 7.0, 60 mM β-glycerophosphate, 150 mM KCl, 6 mM EGTA, 6 mM EDTA, 10% glycerol) supplemented with 1 mM PMSF, 10 μg/ml leupeptin, and 10 μg/ml pepstatin. Cells were frozen in liquid nitrogen, ground using a mortar and pestle, and centrifuged twice for 15 minutes at 4° at 14,000 RPM. 1 mg total protein was adjusted to a final salt concentration of 50 mM with NaCl in a final volume of 500 μl SPGT (50 mM NaCl, PBS (4.3 mM Na_2HPO_4, 1.4 mM KH_2PO_4), 10% glycerol, 0.1% Tween-20) and incubated with 1 μl of an antibody against either Myc (9E10; 1:1000 for western; Covance, Emeryville, CA), HA (16B12; 1:500 for western; Covance, Emeryville, CA), Jnm1 (1:1000 for western; pre-cleared with 100 μg of *jnm1Δ* lysate; Gift from Kelly Tatchell, Louisiana State University, LA), or Arp1 (1:1000 for western; pre-cleared with 100 μg of *arp1Δ* lysate; Gift from Mark Rose, Princeton, NJ) for three hours at 4°. 40 μl of a 50% slurry of Protein G beads (Roche, Nutley, NJ) were added and incubated for 1.5 hours. Beads were washed three times in 1 ml SPGT for 5 minutes each. After final wash, beads were resuspended in 25 μl 2X SDS loading buffer, boiled for 3 minutes, then eluted through a blank mini spin column (Biorad, Hercules, CA) and 25 μl run on 10% SDS-gel followed by wet transfer to nitrocellulose

membrane. Goat anti-mouse IgG light chain (1:12,500; Jackson ImmunoResearch, West Grove, PA) or goat anti-rabbit (1:5,000; Biorad, Hercules, CA) was used as a secondary antibody. SuperSignal ECL (Thermo Scientific, Rockford, IL) was used for detection on film.

Sucrose gradient sedimentation: Cell lysates were prepared as described for coimmunoprecipitation. (500μl of 5 mg/ml) was sedimented on a 10 ml 5-20% sucrose gradient prepared in breakage buffer. The gradient was centrifuged in a SW41 rotor at 34,000 RPM for 17 hours at 4° with no brake as described previously (Clark and Rose, 2006). Fractions (1 ml) were collected and TCA precipitated (Schuyler and Pellman, 2002) before SDS-PAGE and immunoblotting. Yeast alcohol dehydrogenase (7.4S) and thyroglobulin (19.6S) were run as standards (Sigma, St. Louis, MO).

Protein Purification: pAH49, containing GST-Ldb18, was transformed into BL21 *E. coli*. Cultures grown in LB+Kanamycin (100 μg/ml final) were induced with IPTG (1 mM final) at OD of 0.1 at 30° for 4 hours. Uninduced and induced samples run on SDS-PAGE were stained with coomassie blue or immunoblotted with GST antibody.

Protein Modification. To test if Ldb18 modifications vary throughout the cell cycle, AHY1932 was arrested either in α-factor (12.5 μM final) (Zymo Research, Orange, CA), hydroxyurea (100 mM final), nocadozole (25 μg/ml final) for three hours. To see if any bands were due to phosphorylation, 40 μg of cell extract was diluted in phosphatase buffer (50 mM Tris pH 7.5, 5 mM DTT, 0.1 nM EGTA, 2 mM $MnCl_2$) and incubated 20 min at 30° with λ

phosphatase (gift from Goldberg lab) and then immunoblotted after SDS-PAGE.

Microscopy: DAPI staining of cells was carried out as described previously (Sheeman et al., 2003). Cells were grown to mid-log phase and diluted back 1:10 and shifted to 12° for 24 hours. 1 ml of culture was washed twice with PBS (4.3 mM Na_2HPO_4, 1.4 mM KH_2PO_4) and fixed in 3.6% final formaldehyde for 30 minutes at room temperature. The fixed cells were washed twice with PBS, then incubated with 1 μg/ml DAPI 30 minutes in the dark. Cells were washed twice with PBS prior to imaging on a Zeiss Axioplan 2 Imaging microscope (Thornwood, NY) using Openlab software (Improvision, Lexington, MA) with 2x2 binning. Live cells expressing GFP and mCherry constructs were imaged on a spinning disk confocal imaging system (UltraVIEW, Perkin-Elmer, Wellesley, MA) with 2x2 binning. Exposure times were three seconds for GFP, and two seconds for mCherry.

RESULTS

Ldb18 is In the Dynein Pathway for Spindle Orientation

In initial tests to discern Ldb18 function, I found that *ldb18Δ* does not confer resistance or sensitivity to the microtubule destabilizing drug benomyl. However, I did find that *ldb18Δ* demonstrates slight temperature sensitivity at low temperatures (Figure 4.1). To investigate whether Ldb18 is involved in spindle function, I observed microtubules in live *ldb18Δ* cells expressing GFP-Tub1. While anaphase spindles in wild-type cells extend through the bud neck, elongated spindles in *ldb18Δ* cells are frequently observed entirely within the mother cell (Figure 4.2 A). To quantify the spindle orientation defect, I

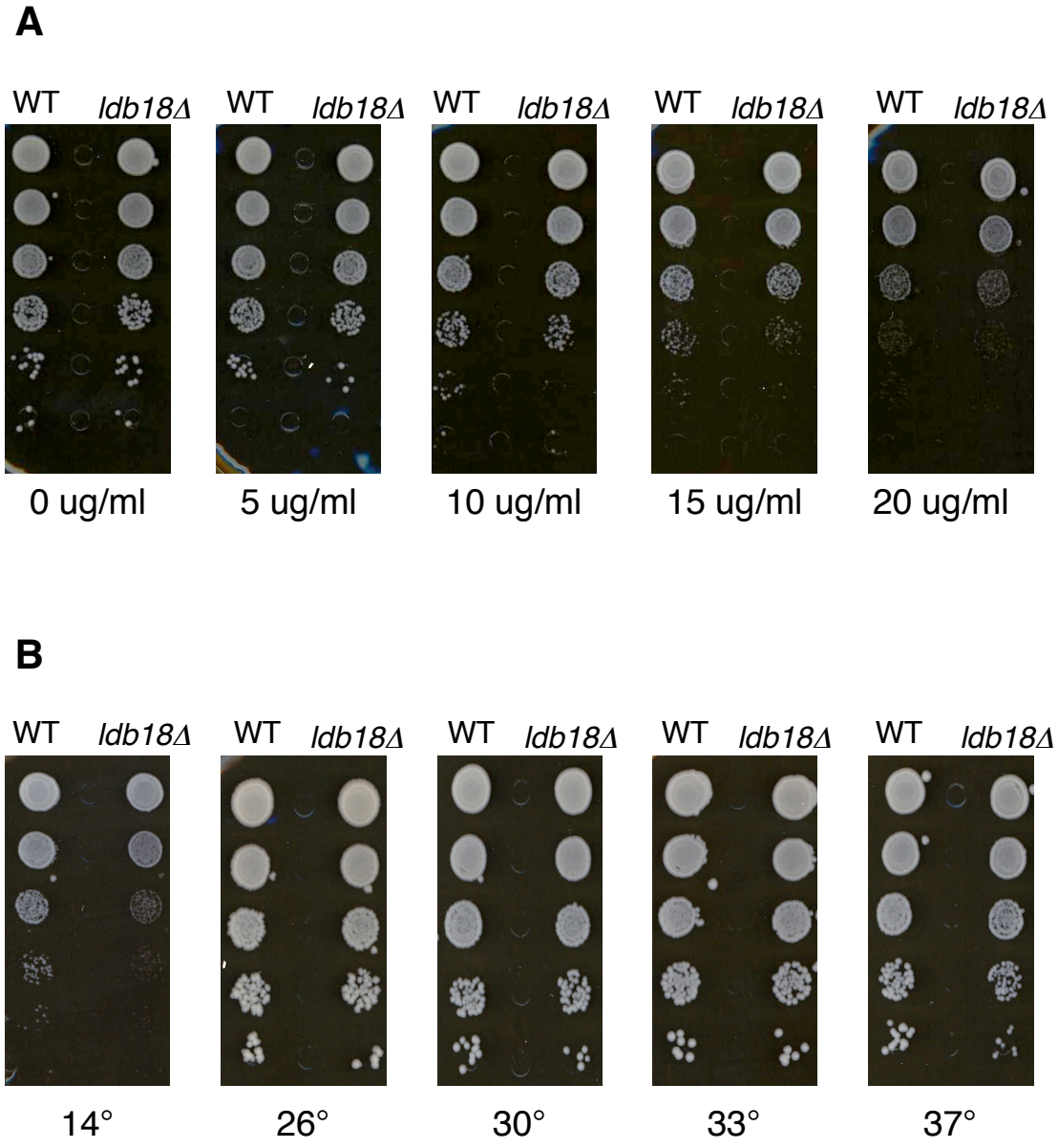

Figure 4.1 Initial characterization of Ldb18. (A) Loss of Ldb18 does not confer benomyl resistance or sensitivity. WT and *ldb18Δ* cells (BY4741, CUY1816) were plated on YPD with indicated concentrations of benomyl in serial dilutions. (B) Deletion of Ldb18 results in slight temperature sensitivity at cold temperatures. Wild type and *ldb18Δ* cells were plated on YPD plates in serial dilutions and incubated at indicated temperatures. WT, wild-type

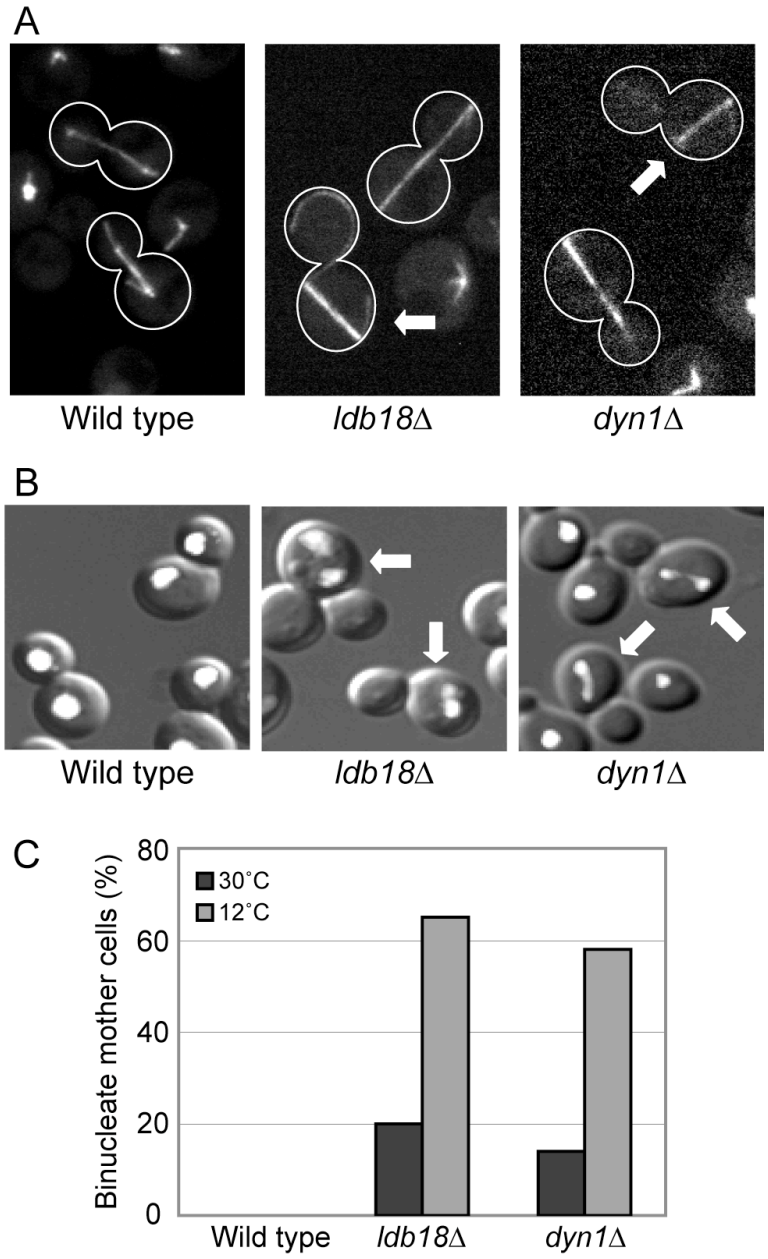

Figure 4.2 Ldb18 plays a role in the dynein pathway of spindle orientation. (A) Wild type (CUY1928), *ldb18Δ* (CUY1929), and *dyn1Δ* (CUY1930) strains expressing GFP-Tub1. Arrows designate cells with elongated spindles in the mother cell. (B) Wild type (BY4741), *ldb18Δ* (CUY1816), and *dyn1Δ* (CUY1823) cells stained with DAPI. Arrows designate binucleate mother cells. (C) Quantification of binucleate mother cells by DAPI indicating spindle elongation within the mother cell. >250 budded cells were counted.

stained cells with DAPI to visualize chromosomal DNA. In wild-type cells, segregated chromosomes are always located in mother cell and bud, respectively. However, in ~20% of *ldb18Δ* cells, segregated chromosomes reside entirely within the mother cell (Figure 4.2 B,C). This number increases to over 60% when cells are grown at 12°. This phenotype, and its increased penetrance at low temperatures, is typical of mutations that disrupt dynein function (Figure 4.2 A-C) or other components of the dynein-mediated spindle orientation pathway (Eshel et al., 1993; Kahana et al., 1998; McMillan and Tatchell, 1994; Muhua et al., 1994).

Because the Kar9 and dynein pathways are redundant for cell viability, mutations in the dynein pathway will be lethal in combination with mutations in the Kar9 pathway, but not with other mutations in the dynein pathway. To test whether Ldb18 acts in the dynein pathway, *ldb18Δ* was crossed to a number of Kar9 and dynein pathway mutations. *ldb18Δ* is synthetic lethal with all tested deletions of Kar9 pathway genes (*BIM1, BNI1, KAR9, KIP3*), but not with any tested deletions of dynein pathway genes (*ARP1*, *BIK1*, *DYN1*, *JNM1*, *NIP100*, *NUM1*, *PAC11*) (Table 4.3) as determined by spore size of double mutants following tetrad dissection. Thus, both phenotypic and genetic evidence place Ldb18 in the dynein pathway. Analysis by others using available genomic synthetic-lethal and two-hybrid data also suggests a role for Ldb18 in the dynein pathway (Ye et al., 2005; Kelley and Ideker, 2005).

Ldb18 is the p24 Homolog in the Yeast Dynactin Complex

Available genome-wide two-hybrid data identified Jnm1 as a protein that interacts with Ldb18 (Ye et al., 2005; Ito et al., 2001). Jnm1 is a component of the yeast dynactin complex, a homolog of the mammalian

Table 4.3 Synthetic lethal interactions place Ldb18 in the dynein pathway.
Genetically, Ldb18 is involved in the dynein pathway of spindle orientation since spores containing deletions of Ldb18 and components of the dynein pathway are viable, while spores containing deletions of both Ldb18 and Kar9 pathway proteins are dead. - , inviable; -/+ , weak growth; + , viable

Genotype	Viability
Kar 9 Pathway	
ldb18Δbni1Δ	-/+
ldb18Δkip3Δ	-/+
ldb18Δkar9Δ	-/+
ldb18Δbim1Δ	-
Dyn1 Pathway	
ldb18Δbik1Δ	+
ldb18Δdyn1Δ	+
ldb18Δpac11Δ	+
ldb18Δnum1Δ	+
ldb18Δjnm1Δ	+
ldb18Δarp1Δ	+
ldb18Δnip100Δ	+

dynamitin protein, and its loss produces a phenotype similar to what is observed for *ldb18Δ* (McMillan and Tatchell, 1994). To test if Ldb18 is associated with dynactin, the dynactin proteins Nip100, Jnm1, Arp1, and Arp10 were tested for their interaction with Ldb18. In the yeast two-hybrid assay, Ldb18 interacts strongly with Jnm1 and Nip100, and weakly with Arp1 and Arp10 (Table 4.4). The Ldb18-binding region of Nip100 was narrowed down to residues 400-600 that lie between its two coiled-coil domains. Ldb18 also interacts with itself, suggesting that it may dimerize. These results indicate that Ldb18 is a component of the dynactin complex that interacts directly with the shoulder-sidearm components Jnm1 and Nip100.

Interactions between Ldb18 and dynactin components were also assessed by co-immunoprecipitation assays. Immunoprecipitation of Myc epitope-tagged Ldb18 pulls down HA epitope-tagged Nip100, Jmn1, Arp1, and Arp10 (Figure 4.3 B). Similarly, immunoprecipitations of Nip100, Jnm1, and Arp1 also pull down Ldb18 (data not shown). Additionally, Ldb18 migrates with dynactin proteins during sucrose gradient sedimentation as a ~ 20 S complex (Figure 4.3 C). While the intact complex runs farther into the gradient (fraction 7 and 8), it is possible that distinct sub-complexes can form and migrate to differing degrees. It is known that the shoulder-sidearm complex (p24-p50-p150^{glued}) can be isolated biochemically. This group may be represented by fractions 5 and 6. Jnm1 and Ldb18 may also exist as monomers or dimers, which may explain why these proteins exist as a smear throughout the gradient. In contrast, Arp1 forms short filaments, which would migrate farther into the gradient. Immunoblots of Ldb18 detect three major bands; the lower two bands are near the predicted molecular weight for Ldb18-13Myc, while the upper band is approximately 10-13 kDa higher.

Table 4.4 Yeast two-hybrid interactions with Ldb18
Yeast two-hybrid was performed using Ldb18 fused to the binding domain of Gal4 with various dynactin proteins fused to the activation domain of Gal4. Interaction was determined by color change in a β-galactosidase filter assay. Strength of interaction as determined by visual inspection is indicated. - , negative; +/- , weak interaction; ++ , good interaction; +++ , strong interaction

Gal-4 Activation Domain	Interaction
Ldb18	++
Jnm1	+++
Nip100	+++
Nip100 (AA 400-600)	++
Arp1	+/-
Arp10	+/-

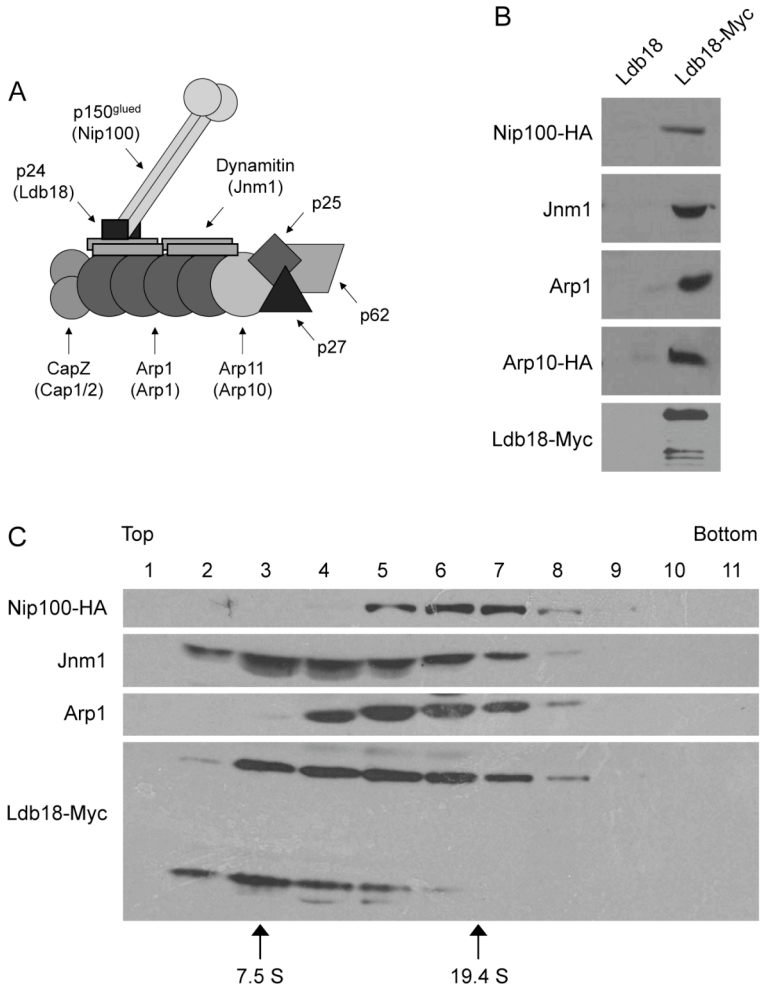

Figure 4.3 Ldb18 is a component of the dynactin complex. (A) Diagram of the mammalian dynactin complex. Yeast homologs are indicated in parentheses. (B) Ldb18 can coimmunoprecipitate with all components of the dynactin complex. Lysates from Ldb18-13Myc (CUY1932), Ldb18-13Myc Nip100-3HA (CUY1933), and Ldb18-13Myc Arp10-HA (CUY1934) strains were immunoprecipitated using a Myc antibody. Strains lacking Ldb18-13Myc (CUY26, MY8912, and MY8895) were used as controls. Immunoprecipitated proteins were run on SDS-PAGE and immunoblotted using Myc antibody and either a Jnm1, Arp1, or HA antibody. (C) Lysate from an Ldb18-13Myc Nip100-3HA strain (CUY1933) was run over a 5-20% sucrose gradient. Fractions were run on SDS-PAGE and immunoblotted using Myc, HA, Jnm1 and Arp1 antibodies. Arrows indicate migration of size standards: yeast alcohol dehydrogenase (7.4S) and thyroglobulin (19.6S).

Interestingly, only the upper band co-migrates with the dynactin complex on sucrose gradients, indicating that post-translational modification of Ldb18 may be needed for its incorporation into the dynactin complex. The nature of this Ldb18 modification is discussed below.

Yeast homologs have not been identified for several mammalian dynactin components, including the shoulder-sidearm protein p24 and the pointed-end proteins p25, p27, and p65. BLAST searches with Ldb18 do not identify any metazoan proteins. However, the size of Ldb18 (21 kD), and its interaction with the yeast homologs of dynamitin (Jnm1) and $p150^{Glued}$ (Nip100), suggest that Ldb18 may be the homolog of p24. An alignment of the Ldb18 and human p24 sequences shows that they share 16% identity and 29.8% similarity (Figure 4.4 A). To demonstrate that this percent identity is significant and not due to chance alone, I collaborated with Tim Sackton to do a permutation analysis by randomizing the p24 sequence and calculating the percent identity between each permutated sequence with Ldb18 (n=10,000). Overall, the mean percent identity of the randomly permutated sequences with Ldb18 is lower than the actual identity (6.2% versus 16.9%) (p-value <0.0001, permutation test). The maximum percent identity observed between Ldb18 and the permutated p24 sequences was 14.6%, still lower than the actual value. The percent identity and similarity between Ldb18 and p24 is comparable to the percentages between other known and accepted dynactin homolog pairs – Nip100-$p150^{Glued}$ (21.9% similar and 12.7% identical) Jnm1-dynamitin (26.7% similar and 15.8% identical), Arp10-Arp11 (24% similar and 12.2% identical). In addition, the two proteins share similar predicted secondary structure. Both p24 and Ldb18 are predicted to contain long stretches of alpha helical structure (Karki et al., 1998; Pfister et al., 1998). By

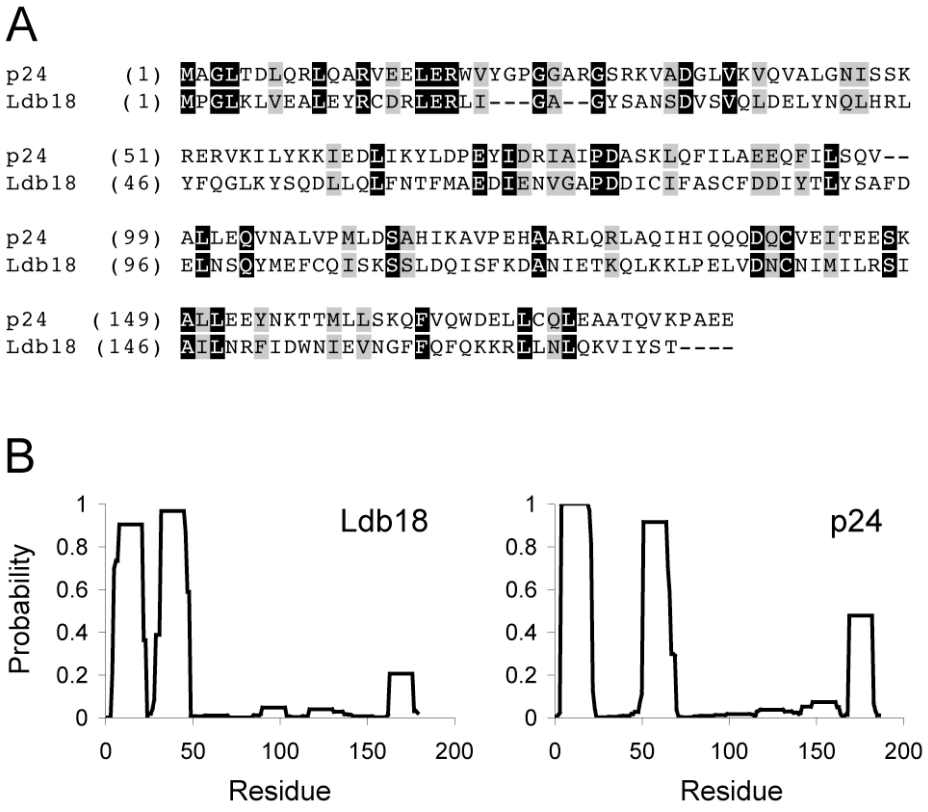

Figure 4.4 Ldb18 shares sequential and structural properties with mammalian p24, a component of the dynactin complex. (A) Sequence alignment of yeast Ldb18 and human p24. Similar residues are shaded in gray and identical residues are shaded in black. (B) Ldb18 and p24 are both predicted to contain coiled-coil domains near the amino terminus using a 14 residue window in the COILS algorithm.

contrast, the other two dynactin proteins of similar molecular weight, p25 and p27, are predicted to adopt a left-handed β helix, a motif not commonly encountered (Parisi et al., 2004). Sequence analysis using the COILS algorithm suggests that both p24 and Ldb18 contain coiled-coil domains near their amino termini and possibly at their carboxyl termini (Figure 4.4 B). It is the amino termini of these proteins that share the most similarity. Hence, based on sequence alignment, similar secondary structure, and strong interactions with Nip100 and Jnm1, Ldb18 is likely the yeast homolog of the dynactin component p24.

Yeast dynactin localizes to the spindle pole bodies and to the distal ends of cytoplasmic microtubules (Grava et al., 2006; Kahana et al., 1998; McMillan and Tatchell, 1994). To determine the localization of Ldb18 in live cells, I fused three tandem copies of GFP to the carboxyl terminus of the protein. Ldb18-3GFP was visualized in live cells also expressing either the spindle pole body marker Spc42-RFP, or mCherry-Tub1 (Figure 4.5 A-D). Ldb18 localizes to the spindle pole body, often on the daughter-bound pole. Asymmertric localization on the daughter-bound SPB has been reported for Dyn1, and to a lesser extent for Jnm1 (Grava et al., 2006). Additional Ldb18 foci can also be observed at the distal end of an astral microtubule. Thus, Ldb18 localization is consistent with it being a component of the dynactin complex.

Ldb18 is Required for Dynactin Integrity

When the dynactin complex is disrupted, a subcomplex of p24, dynamitin, and $p150^{Glued}$ can be isolated (Eckley et al., 1999); however, the precise nature of the interactions among these shoulder-sidearm proteins is

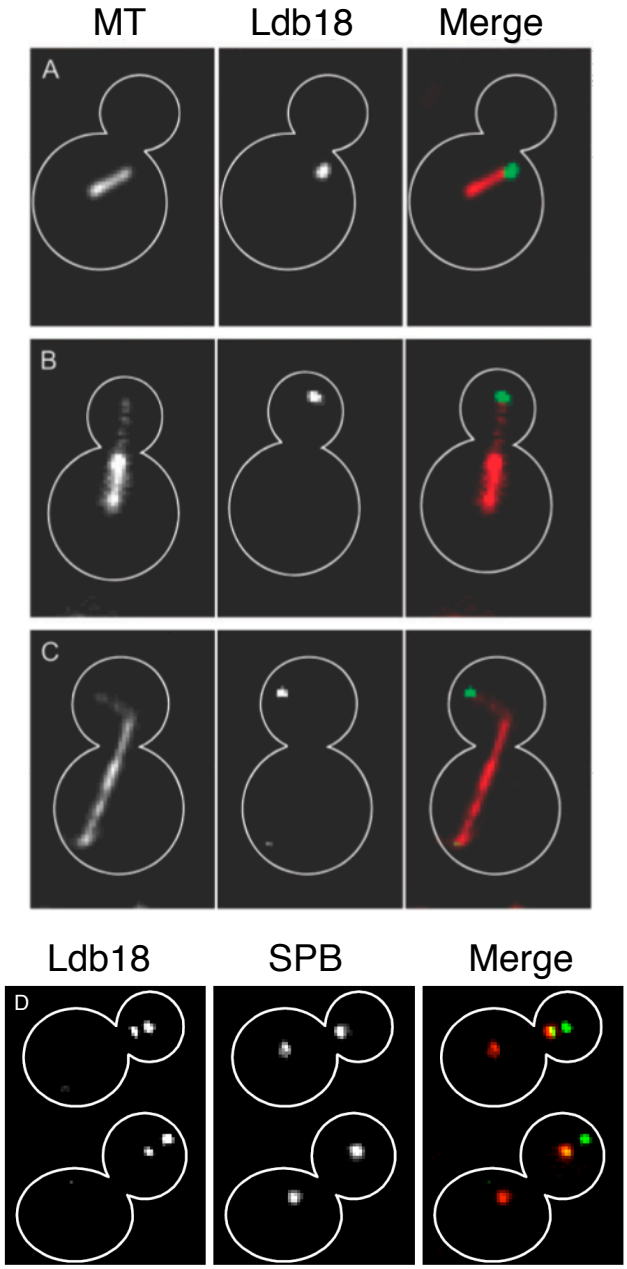

Figure 4.5 Localization of Ldb18. Z-series projections of cells (CUY1951) expressing Ldb18-3GFP (green) and mCherry-Tub1 (red) to visualize microtubules. Ldb18 localizes near the daughter-bound SPB (A), and at the plus-ends of astral microtubules (B and C). (D) Z-series projections of cells (CUY1931) expressing Ldb18-3GFP (green) and Spc42-RFP (red) to mark spindle pole bodies. MT-microtubule; SPB, Spindle Pole Body

not known. The phenotype of *ldb18Δ* cells suggests that Ldb18 is required for dynactin function. To test whether Ldb18 is needed for the integrity of the dynactin complex, I measured the co-precipitation of Jnm1 with Nip100 and Arp1 in wild-type and *ldb18Δ* cells. Loss of Ldb18 does not affect the interaction between Jnm1 and the Arp1 filament (Figure 4.6 A). However, the interaction between Jnm1 and Nip100 is disrupted in the absence of Ldb18 (Figure 4.6 B), indicating that p24 is important in mediating the $p150^{Glued}$-dynamitin interaction. Similar results were obtained by measuring the co-precipitation of Arp1 and Nip100 with Jnm1 (data not shown). The amount of Jnm1 that is precipitated with Nip100 in the *ldb18Δ* strain is ~1/25 of the Jnm1 precipitated in the wild-type strain (Figure 4.6 C). Thus, loss of Ldb18 reduced the Jnm1-Nip100 interaction by ~95%. This result is consistent with Ldb18 being part of the shoulder-sidearm dynactin subcomplex. Earlier studies demonstrated reduced Nip100 binding to the Arp1 filament in *jnm1Δ* cells (Kahana et al., 1998), indicating Jnm1 was responsible for sidearm attachment. In *ldb18Δ* cells, Jnm1 still interacts with Arp1 and only Nip100 dissociates from the complex. Thus, Ldb18 is essential for dynactin function because it is required to tether the microtubule and the dynein-binding Nip100 arm to the dynactin complex through its interaction with Jnm1.

Post-Translational Modification of Ldb18

As described above, immunoblots of Ldb18-13Myc detect multiple bands, indicating possible post-translational modification. A doublet is found near the predicted molecular weight of Ldb18-13Myc (41 kDa), but there is also a prominent band that migrates ~10-13 kDa slower (Figure 4.7 A). The higher migrating band can also be identified in immunoblots for Ldb18-3GFP

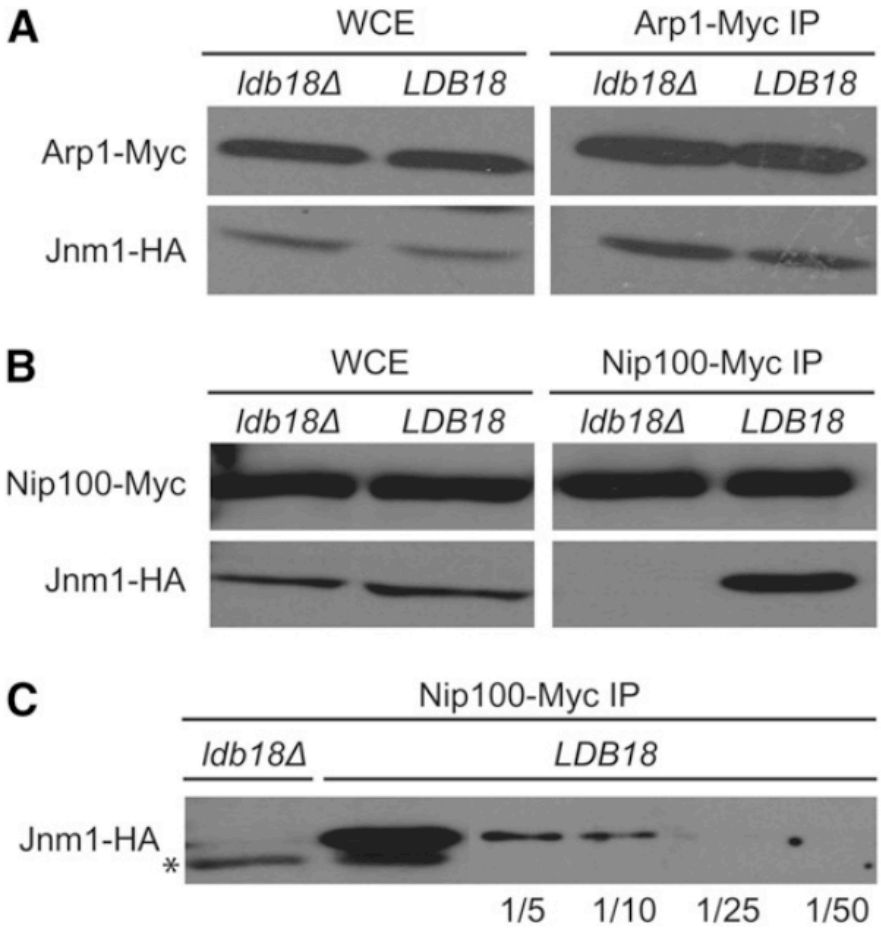

Figure 4.6 Ldb18 is involved in shoulder-sidearm interactions. *LDB18* and *ldb18Δ* strains expressing Jnm1-3HA and Nip100-13Myc or Arp1-13Myc wre constructed (CUY1935, CUY1936, CUY1937, CUY1938). Lysates were immunoprecipitated using a Myc antibody. Samples were separated by SDS-PAGE and blotted using Myc and HA antibodies. Loss of LDb18 does not affect the interaction of Jnm1 with Arp1 (A), but disrupts its interaction with Nip100 (B). (C) Extended exposure of the Nip100-Myc immunoprecipitation shown in the bottom right panel of (B) with serial dilutions of the Nip100-Myc immunoprecipitation from the *LDB18* strain. *, IgG heavy chain; WCE, Whole Cell Extracts; IP, immunoprecipitation

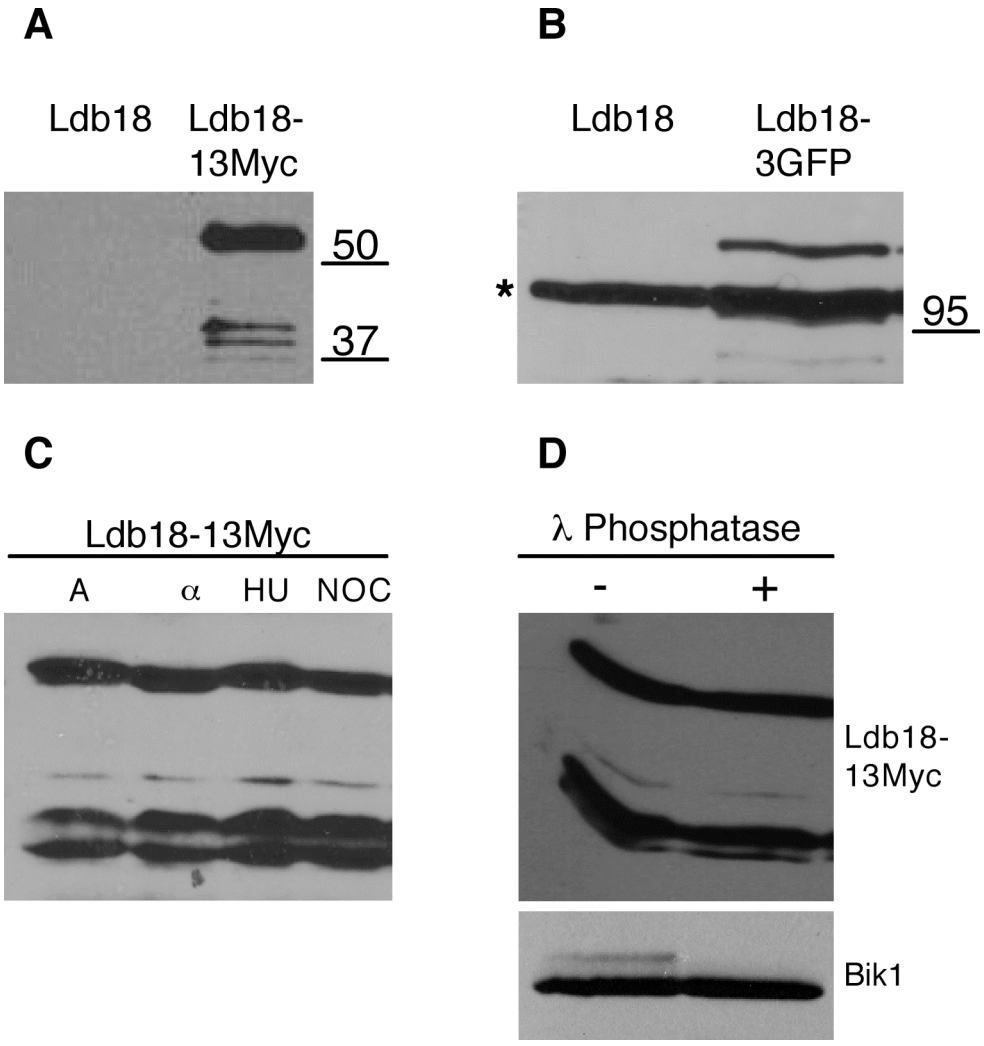

Figure 4.7 Ldb18 is post-translationally modified. Extracts from untagged Ldb18, Ldb18-13Myc, and Ldb18-3GFP (CUY26, CUY1932, CUY1813) blotted with antibodies against Myc (A) or GFP (B). The predicted molecular weight for Ldb18-13Myc is 41 kDa, while Ldb18-3GFP is 103 kDa. Ldb18-3GFP co-migrates in a background band detected by the GFP antibody, but a higher molecular weight species is detected ~13 kDa higher. Molecular size markers on blots are indicated. Asterisks denote background band. (C) Ldb18-13Myc extracts arrested in α-factor (α), hydroxyurea (HU), and nocadozole (NOC) and blotted with a Myc antibody. Extract from asynchronous cultures (A) was included for comparison (D) Ldb18-13Myc extract treated with λ phosphatase for 20 min and blotted with a Myc antibody does not differ from untreated extract. Immunoblots of treated and untreated wild-type extracts (CUY26) with antibodies against Bik1 demonstrate the effectiveness of the phosphatase.

(predicted weight 103 kDa) (Figure 4.7 B). To determine if Ldb18 has intrinsic properties that cause the protein to migrate differently than predicted in SDS-PAGE, I cloned Ldb18 into an *E. coli* GST-expression vector. As post-translational modifications in bacterial systems are limited (Eichler and Adams, 2005), I expected to express GST-Ldb18 in its native unmodified form. After induction, bacterial extracts show the appearance of a specific band that can be identified with a GST antibody at the predicted molecular weight of 48 kDa. While smaller bands also emerge, likely representing degradation products, no bands at a higher molecular weight are observed (Figure 4.8), indicating Ldb18 is modified in yeast cells.

Protein modifications can regulate protein localization or activity throughout the cell cycle. Since dynein/dynactin acts primarily in anaphase, it is possible that the Ldb18 modification varies through the cell cycle. No observable differences in regard to the modification bands could be detected in Ldb18-13Myc cells arrested with either α-factor (G1), hydroxyurea (late S/early mitosis), or nocodazole (metaphase) (Figure 4.7 C). To investigate the modification state in anaphase, cells were arrested in metaphase by depletion of Cdc20 and subsequently released. Samples from the released culture were taken at 15 minute intervals. Preliminary results suggest there is no redistribution of the band pattern throughout anaphase (data not shown). Hence, the Ldb18 modification does not appear to vary with the cell cycle.

Post-translational protein modifications involve addition of a functional group (phosphorylation, methylation, acetylation) or a small peptide. Based on the size difference between the bands, I investigated whether Ldb18 is modified by a small peptide from the ubiquitin-related family. Ubiquitin (yeast Ubi4, 8.6 kDa), Small-Ubiquitin Modifier (SUMO) (yeast Smt3, 11.6 kDa),

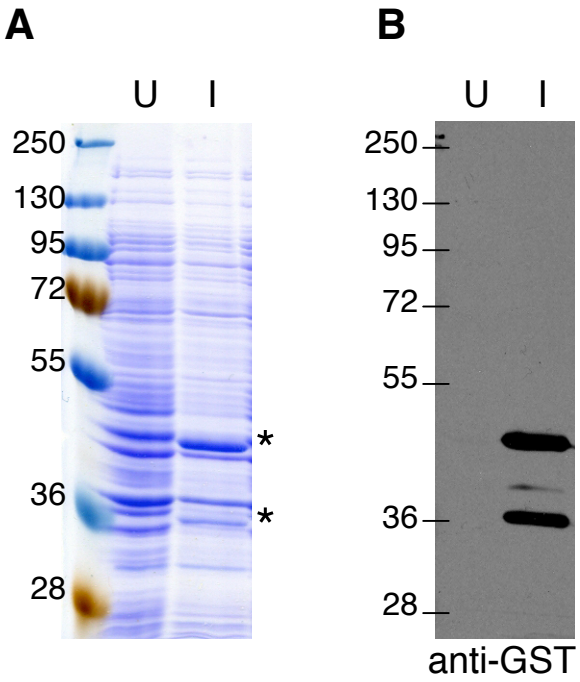

Figure 4.8 Ldb18 expressed in E. coli migrates at the predicted molecular weight. (A) Coomassie Blue staining of uninduced and induced samples from *E. coli* BL21 cells. GST-Ldb18 has a predicted molecular weight of 48 kDa. Asterisks denotes unique bands in the induced extract. (B) Immunoblot of uninduced and induced extract with a GST antibody. The bands correspond with the coomassie staining. A major degradation product is also identified. U, uninduced; I, induced

NEDD8 (yeast Rub1, 8.7 kDa), and Urm (yeast Urm1, 11 kDa) covalently bind proteins via an isopeptide bond between the carboxyl-terminal carboxylate and the amine group of lysine residues on the target protein (reviewed in Hochstrasser, 2000). In an attempt to identify the larger band, immunoprecipitated Ldb18-13Myc was immunoblotted using antibodies against ubiquitin and SUMO. Neither antibody recognize the top band (data not shown). Although the antibodies recognize protein species in whole cell extracts, no positive control of a known ubiquitin- or SUMO-modified protein was tested.

Urmylation was first identified in budding yeast based on homology to bacterial sulfur transfer proteins, whose biochemistry mechanistically resembles early ubiquitin activation (Furukawa et al., 2000; Goehring et al., 2003b). Urm1 in yeast is covalently conjugated to Ahp1, a protein involved in oxidative stress (Goehring et al., 2003a). The urmylation activating protein Uba4 was identified in a screen looking for synthetic-lethal relationships with Jnm1 and Arp1 (Schoner et al., 2008). *urm1Δ* and *uba4Δ* cells are viable, hence I examined Ldb18 modifications in these strains. Interestingly, the upper modification band of Ldb18 is absent, suggesting that the band contains the peptide Urm1 (Figure 4.9 A). Attempts to identify the top band of immunoprecipitated Ldb18-13Myc with an Urm1 antibody (Goehring et al., 2003b) were not successful (data not shown). However, it should be noted that this antibody does not reliably detect Urm1 species (Charles Kubicek, personal communication).

A variety of phenotypes have been reported for *urm1Δ,* including no growth at 37°, sensitivity to rapamycin, lack of invasive growth under starvation conditions, and slight loss of asymmetric Kar9 SPB localization

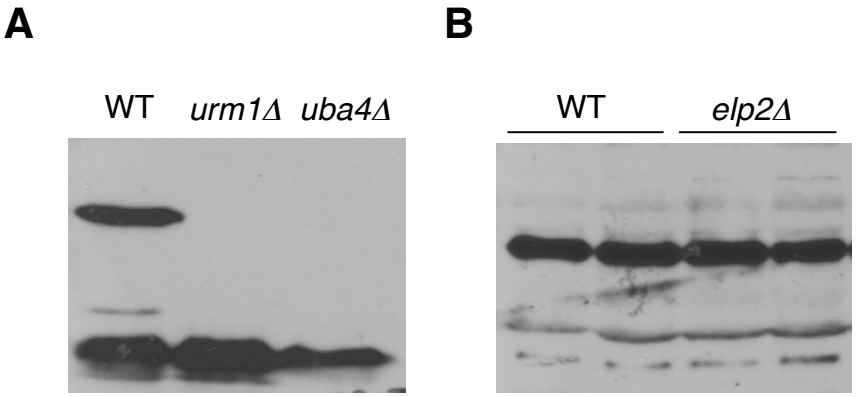

C

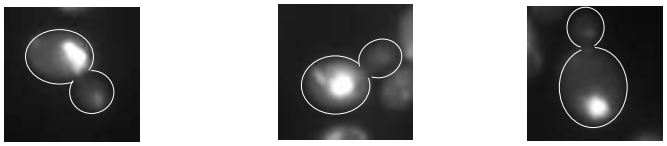

Wild type	98 (57.6%)	62 (36.5%)	10 (5.9%)
urm1Δ	79 (42.0%)	56 (29.8%)	53 (28.2%)
uba4Δ	38 (41.8%)	26 (28.6%)	27 (29.7%)

Figure 4.9 Urmylation of Ldb18. (A) Immunoblots of whole cell extracts using a Myc antibody show that the upper band from Ldb18-13Myc is absent in *urm1Δ* and *uba4Δ* backgrounds (AHY191). (B) Extracts blotted with a Myc antibody show Ldb18-13Myc is not affected by loss of tRNA modification. Whole cell extracts are from individual spores from a Ldb18-13Myc (CUY1932) X *elp2Δ* (CUY2005) cross. (C) WT (BY4741), *urm1Δ* (CUY1994), *uba4Δ* (CUY1995) were stained with DAPI after growth at 12° overnight. The mother cell of small-medium budded cells was divided into thirds and scored based on the position of the nucleus. Shown are number and percentages of cells in each category. WT, wild type

(Schoner et al., 2008; Furukawa et al., 2000; Goehring et al., 2003b). To determine if loss of Urm1 results in a dynein pathway defect, I stained cells grown at 12° with DAPI to assay chromosome segregation. Unlike *dyn1Δ* or *ldb18Δ* in which a high percentage of cells separate chromosomes entirely within the mother cell, *urm1Δ* and *uba4Δ* cells have segregated chromosomes in the both mother and daughter similar to wild-type cells (data not shown). There is, however, an increase in the number of medium-budded cells that do not position the nucleus near the bud neck, reminiscent of defects in the Kar9 pathway for spindle orientation (Figure 4.9 C). Recent work by a number of yeast and mammalian labs have implicated Urm1 as a sulfur transfer protein in the modification of specific tRNAs, independent of its proposed role as a protein modifier (Leidel et al., 2009; Huang et al., 2008; Nakai et al., 2008; Schlieker et al., 2008). tRNA modification, often near the wobble position of the anti-codon, is important to ensure ribosome stability (Ashraf et al., 1999). Since unmodfied tRNA can lead to errors in codon usage and affect protein stability, it is possible that the Ldb18 band loss in *urm1Δ* occurs by an indirect mechanism. Deletion of Elp2, a component of the elongator complex also involved in modification of tRNA, does not affect Ldb18 modification (Figure 4.9 B). Hence, proper tRNA processing is not required for Ldb18 modification.

In addition to the observed larger protein shift, a doublet is detected near the predicted size. Addition of a phosphate is a common protein modification that can alter protein function. Phosphorylation is emerging as an important regulator for subsequent ubiquitin or SUMO modifications on proteins (Hietakangas et al., 2006). Treatment of cell lysates with λ phosphatase does collapse the phosphorylation bands of Bik1, a microtubule-associated protein, but there is no effect on either the Ldb18-13Myc doublet

bands or the higher migrating band (Figure 4.7 D). The nature of this smaller modification remains unclear.

DISCUSSION

Ldb18 is the Yeast Homolog of p24, a Protein in the Shoulder-Side Arm Subcomplex of Dynactin

The genetic and biochemical data indicate that Ldb18 is the yeast homolog of the mammalian dynactin protein p24 and is essential for Nip100 ($p150^{Glued}$) attachment to dynactin. Nip100 is the primary subunit of dynactin responsible for dynein binding. Hence, the dynactin complex in *ldb18Δ* cells cannot effectively "off-load" dynein from the microtubule plus end to the cortex to pull the spindle through the neck. Increased dynein accumulation at microtubule plus ends and absence from the cortex is observed for *ldb18Δ* (Moore et al., 2008). I identified *ldb18Δ*, as well as deletions of a number of other genes in the dynein pathway (*DYN1, NIP100, JNM1, ARP1*), through the SGA screen with *stu1-5*. In the last chapter, I discussed that dynein/dynactin and Stu1 are synthetic lethal due to their redundant roles in SPB separation.

Yeast homologs for most of the proteins comprising the mammalian dynactin complex have now been identified, with the exception of the pointed-end complex proteins p25, p27, and p62. Neither sequence homology searches nor genome-wide screens assaying for a binucleate phenotype has produced any candidates (Li et al., 2005; Lee et al., 2005; Moore et al., 2008). If these proteins exist in yeast, they likely do not contribute significantly to dynactin function. Mammalian dynactin structure does not appear to be affected by loss of p62 (Lee et al., 2001), while p25 and p27 can be found in soluble pools independent of dynactin (Schroer, 2004). p25, p27, and p62 are

proposed to mediate protein-protein interactions with various cellular targets (reviewed in Schroer, 2004), hence it is possible that these specific interactions do not exist in yeast.

Dynactin Involvement in Cell Wall Integrity Checkpoint

Recent evidence suggests that yeast dynactin is involved in monitoring the integrity of the cell wall during the early stages of the cell cycle. Normally, cells with mutations that block or alter cell wall synthesis arrest in G2 with duplicated chromosomes, duplicated but unseparated SPBs, and small buds. Cells lacking Arp1, Jnm1, or Nip100 fail to arrest in response to cell wall defects, indicating a role for the dynactin complex in the checkpoint. Bypass of the checkpoint is not observed in cells lacking other dynein pathway proteins (Dyn1, Pac11, Num1, Pac1, and Bik1), showing that monitoring of the cell wall is specific to the dynactin complex (Suzuki et al., 2004). Analysis of Arp1 alanine-scanning mutants reveals that the functions of nuclear migration and cell wall checkpoint can be separated and therefore independent (Igarashi et al., 2005). Using an *in vivo* membrane association assay, Arp1 membrane association was independent of both dynein and the cortical patch protein Num1, but required the presence of Jnm1 and Nip100 (Clark and Rose, 2006). The mechanism for how dynactin is involved in the checkpoint is not worked out, but it is hypothesized that dynactin could serve as a scaffold for other proteins to monitor the cell wall. Preliminary evidence suggests that Arp1 no longer associates with the membrane in strain backgrounds that invoke the checkpoint, indicating Arp1 is sensitive to cell wall changes (Clark and Rose, 2006).

It is possible Ldb18 also plays a role in cell wall monitoring. Nip100 is required for Arp1 membrane targeting, and I demonstrated that Nip100 association with the dynactin complex requires Ldb18. To determine if Ldb18 is involved in the checkpoint, Ldb18 can be deleted in a strain background that affects genes involved in glucan synthesis. This temperature-sensitive strain (*fks1^{ts}, fks2Δ*) arrests in restrictive conditions (Suzuki et al., 2004). If Ldb18 is required for the checkpoint, the *ldb18Δ fks1^{ts} fks2Δ* strain will instead be viable. Alternatively, one can treat *ldb18Δ* cells with Echinocandin B_{27}, which inhibits yeast β(1→ 3) glucan synthase activity and activates the checkpoint. Following α-factor G1 arrest and release, drug-treated wild-type cells arrest with unseparated SPBs (Suzuki et al., 2004). A role for Ldb18 in the checkpoint would be indicated by appearance of separated SPBs and spindle formation following drug treatment in *ldb18Δ*.

Ldb18's possible involvement in the cell wall checkpoint sheds light on why a protein involved in nuclear migration would turn up in the low dye binding (LDB) genomic screen looking for defects in cell wall protein modifications (Corbacho et al., 2005). It is possible that very soon after the *ldb18Δ* strain was diluted back, a second spontaneous mutation that affects cell wall integrity arose. Normally, that particular cell would either arrest terminally or just long enough to correct the problem. However, in the absence of the checkpoint, this cell can continue through the cell cycle resulting in a daughter cell that now harbors the second mutation. As this continues, the result is a culture of cells with compromised cell wall composition, and therefore does not bind the cationic dye. Reduction of dye binding in *ldb18Δ* was less than 20%, indicating that Ldb18 is likely not involved directly with post-translational modification of cell wall proteins.

Jnm1, known to be required for the cell wall checkpoint, was also identified in the Ldb screen (Corbacho et al., 2005).

Modification and Implications for Regulation of Ldb18 and Dynactin

Antibodies recognize epitope-tagged Ldb18 as a species that migrates not only at the predicted molecular weight, but also as a species of an additional ~10-13 kDa, suggesting Ldb18 undergoes post-translational modification. These bands are not believed to be artifacts, as the higher-migrating species are present in two different epitope-tagged strains and purified protein from *E. coli* migrates at the predicted weight. Based on the size of the shift, I investigated members of the ubiquitin related proteins (reviewed in Hochstrasser, 2000). There was no positive identification using antibodies against ubiquitin or SUMO. However, these experiments can be repeated using appropriate positive controls. SUMO may not be a viable candidate, as Ldb18 does not contain a ψKxE SUMO consensus sequence (Rodriguez et al., 2001). Other members of the ubiquitin family that can be tested include Rub1 and Apg12, which so far have limited targets in yeast (Mizushima et al., 1998; Chiba and Tanaka, 2004).

An intriguing possibility is that Ldb18 is urmylated. While Ldb18 modification is notably absent in an *urm1Δ* background, there are some additional factors to consider. First, reports indicate that Urm-modified species are only readily observed when extracts are treated with the isopeptidase inhibitor N-ethylmaleimide (NEM). Yet, I observe a robust signal for the modified band without addition of NEM. NEM is commonly used to protect against deubiquitinases and desumolyation, so it would be interesting to observe if levels of the modified band change, namely increase, in the

presence of NEM. Second, large-scale pull-down purifications with Urm1 to identify potential targets have not reported isolation of Ldb18. However, Ahp1, a protein involved in the oxidative stress response and the only identified target of Urm1, has also not been identified (Goehring et al., 2003a; Charles Kubicek, personal communication). Third, Urm in yeast and mammalian cells is a major sulfur carrier in tRNA modification pathways (Leidel et al., 2009; Huang et al., 2008; Nakai et al., 2008; Schlieker et al., 2008). tRNA modifications are important for transcript fidelity, making it possible that loss of modification on Ldb18 is a secondary effect. However, based on the presence of the Ldb18 modification band in *elp2Δ,* this may not be the case.

One approach to positively identify the nature of the post-translational modification is through tandem mass spectrometry (MS/MS) using purified protein (Witze et al., 2007; Hoffman et al., 2008). The Ldb18 amino acid sequence contains a handful of lysine residues, which are typically modified by the ubiquitin related proteins. These residues can be systematically mutated to determine critical residues.

One consequence of Ldb18 modification is that it may serve as a means for possible dynactin regulation. It is curious that only the higher-migrating band co-fractionates with the presumably intact dynactin complex in sucrose gradients, suggesting that Ldb18 modification is needed for full dynactin assembly. Future experiments to test whether the modification is significant for dynactin function and structure include using co-immunoprecipitation to determine to what degree unmodified Ldb18 (*urm1Δ* background) can interact with dynactin complex proteins. The Nip100-Jnm1 and Jnm1-Arp1 interactions can also be tested to see if they resemble *ldb18Δ*. Sucrose gradient analysis can determine if loss of Urm1 significantly changes

dynactin protein distribution. Additionally, the localization of Ldb18, and other dynactin proteins, can be studied for any changes in an *urm1Δ* background. To date, the asymmetric SPB localization of Kar9, which in turn affects dynein localization, is slightly altered in *urm1Δ* (Schoner et al., 2008). It may be the case that Urm1 affects the asymmetric SPB localization of Ldb18 as well.

If a fully-assembled dynactin complex depends on Ldb18 modification, then disruption of the modification could yield the same phenotype found in dynactin null mutants. Without dynactin, dynein accumulates at microtubule plus ends, unable to off-load to the cortex and pull the spindle through the bud-neck. However, neither *urm1Δ* nor *uba4Δ* cells exhibit a dynein phenotype, but instead the data suggests a possible role in the Kar9 pathway for spindle positioning. This *urm1Δ* phenotype is in line with the reported Kar9 localization defect. Additional evidence suggests that Urm1 may not be involved in the dynein pathway. She1 is a protein postulated to be a negative regulator of dynein function, with overactive dynein in a *she1Δ* contributing to astral microtubule release from the SPB early in the cell cycle and excessive spindle movement (Woodruff et al., 2009; Zane Bergman personal communication). A *she1Δ urm1Δ* strain does not show a reduced, or enhanced, phenotype, indicating that dynein activity is not affected by loss of Urm1 (Zane Bergman, personal communication). She1 is believed to regulate dynein activity by temporally restricting dynactin subunit localization thereby preventing premature association with each other and dynein. In *she1Δ*, all of the dynactin proteins localize to astral microtubule ends prematurely and in higher quantities (Woodruff et al., 2009). Ldb18 in particular normally associates with SPBs early, and later transitions to the microtubule tip in anaphase. One possibility is that She1 affects localization by regulating

proteins directly or indirectly by post-translational modification. Yet, Ldb18 modifications are unchanged in *she1Δ* (Zane Bergman, personal communication). The change in localization may not be influenced by modification, since one would expect this modification to be cell cycle dependent, yet there is no change observed in extracts arrested at different cell cycle stages.

Understanding regulation mechanisms of dynactin in mammalian cells is an area of ongoing study, yet some insights have been gleaned in recent years. In the early embryo, dynein/dynactin is involved in spindle rotation in the initial cell divisions. Dynactin localization is influenced by the Wnt and Src signaling pathways, but the precise mechanism is still unclear (Zhang et al., 2008). In vesicle transport, the cell-cell adhesion protein α-E-catenin modulates dynactin-mediated organelle transport (Lien et al., 2008). α-E-catenin binds dynactin directly and is believed to mediate cross-talk between actin and other cytoskeletal structures. More work still needs to be done to find the upstream mediators of dynactin regulation.

CHAPTER FIVE

Summary

Work presented here highlights proteins involved in formation and maintenance of mitotic spindles in budding yeast. Stu1 localizes to kinetochores and provides stability to kinetochore microtubules in order to provide an outward force to maintain a short spindle. Stu1 may also be involved in stabilization of polar microtubules, but to a lesser extent. Later in mitosis when the spindle is elongating, the motor dynein pulls the spindle through the bud neck. Ldb18 is an integral part of the dynactin complex, which in turn activates dynein function.

There is a genetic relationship between Stu1 and proteins in the dynein/dynactin pathway as described in detail in the discussion of chapter three. Genes that are synthetic lethal often have overlapping function. Here, Stu1 and dynein are both likely involved in generating an outward force to maintain separation of the spindle pole bodies (Figure 5.1), which may be a clue that Stu1 has a role in anaphase. Loss of dynein does not result in spindle collapse, but dynein may still be important in the later stages of spindle elongation. Dynein anchored at the cortex in both the daughter and mother cell could provide opposing pulling forces on the spindle pole bodies. Evidence supports the idea that dynein is involved in spindle elongation to some degree (Gerson-Gurwitz et al., 2009). In addition, dynein/dynacin proteins are not only synthetic lethal with Stu1, but the midzone motor protein Cin8 as well (Geiser et al., 1997; Tong et al., 2001), indicating that there is an overlapping relationship with proteins that separate spindle pole bodies.

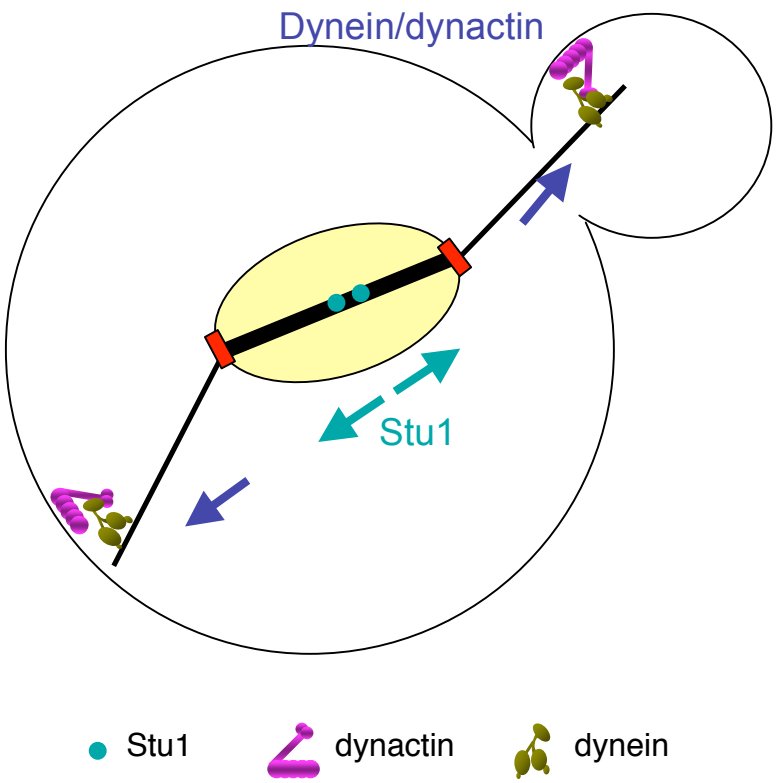

Figure 5.1 Model of Stu1 and Ldb18 contributions to spindle stability. Diagram illustrating the forces contributed by Stu1 and dynein in order to maintain spindle pole body separation in budding yeast during anaphase. Stu1 in the spindle maintains an outward spindle pole body separating force by stabilizing kinetochore microtubules. In anaphase, Stu1 at the midzone could push SPBs outward by microtubule stabilization or subunit incorporation. Dynein, possibly anchored in both the mother and daughter cell late in anaphase by dynactin, uses minus-end directed motor activity to generate pulling forces on the spindle poles, primarily to pull the elongating spindle through the bud neck. When both of these separating forces are absent or compromised, a synthetic lethal phenotype results.

Attempts to measure elongating spindle length in *stu1-5 ldb18Δ* double mutants at the semi-restrictive temperature were not completed, but a prediction would be that these spindles would be shorter than the single mutants, thus eventually leading to the synthetic lethal phenotype.

While the precise mechanism of how Stu1 stabilizes microtubules has yet to be elucidated, it is likely that Stu1 stimulates incorporation of tubulin subunits at the plus end similar to mammalian CLASP (Maiato et al., 2005). Future work should focus on determining the individual effect of purified Stu1 on microtubule dynamics through *in vitro* assays. Determining if purified Stu1 binds tubulin subunits can give some insights into a possible mechanism for microtubule stabilization or promotion of polymerization. One can also test if Stu1 can interact with other purified +TIPs such as Bik1 and Bim1. Additionally, it would be valuable to determine what role, if any, Stu1 may have in the spindle assembly checkpoint. Stu1 is well positioned at the kinetochore to signal when microtubule-kinetochore attachment is properly established. Stu1 binds checkpoint proteins Mad1 and Mad3 by yeast two-hybrid, and curiously *stu1-5 ndc80-1* appears to bypass the checkpoint. Integrating the vast amount of research regarding the +TIPs will yield insights into how microtubule dynamics translates into overall function.

BIBLIOGRAPHY

Adames, N.R., and J.A. Cooper. 2000. Microtubule interactions with the cell cortex causing nuclear movements in Saccharomyces cerevisiae. *J.Cell Biol.* 149:863-874.

Akhmanova, A., C.C. Hoogenraad, K. Drabek, T. Stepanova, B. Dortland, T. Verkerk, W. Vermeulen, B.M. Burgering, C.I. De Zeeuw, F. Grosveld, and N. Galjart. 2001. Clasps are CLIP-115 and -170 associating proteins involved in the regional regulation of microtubule dynamics in motile fibroblasts. *Cell.* 104:923-935.

Akhmanova, A., and M.O. Steinmetz. 2008. Tracking the ends: a dynamic protein network controls the fate of microtubule tips. *Nat.Rev.Mol.Cell Biol.* 9:309-322.

Al-Bassam, J., N.A. Larsen, A.A. Hyman, and S.C. Harrison. 2007. Crystal structure of a TOG domain: conserved features of XMAP215/Dis1-family TOG domains and implications for tubulin binding. *Structure.* 15:355-362.

Ambrose, J.C., T. Shoji, A.M. Kotzer, J.A. Pighin, and G.O. Wasteneys. 2007. The Arabidopsis CLASP gene encodes a microtubule-associated protein involved in cell expansion and division. *Plant Cell.* 19:2763-2775.

Ambrose, J.C., and G.O. Wasteneys. 2008. CLASP modulates microtubule-cortex interaction during self-organization of acentrosomal microtubules. *Mol.Biol.Cell.* 19:4730-4737.

Aoki, K., and M.M. Taketo. 2007. Adenomatous polyposis coli (APC): a multi-functional tumor suppressor gene. *J.Cell.Sci.* 120:3327-3335.

Aonuma, M., M. Miyamoto, Y.H. Inoue, K. Tamai, H. Sakai, N. Kamasawa, and A. Matsukage. 2005. Microtubule bundle formation and cell death induced by the human CLASP/Orbit N-terminal fragment. *Cell Struct.Funct.* 30:7-13.

Ashraf, S.S., E. Sochacka, R. Cain, R. Guenther, A. Malkiewicz, and P.F. Agris. 1999. Single atom modification (O-->S) of tRNA confers ribosome binding. *RNA.* 5:188-194.

Baas, P.W., A. Karabay, and L. Qiang. 2005. Microtubules cut and run. *Trends Cell Biol.* 15:518-524.

Barr, A.R., and F. Gergely. 2007. Aurora-A: the maker and breaker of spindle poles. *J.Cell.Sci.* 120:2987-2996.

Barr, F.A., H.H. Sillje, and E.A. Nigg. 2004. Polo-like kinases and the orchestration of cell division. *Nat.Rev.Mol.Cell Biol.* 5:429-440.

Belgareh, N., G. Rabut, S.W. Bai, M. van Overbeek, J. Beaudouin, N. Daigle, O.V. Zatsepina, F. Pasteau, V. Labas, M. Fromont-Racine, J. Ellenberg, and V. Doye. 2001. An evolutionarily conserved NPC subcomplex, which redistributes in part to kinetochores in mammalian cells. *J.Cell Biol.* 154:1147-1160.

Bender, A., and J.R. Pringle. 1991. Use of a screen for synthetic lethal and multicopy suppressee mutants to identify two new genes involved in morphogenesis in Saccharomyces cerevisiae. *Mol.Cell.Biol.* 11:1295-1305.

Berbari, N.F., A.K. O'Connor, C.J. Haycraft, and B.K. Yoder. 2009. The primary cilium as a complex signaling center. *Curr.Biol.* 19:R526-35.

Berlin, V., C.A. Styles, and G.R. Fink. 1990. BIK1, a protein required for microtubule function during mating and mitosis in Saccharomyces cerevisiae, colocalizes with tubulin. *J.Cell Biol.* 111:2573-2586.

Bhat, K.M., and V. Setaluri. 2007. Microtubule-associated proteins as targets in cancer chemotherapy. *Clin.Cancer Res.* 13:2849-2854.

Bieling, P., S. Kandels-Lewis, I.A. Telley, J. van Dijk, C. Janke, and T. Surrey. 2008. CLIP-170 tracks growing microtubule ends by dynamically recognizing composite EB1/tubulin-binding sites. *J.Cell Biol.* 183:1223-1233.

Bieling, P., L. Laan, H. Schek, E.L. Munteanu, L. Sandblad, M. Dogterom, D. Brunner, and T. Surrey. 2007. Reconstitution of a microtubule plus-end tracking system in vitro. *Nature.* 450:1100-1105.

Blake-Hodek, K. 2009. Regulation of microtubule dynamics by Saccharomyces cerevisiae plus-end binding proteins. .

Boone, C., H. Bussey, and B.J. Andrews. 2007. Exploring genetic interactions and networks with yeast. *Nat.Rev.Genet.* 8:437-449.

Bouck, D.C., and K.S. Bloom. 2005. The kinetochore protein Ndc10p is required for spindle stability and cytokinesis in yeast. *Proc.Natl.Acad.Sci.U.S.A.* 102:5408-5413.

Brackley, K.I., and J. Grantham. 2009. Activities of the chaperonin containing TCP-1 (CCT): implications for cell cycle progression and cytoskeletal organisation. *Cell Stress Chaperones.* 14:23-31.

Bratman, S.V., and F. Chang. 2007. Stabilization of overlapping microtubules by fission yeast CLASP. *Dev.Cell.* 13:812-827.

Brew, C.T., and T.C. Huffaker. 2002. The yeast ubiquitin protease, Ubp3p, promotes protein stability. *Genetics.* 162:1079-1089.

Brinkley, B.R., and E. Stubblefield. 1966. The fine structure of the kinetochore of a mammalian cell in vitro. *Chromosoma.* 19:28-43.

Brouhard, G.J., J.H. Stear, T.L. Noetzel, J. Al-Bassam, K. Kinoshita, S.C. Harrison, J. Howard, and A.A. Hyman. 2008. XMAP215 is a processive microtubule polymerase. *Cell.* 132:79-88.

Brust-Mascher, I., and J.M. Scholey. 2002. Microtubule flux and sliding in mitotic spindles of Drosophila embryos. *Mol.Biol.Cell.* 13:3967-3975.

Busch, K.E., J. Hayles, P. Nurse, and D. Brunner. 2004. Tea2p kinesin is involved in spatial microtubule organization by transporting tip1p on microtubules. *Dev.Cell.* 6:831-843.

Buster, D.W., D. Zhang, and D.J. Sharp. 2007. Poleward tubulin flux in spindles: regulation and function in mitotic cells. *Mol.Biol.Cell.* 18:3094-3104.

Carazo-Salas, R.E., O.J. Gruss, I.W. Mattaj, and E. Karsenti. 2001. Ran-GTP coordinates regulation of microtubule nucleation and dynamics during mitotic-spindle assembly. *Nat.Cell Biol.* 3:228-234.

Carvalho, P., M.L. Gupta Jr, M.A. Hoyt, and D. Pellman. 2004. Cell cycle control of kinesin-mediated transport of Bik1 (CLIP-170) regulates microtubule stability and dynein activation. *Dev.Cell.* 6:815-829.

Carvalho, P., J.S. Tirnauer, and D. Pellman. 2003. Surfing on microtubule ends. *Trends Cell Biol.* 13:229-237.

Cassimeris, L. 1993. Regulation of microtubule dynamic instability. *Cell Motil.Cytoskeleton.* 26:275-281.

Chan, L.Y., and A. Amon. 2009. The protein phosphatase 2A functions in the spindle position checkpoint by regulating the checkpoint kinase Kin4. *Genes Dev.* 23:1639-1649.

Cheeseman, I.M., S. Anderson, M. Jwa, E.M. Green, J. Kang, J.R. Yates 3rd, C.S. Chan, D.G. Drubin, and G. Barnes. 2002. Phospho-regulation of kinetochore-microtubule attachments by the Aurora kinase Ipl1p. *Cell.* 111:163-172.

Cheeseman, I.M., C. Brew, M. Wolyniak, A. Desai, S. Anderson, N. Muster, J.R. Yates, T.C. Huffaker, D.G. Drubin, and G. Barnes. 2001. Implication of a novel multiprotein Dam1p complex in outer kinetochore function. *J.Cell Biol.* 155:1137-1145.

Cheeseman, I.M., J.S. Chappie, E.M. Wilson-Kubalek, and A. Desai. 2006. The conserved KMN network constitutes the core microtubule-binding site of the kinetochore. *Cell.* 127:983-997.

Cheeseman, I.M., and A. Desai. 2008. Molecular architecture of the kinetochore-microtubule interface. *Nat.Rev.Mol.Cell Biol.* 9:33-46.

Cheeseman, I.M., I. MacLeod, J.R. Yates 3rd, K. Oegema, and A. Desai. 2005. The CENP-F-like proteins HCP-1 and HCP-2 target CLASP to kinetochores to mediate chromosome segregation. *Curr.Biol.* 15:771-777.

Chiba, T., and K. Tanaka. 2004. Cullin-based ubiquitin ligase and its control by NEDD8-conjugating system. *Curr.Protein Pept.Sci.* 5:177-184.

Chiron, S., A. Bobkova, H. Zhou, and M.P. Yaffe. 2008. CLASP regulates mitochondrial distribution in Schizosaccharomyces pombe. *J.Cell Biol.* 182:41-49.

Ciferri, C., S. Pasqualato, E. Screpanti, G. Varetti, S. Santaguida, G. Dos Reis, A. Maiolica, J. Polka, J.G. De Luca, P. De Wulf, M. Salek, J. Rappsilber, C.A. Moores, E.D. Salmon, and A. Musacchio. 2008. Implications for kinetochore-microtubule attachment from the structure of an engineered Ndc80 complex. *Cell.* 133:427-439.

Clark, S.W., and M.D. Rose. 2006. Arp10p is a pointed-end-associated component of yeast dynactin. *Mol.Biol.Cell.* 17:738-748.

Corbacho, I., I. Olivero, and L.M. Hernandez. 2005. A genome-wide screen for Saccharomyces cerevisiae nonessential genes involved in mannosyl phosphate transfer to mannoprotein-linked oligosaccharides. *Fungal Genet.Biol.* 42:773-790.

DeLuca, J.G., Y. Dong, P. Hergert, J. Strauss, J.M. Hickey, E.D. Salmon, and B.F. McEwen. 2005. Hec1 and nuf2 are core components of the kinetochore outer plate essential for organizing microtubule attachment sites. *Mol.Biol.Cell.* 16:519-531.

Desai, A., and T.J. Mitchison. 1997. Microtubule polymerization dynamics. *Annu.Rev.Cell Dev.Biol.* 13:83-117.

Dimitrov, A., M. Quesnoit, S. Moutel, I. Cantaloube, C. Pous, and F. Perez. 2008. Detection of GTP-tubulin conformation in vivo reveals a role for GTP remnants in microtubule rescues. *Science.* 322:1353-1356.

Doe, C.Q. 2008. Neural stem cells: balancing self-renewal with differentiation. *Development.* 135:1575-1587.

Drabek, K., M. van Ham, T. Stepanova, K. Draegestein, R. van Horssen, C.L. Sayas, A. Akhmanova, T. Ten Hagen, R. Smits, R. Fodde, F. Grosveld, and N. Galjart. 2006. Role of CLASP2 in microtubule stabilization and the regulation of persistent motility. *Curr.Biol.* 16:2259-2264.

Dzhindzhev, N.S., S.L. Rogers, R.D. Vale, and H. Ohkura. 2005. Distinct mechanisms govern the localisation of Drosophila CLIP-190 to unattached kinetochores and microtubule plus-ends. *J.Cell.Sci.* 118:3781-3790.

Eckley, D.M., S.R. Gill, K.A. Melkonian, J.B. Bingham, H.V. Goodson, J.E. Heuser, and T.A. Schroer. 1999. Analysis of dynactin subcomplexes reveals a novel actin-related protein associated with the arp1 minifilament pointed end. *J.Cell Biol.* 147:307-320.

Efimov, A., A. Kharitonov, N. Efimova, J. Loncarek, P.M. Miller, N. Andreyeva, P. Gleeson, N. Galjart, A.R. Maia, I.X. McLeod, J.R. Yates 3rd, H. Maiato, A. Khodjakov, A. Akhmanova, and I. Kaverina. 2007. Asymmetric CLASP-dependent nucleation of noncentrosomal microtubules at the trans-Golgi network. *Dev.Cell.* 12:917-930.

Eichler, J., and M.W. Adams. 2005. Posttranslational protein modification in Archaea. *Microbiol.Mol.Biol.Rev.* 69:393-425.

Emanuele, M.J., M.L. McCleland, D.L. Satinover, and P.T. Stukenberg. 2005. Measuring the stoichiometry and physical interactions between components elucidates the architecture of the vertebrate kinetochore. *Mol.Biol.Cell.* 16:4882-4892.

Enos, A.P., and N.R. Morris. 1990. Mutation of a gene that encodes a kinesin-like protein blocks nuclear division in A. nidulans. *Cell.* 60:1019-1027.

Eshel, D., L.A. Urrestarazu, S. Vissers, J.C. Jauniaux, J.C. van Vliet-Reedijk, R.J. Planta, and I.R. Gibbons. 1993. Cytoplasmic dynein is required for normal nuclear segregation in yeast. *Proc.Natl.Acad.Sci.U.S.A.* 90:11172-11176.

Ferrezuelo, F., M. Aldea, and B. Futcher. 2009. Bck2 is a phase-independent activator of cell cycle-regulated genes in yeast. *Cell.Cycle.* 8:239-252.

Fraschini, R., M. Venturetti, E. Chiroli, and S. Piatti. 2008. The spindle position checkpoint: how to deal with spindle misalignment during asymmetric cell division in budding yeast. *Biochem.Soc.Trans.* 36:416-420.

Furukawa, K., N. Mizushima, T. Noda, and Y. Ohsumi. 2000. A protein conjugation system in yeast with homology to biosynthetic enzyme reaction of prokaryotes. *J.Biol.Chem.* 275:7462-7465.

Galjart, N. 2005. CLIPs and CLASPs and cellular dynamics. *Nat.Rev.Mol.Cell Biol.* 6:487-498.

Gard, D.L., and M.W. Kirschner. 1987. A microtubule-associated protein from Xenopus eggs that specifically promotes assembly at the plus-end. *J.Cell Biol.* 105:2203-2215.

Geiser, J.R., E.J. Schott, T.J. Kingsbury, N.B. Cole, L.J. Totis, G. Bhattacharyya, L. He, and M.A. Hoyt. 1997. Saccharomyces cerevisiae genes required in the absence of the CIN8-encoded spindle motor act in functionally diverse mitotic pathways. *Mol.Biol.Cell.* 8:1035-1050.

Gerson-Gurwitz, A., N. Movshovich, R. Avunie, V. Fridman, K. Moyal, B. Katz, M.A. Hoyt, and L. Gheber. 2009. Mid-anaphase arrest in S. cerevisiae cells eliminated for the function of Cin8 and dynein. *Cell Mol.Life Sci.* 66:301-313.

Gill, S.R., T.A. Schroer, I. Szilak, E.R. Steuer, M.P. Sheetz, and D.W. Cleveland. 1991. Dynactin, a conserved, ubiquitously expressed component of an activator of vesicle motility mediated by cytoplasmic dynein. *J.Cell Biol.* 115:1639-1650.

Goehring, A.S., D.M. Rivers, and G.F. Sprague Jr. 2003a. Attachment of the ubiquitin-related protein Urm1p to the antioxidant protein Ahp1p. *Eukaryot.Cell.* 2:930-936.

Goehring, A.S., D.M. Rivers, and G.F. Sprague Jr. 2003b. Urmylation: a ubiquitin-like pathway that functions during invasive growth and budding in yeast. *Mol.Biol.Cell.* 14:4329-4341.

Goshima, G., and R.D. Vale. 2003. The roles of microtubule-based motor proteins in mitosis: comprehensive RNAi analysis in the Drosophila S2 cell line. *J.Cell Biol.* 162:1003-1016.

Grallert, A., C. Beuter, R.A. Craven, S. Bagley, D. Wilks, U. Fleig, and I.M. Hagan. 2006. S. pombe CLASP needs dynein, not EB1 or CLIP170, to induce microtubule instability and slows polymerization rates at cell tips in a dynein-dependent manner. *Genes Dev.* 20:2421-2436.

Grava, S., F. Schaerer, M. Faty, P. Philippsen, and Y. Barral. 2006. Asymmetric recruitment of dynein to spindle poles and microtubules promotes proper spindle orientation in yeast. *Dev.Cell.* 10:425-439.

Guarente, L. 1993. Synthetic enhancement in gene interaction: a genetic tool come of age. *Trends Genet.* 9:362-366.

Gupta, M.L.,Jr, P. Carvalho, D.M. Roof, and D. Pellman. 2006. Plus end-specific depolymerase activity of Kip3, a kinesin-8 protein, explains its role in positioning the yeast mitotic spindle. *Nat.Cell Biol.* 8:913-923.

Hammond, J.W., D. Cai, and K.J. Verhey. 2008. Tubulin modifications and their cellular functions. *Curr.Opin.Cell Biol.* 20:71-76.

Hannak, E., and R. Heald. 2006. Xorbit/CLASP links dynamic microtubules to chromosomes in the Xenopus meiotic spindle. *J.Cell Biol.* 172:19-25.

Hartman, J.L.,4th, B. Garvik, and L. Hartwell. 2001. Principles for the buffering of genetic variation. *Science.* 291:1001-1004.

He, X., D.R. Rines, C.W. Espelin, and P.K. Sorger. 2001. Molecular analysis of kinetochore-microtubule attachment in budding yeast. *Cell.* 106:195-206.

Heck, M.M., A. Pereira, P. Pesavento, Y. Yannoni, A.C. Spradling, and L.S. Goldstein. 1993. The kinesin-like protein KLP61F is essential for mitosis in Drosophila. *J.Cell Biol.* 123:665-679.

Heil-Chapdelaine, R.A., J.R. Oberle, and J.A. Cooper. 2000. The cortical protein Num1p is essential for dynein-dependent interactions of microtubules with the cortex. *J.Cell Biol.* 151:1337-1344.

Hietakangas, V., J. Anckar, H.A. Blomster, M. Fujimoto, J.J. Palvimo, A. Nakai, and L. Sistonen. 2006. PDSM, a motif for phosphorylation-dependent SUMO modification. *Proc.Natl.Acad.Sci.U.S.A.* 103:45-50.

Higuchi, T., and F. Uhlmann. 2005. Stabilization of microtubule dynamics at anaphase onset promotes chromosome segregation. *Nature.* 433:171-176.

Hochstrasser, M. 2000. Biochemistry. All in the ubiquitin family. *Science.* 289:563-564.

Hoffman, M.D., M.J. Sniatynski, and J. Kast. 2008. Current approaches for global post-translational modification discovery and mass spectrometric analysis. *Anal.Chim.Acta.* 627:50-61.

Holtzman, D.A., S. Yang, and D.G. Drubin. 1993. Synthetic-lethal interactions identify two novel genes, SLA1 and SLA2, that control membrane cytoskeleton assembly in Saccharomyces cerevisiae. *J.Cell Biol.* 122:635-644.

Ho, Y., A. Gruhler, A. Heilbut, G.D. Bader, L. Moore, S.L. Adams, A. Millar, P. Taylor, K. Bennett, K. Boutilier, L. Yang, C. Wolting, I. Donaldson, S. Schandorff, J. Shewnarane, M. Vo, J. Taggart, M. Goudreault, B. Muskat, C. Alfarano, D. Dewar, Z. Lin, K. Michalickova, A.R. Willems, H. Sassi, P.A. Nielsen, K.J. Rasmussen, J.R. Andersen, L.E. Johansen, L.H. Hansen, H. Jespersen, A. Podtelejnikov, E. Nielsen, J. Crawford, V. Poulsen, B.D. Sorensen, J. Matthiesen, R.C. Hendrickson, F. Gleeson, T. Pawson, M.F. Moran, D. Durocher, M. Mann, C.W. Hogue, D. Figeys, and M. Tyers. 2002. Systematic identification of protein complexes in Saccharomyces cerevisiae by mass spectrometry. *Nature.* 415:180-183.

Hoogenraad, C.C., A. Akhmanova, N. Galjart, and C.I. De Zeeuw. 2004. LIMK1 and CLIP-115: linking cytoskeletal defects to Williams syndrome. *Bioessays.* 26:141-150.

Hook, P., and R.B. Vallee. 2006. The dynein family at a glance. *J.Cell.Sci.* 119:4369-4371.

Howard, J., and A.A. Hyman. 2007. Microtubule polymerases and depolymerases. *Curr.Opin.Cell Biol.* 19:31-35.

Hoyt, M.A., L. He, K.K. Loo, and W.S. Saunders. 1992. Two Saccharomyces cerevisiae kinesin-related gene products required for mitotic spindle assembly. *J.Cell Biol.* 118:109-120.

Hoyt, M.A., J.P. Macke, B.T. Roberts, and J.R. Geiser. 1997. Saccharomyces cerevisiae PAC2 functions with CIN1, 2 and 4 in a pathway leading to normal microtubule stability. *Genetics.* 146:849-857.

Hoyt, M.A., T. Stearns, and D. Botstein. 1990. Chromosome instability mutants of Saccharomyces cerevisiae that are defective in microtubule-mediated processes. *Mol.Cell.Biol.* 10:223-234.

Huang, B., J. Lu, and A.S. Bystrom. 2008. A genome-wide screen identifies genes required for formation of the wobble nucleoside 5-methoxycarbonylmethyl-2-thiouridine in Saccharomyces cerevisiae. *RNA.* 14:2183-2194.

Huffaker, T.C., M.A. Hoyt, and D. Botstein. 1987. Genetic analysis of the yeast cytoskeleton. *Annu.Rev.Genet.* 21:259-284.

Hwang, E. 2005. Nuclear migration and microtubule plus-end tracking proteins in yeast.

Hwang, E., J. Kusch, Y. Barral, and T.C. Huffaker. 2003. Spindle orientation in Saccharomyces cerevisiae depends on the transport of microtubule ends along polarized actin cables. *J.Cell Biol.* 161:483-488.

Igarashi, R., M. Suzuki, S. Nogami, and Y. Ohya. 2005. Molecular dissection of ARP1 regions required for nuclear migration and cell wall integrity checkpoint functions in Saccharomyces cerevisiae. *Cell Struct.Funct.* 30:57-67.

Inoue, Y.H., M. do Carmo Avides, M. Shiraki, P. Deak, M. Yamaguchi, Y. Nishimoto, A. Matsukage, and D.M. Glover. 2000. Orbit, a novel microtubule-associated protein essential for mitosis in Drosophila melanogaster. *J.Cell Biol.* 149:153-166.

Inoue, Y.H., M.S. Savoian, T. Suzuki, E. Mathe, M.T. Yamamoto, and D.M. Glover. 2004. Mutations in orbit/mast reveal that the central spindle is comprised of two microtubule populations, those that initiate cleavage and those that propagate furrow ingression. *J.Cell Biol.* 166:49-60.

Iouk, T., O. Kerscher, R.J. Scott, M.A. Basrai, and R.W. Wozniak. 2002. The yeast nuclear pore complex functionally interacts with components of the spindle assembly checkpoint. *J.Cell Biol.* 159:807-819.

Ito, T., T. Chiba, R. Ozawa, M. Yoshida, M. Hattori, and Y. Sakaki. 2001. A comprehensive two-hybrid analysis to explore the yeast protein interactome. *Proc.Natl.Acad.Sci.U.S.A.* 98:4569-4574.

Jaworski, J., C.C. Hoogenraad, and A. Akhmanova. 2008. Microtubule plus-end tracking proteins in differentiated mammalian cells. *Int.J.Biochem.Cell Biol.* 40:619-637.

Jimbo, T., Y. Kawasaki, R. Koyama, R. Sato, S. Takada, K. Haraguchi, and T. Akiyama. 2002. Identification of a link between the tumour suppressor APC and the kinesin superfamily. *Nat.Cell Biol.* 4:323-327.

Kahana, J.A., G. Schlenstedt, D.M. Evanchuk, J.R. Geiser, M.A. Hoyt, and P.A. Silver. 1998. The yeast dynactin complex is involved in partitioning the mitotic spindle between mother and daughter cells during anaphase B. *Mol.Biol.Cell.* 9:1741-1756.

Kalab, P., A. Pralle, E.Y. Isacoff, R. Heald, and K. Weis. 2006. Analysis of a RanGTP-regulated gradient in mitotic somatic cells. *Nature.* 440:697-701.

Kalab, P., K. Weis, and R. Heald. 2002. Visualization of a Ran-GTP gradient in interphase and mitotic Xenopus egg extracts. *Science.* 295:2452-2456.

Kapoor, T.M., M.A. Lampson, P. Hergert, L. Cameron, D. Cimini, E.D. Salmon, B.F. McEwen, and A. Khodjakov. 2006. Chromosomes can congress to the metaphase plate before biorientation. *Science.* 311:388-391.

Karki, S., B. LaMonte, and E.L. Holzbaur. 1998. Characterization of the p22 subunit of dynactin reveals the localization of cytoplasmic dynein and dynactin to the midbody of dividing cells. *J.Cell Biol.* 142:1023-1034.

Karsenti, E., J. Newport, and M. Kirschner. 1984. Respective roles of centrosomes and chromatin in the conversion of microtubule arrays from interphase to metaphase. *J.Cell Biol.* 99:47s-54s.

Kelley, R., and T. Ideker. 2005. Systematic interpretation of genetic interactions using protein networks. *Nat.Biotechnol.* 23:561-566.

Kerscher, O., P. Hieter, M. Winey, and M.A. Basrai. 2001. Novel role for a Saccharomyces cerevisiae nucleoporin, Nup170p, in chromosome segregation. *Genetics.* 157:1543-1553.

Khmelinskii, A., C. Lawrence, J. Roostalu, and E. Schiebel. 2007. Cdc14-regulated midzone assembly controls anaphase B. *J.Cell Biol.* 177:981-993.

Khodjakov, A., R.W. Cole, B.R. Oakley, and C.L. Rieder. 2000. Centrosome-independent mitotic spindle formation in vertebrates. *Curr.Biol.* 10:59-67.

Khodjakov, A., S. La Terra, and F. Chang. 2004. Laser microsurgery in fission yeast; role of the mitotic spindle midzone in anaphase B. *Curr.Biol.* 14:1330-1340.

Kirik, V., U. Herrmann, C. Parupalli, J.C. Sedbrook, D.W. Ehrhardt, and M. Hulskamp. 2007. CLASP localizes in two discrete patterns on cortical microtubules and is required for cell morphogenesis and cell division in Arabidopsis. *J.Cell.Sci.* 120:4416-4425.

Kirschner, M.W., and T. Mitchison. 1986. Microtubule dynamics. *Nature.* 324:621.

Komarova, Y., C.O. De Groot, I. Grigoriev, S.M. Gouveia, E.L. Munteanu, J.M. Schober, S. Honnappa, R.M. Buey, C.C. Hoogenraad, M. Dogterom, G.G. Borisy, M.O. Steinmetz, and A. Akhmanova. 2009. Mammalian end binding proteins control persistent microtubule growth. *J.Cell Biol.* 184:691-706.

Kotwaliwale, C.V., S.B. Frei, B.M. Stern, and S. Biggins. 2007. A pathway containing the Ipl1/aurora protein kinase and the spindle midzone protein Ase1 regulates yeast spindle assembly. *Dev.Cell.* 13:433-445.

Lansbergen, G., I. Grigoriev, Y. Mimori-Kiyosue, T. Ohtsuka, S. Higa, I. Kitajima, J. Demmers, N. Galjart, A.B. Houtsmuller, F. Grosveld, and A. Akhmanova. 2006. CLASPs attach microtubule plus ends to the cell cortex through a complex with LL5beta. *Dev.Cell.* 11:21-32.

Lansbergen, G., Y. Komarova, M. Modesti, C. Wyman, C.C. Hoogenraad, H.V. Goodson, R.P. Lemaitre, D.N. Drechsel, E. van Munster, T.W. Gadella Jr, F. Grosveld, N. Galjart, G.G. Borisy, and A. Akhmanova. 2004. Conformational changes in CLIP-170 regulate its binding to microtubules and dynactin localization. *J.Cell Biol.* 166:1003-1014.

Laycock, J.E., M.S. Savoian, and D.M. Glover. 2006. Antagonistic activities of Klp10A and Orbit regulate spindle length, bipolarity and function in vivo. *J.Cell.Sci.* 119:2354-2361.

Lee, H., U. Engel, J. Rusch, S. Scherrer, K. Sheard, and D. Van Vactor. 2004. The microtubule plus end tracking protein Orbit/MAST/CLASP acts downstream of the tyrosine kinase Abl in mediating axon guidance. *Neuron.* 42:913-926.

Lee, I.H., S. Kumar, and M. Plamann. 2001. Null mutants of the neurospora actin-related protein 1 pointed-end complex show distinct phenotypes. *Mol.Biol.Cell.* 12:2195-2206.

Lee, W.L., M.A. Kaiser, and J.A. Cooper. 2005. The offloading model for dynein function: differential function of motor subunits. *J.Cell Biol.* 168:201-207.

Lee, W.L., J.R. Oberle, and J.A. Cooper. 2003. The role of the lissencephaly protein Pac1 during nuclear migration in budding yeast. *J.Cell Biol.* 160:355-364.

Leidel, S., P.G. Pedrioli, T. Bucher, R. Brost, M. Costanzo, A. Schmidt, R. Aebersold, C. Boone, K. Hofmann, and M. Peter. 2009. Ubiquitin-related modifier Urm1 acts as a sulphur carrier in thiolation of eukaryotic transfer RNA. *Nature.* 458:228-232.

Lemos, C.L., P. Sampaio, H. Maiato, M. Costa, L.V. Omel'yanchuk, V. Liberal, and C.E. Sunkel. 2000. Mast, a conserved microtubule-associated protein required for bipolar mitotic spindle organization. *EMBO J.* 19:3668-3682.

Levy, J.R., and E.L. Holzbaur. 2006. Cytoplasmic dynein/dynactin function and dysfunction in motor neurons. *Int.J.Dev.Neurosci.* 24:103-111.

Li, J., W.L. Lee, and J.A. Cooper. 2005. NudEL targets dynein to microtubule ends through LIS1. *Nat.Cell Biol.* 7:686-690.

Lien, W.H., V.I. Gelfand, and V. Vasioukhin. 2008. Alpha-E-catenin binds to dynamitin and regulates dynactin-mediated intracellular traffic. *J.Cell Biol.* 183:989-997.

Lin, H., P. de Carvalho, D. Kho, C.Y. Tai, P. Pierre, G.R. Fink, and D. Pellman. 2001. Polyploids require Bik1 for kinetochore-microtubule attachment. *J.Cell Biol.* 155:1173-1184.

Liu, J., Z. Wang, K. Jiang, L. Zhang, L. Zhao, S. Hua, F. Yan, Y. Yang, D. Wang, C. Fu, X. Ding, Z. Guo, and X. Yao. 2009. PRC1 Cooperates with CLASP1 to Organize Central Spindle Plasticity in Mitosis. *J.Biol.Chem.* 284:23059-23071.

Lopez-Fanarraga, M., J. Avila, A. Guasch, M. Coll, and J.C. Zabala. 2001. Review: postchaperonin tubulin folding cofactors and their role in microtubule dynamics. *J.Struct.Biol.* 135:219-229.

Lupas, A., M. Van Dyke, and J. Stock. 1991. Predicting coiled coils from protein sequences. *Science.* 252:1162-1164.

Ma, L., J. McQueen, L. Cuschieri, J. Vogel, and V. Measday. 2007. Spc24 and Stu2 promote spindle integrity when DNA replication is stalled. *Mol.Biol.Cell.* 18:2805-2816.

Maddox, P.S., K.S. Bloom, and E.D. Salmon. 2000. The polarity and dynamics of microtubule assembly in the budding yeast Saccharomyces cerevisiae. *Nat.Cell Biol.* 2:36-41.

Maiato, H., E.A. Fairley, C.L. Rieder, J.R. Swedlow, C.E. Sunkel, and W.C. Earnshaw. 2003. Human CLASP1 is an outer kinetochore component that regulates spindle microtubule dynamics. *Cell.* 113:891-904.

Maiato, H., A. Khodjakov, and C.L. Rieder. 2005. Drosophila CLASP is required for the incorporation of microtubule subunits into fluxing kinetochore fibres. *Nat.Cell Biol.* 7:42-47.

Maiato, H., C.L. Rieder, and A. Khodjakov. 2004. Kinetochore-driven formation of kinetochore fibers contributes to spindle assembly during animal mitosis. *J.Cell Biol.* 167:831-840.

Maiato, H., P. Sampaio, C.L. Lemos, J. Findlay, M. Carmena, W.C. Earnshaw, and C.E. Sunkel. 2002. MAST/Orbit has a role in microtubule-kinetochore attachment and is essential for chromosome alignment and maintenance of spindle bipolarity. *J.Cell Biol.* 157:749-760.

Markus, S.M., J.J. Punch, and W.L. Lee. 2009. Motor- and tail-dependent targeting of dynein to microtubule plus ends and the cell cortex. *Curr.Biol.* 19:196-205.

Mathe, E., Y.H. Inoue, W. Palframan, G. Brown, and D.M. Glover. 2003. Orbit/Mast, the CLASP orthologue of Drosophila, is required for asymmetric stem cell and cystocyte divisions and development of the polarised microtubule network that interconnects oocyte and nurse cells during oogenesis. *Development.* 130:901-915.

Mayer, M.L., S.P. Gygi, R. Aebersold, and P. Hieter. 2001. Identification of RFC(Ctf18p, Ctf8p, Dcc1p): an alternative RFC complex required for sister chromatid cohesion in S. cerevisiae. *Mol.Cell.* 7:959-970.

Mayer, M.L., I. Pot, M. Chang, H. Xu, V. Aneliunas, T. Kwok, R. Newitt, R. Aebersold, C. Boone, G.W. Brown, and P. Hieter. 2004. Identification of protein complexes required for efficient sister chromatid cohesion. *Mol.Biol.Cell.* 15:1736-1745.

Mayer, T.U., T.M. Kapoor, S.J. Haggarty, R.W. King, S.L. Schreiber, and T.J. Mitchison. 1999. Small molecule inhibitor of mitotic spindle bipolarity identified in a phenotype-based screen. *Science.* 286:971-974.

McMillan, J.N., and K. Tatchell. 1994. The JNM1 gene in the yeast Saccharomyces cerevisiae is required for nuclear migration and spindle orientation during the mitotic cell cycle. *J.Cell Biol.* 125:143-158.

Measday, V., K. Baetz, J. Guzzo, K. Yuen, T. Kwok, B. Sheikh, H. Ding, R. Ueta, T. Hoac, B. Cheng, I. Pot, A. Tong, Y. Yamaguchi-Iwai, C. Boone, P. Hieter, and B. Andrews. 2005. Systematic yeast synthetic lethal and synthetic dosage lethal screens identify genes required for chromosome segregation. *Proc.Natl.Acad.Sci.U.S.A.* 102:13956-13961.

Miller, P.M., A.W. Folkmann, A.R. Maia, N. Efimova, A. Efimov, and I. Kaverina. 2009. Golgi-derived CLASP-dependent microtubules control Golgi organization and polarized trafficking in motile cells. *Nat.Cell Biol.*

Miller, R.K., and M.D. Rose. 1998. Kar9p is a novel cortical protein required for cytoplasmic microtubule orientation in yeast. *J.Cell Biol.* 140:377-390.

Mimori-Kiyosue, Y., I. Grigoriev, G. Lansbergen, H. Sasaki, C. Matsui, F. Severin, N. Galjart, F. Grosveld, I. Vorobjev, S. Tsukita, and A. Akhmanova. 2005. CLASP1 and CLASP2 bind to EB1 and regulate microtubule plus-end dynamics at the cell cortex. *J.Cell Biol.* 168:141-153.

Mimori-Kiyosue, Y., I. Grigoriev, H. Sasaki, C. Matsui, A. Akhmanova, S. Tsukita, and I. Vorobjev. 2006. Mammalian CLASPs are required for mitotic spindle organization and kinetochore alignment. *Genes Cells.* 11:845-857.

Miranda, J.J., P. De Wulf, P.K. Sorger, and S.C. Harrison. 2005. The yeast DASH complex forms closed rings on microtubules. *Nat.Struct.Mol.Biol.* 12:138-143.

Mitchison, T.J., and E.D. Salmon. 2001. Mitosis: a history of division. *Nat.Cell Biol.* 3:E17-21.

Mizushima, N., T. Noda, T. Yoshimori, Y. Tanaka, T. Ishii, M.D. George, D.J. Klionsky, M. Ohsumi, and Y. Ohsumi. 1998. A protein conjugation system essential for autophagy. *Nature.* 395:395-398.

Montpetit, B., K. Thorne, I. Barrett, K. Andrews, R. Jadusingh, P. Hieter, and V. Measday. 2005. Genome-wide synthetic lethal screens identify an interaction between the nuclear envelope protein, Apq12p, and the kinetochore in Saccharomyces cerevisiae. *Genetics.* 171:489-501.

Moore, J.K., S. D'Silva, and R.K. Miller. 2006. The CLIP-170 homologue Bik1p promotes the phosphorylation and asymmetric localization of Kar9p. *Mol.Biol.Cell.* 17:178-191.

Moore, J.K., J. Li, and J.A. Cooper. 2008. Dynactin function in mitotic spindle positioning. *Traffic.* 9:510-527.

Moore, J.K., and R.K. Miller. 2007. The cyclin-dependent kinase Cdc28p regulates multiple aspects of Kar9p function in yeast. *Mol.Biol.Cell.* 18:1187-1202.

Muhua, L., T.S. Karpova, and J.A. Cooper. 1994. A yeast actin-related protein homologous to that in vertebrate dynactin complex is important for spindle orientation and nuclear migration. *Cell.* 78:669-679.

Musacchio, A., and E.D. Salmon. 2007. The spindle-assembly checkpoint in space and time. *Nat.Rev.Mol.Cell Biol.* 8:379-393.

Nakai, Y., M. Nakai, and H. Hayashi. 2008. Thio-modification of yeast cytosolic tRNA requires a ubiquitin-related system that resembles bacterial sulfur transfer systems. *J.Biol.Chem.* 283:27469-27476.

Nathke, I. 2004. APC at a glance. *J.Cell.Sci.* 117:4873-4875.

Norden, C., M. Mendoza, J. Dobbelaere, C.V. Kotwaliwale, S. Biggins, and Y. Barral. 2006. The NoCut pathway links completion of cytokinesis to spindle midzone function to prevent chromosome breakage. *Cell.* 125:85-98.

Novick, P., B.C. Osmond, and D. Botstein. 1989. Suppressors of yeast actin mutations. *Genetics.* 121:659-674.

Pan, X., P. Ye, D.S. Yuan, X. Wang, J.S. Bader, and J.D. Boeke. 2006. A DNA integrity network in the yeast Saccharomyces cerevisiae. *Cell.* 124:1069-1081.

Pardo, M., and P. Nurse. 2005. The nuclear rim protein Amo1 is required for proper microtubule cytoskeleton organisation in fission yeast. *J.Cell.Sci.* 118:1705-1714.

Parisi, G., M.S. Fornasari, and J. Echave. 2004. Dynactins p25 and p27 are predicted to adopt the LbetaH fold. *FEBS Lett.* 562:1-4.

Pasqualone, D., and T.C. Huffaker. 1994. STU1, a suppressor of a beta-tubulin mutation, encodes a novel and essential component of the yeast mitotic spindle. *J.Cell Biol.* 127:1973-1984.

Pinsky, B.A., C. Kung, K.M. Shokat, and S. Biggins. 2006. The Ipl1-Aurora protein kinase activates the spindle checkpoint by creating unattached kinetochores. *Nat.Cell Biol.* 8:78-83.

Pereira, A.L., A.J. Pereira, A.R. Maia, K. Drabek, C.L. Sayas, P.J. Hergert, M. Lince-Faria, I. Matos, C. Duque, T. Stepanova, C.L. Rieder, W.C. Earnshaw, N. Galjart, and H. Maiato. 2006. Mammalian CLASP1 and CLASP2 cooperate to ensure mitotic fidelity by regulating spindle and kinetochore function. *Mol.Biol.Cell.* 17:4526-4542.

Perez, F., G.S. Diamantopoulos, R. Stalder, and T.E. Kreis. 1999. CLIP-170 highlights growing microtubule ends in vivo. *Cell.* 96:517-527.

Pfister, K.K., S.E. Benashski, J.F. Dillman 3rd, R.S. Patel-King, and S.M. King. 1998. Identification and molecular characterization of the p24 dynactin light chain. *Cell Motil.Cytoskeleton.* 41:154-167.

Reis, R., T. Feijao, S. Gouveia, A.J. Pereira, I. Matos, P. Sampaio, H. Maiato, and C.E. Sunkel. 2009. Dynein and Mast/Orbit/CLASP have antagonistic roles in regulating kinetochore-microtubule plus-end dynamics. *J.Cell.Sci.* 122:2543-2553.

Rieder, C.L., and S.P. Alexander. 1990. Kinetochores are transported poleward along a single astral microtubule during chromosome attachment to the spindle in newt lung cells. *J.Cell Biol.* 110:81-95.

Rieder, C.L., and A. Khodjakov. 2003. Mitosis through the microscope: advances in seeing inside live dividing cells. *Science.* 300:91-96.

Robert, M., and P.S. Mathuranath. 2007. Tau and tauopathies. *Neurol.India.* 55:11-16.

Rodriguez, M.S., C. Dargemont, and R.T. Hay. 2001. SUMO-1 conjugation in vivo requires both a consensus modification motif and nuclear targeting. *J.Biol.Chem.* 276:12654-12659.

Rogers, G.C., S.L. Rogers, and D.J. Sharp. 2005. Spindle microtubules in flux. *J.Cell.Sci.* 118:1105-1116.

Roof, D.M., P.B. Meluh, and M.D. Rose. 1992. Kinesin-related proteins required for assembly of the mitotic spindle. *J.Cell Biol.* 118:95-108.

Rosenblatt, J. 2005. Spindle assembly: asters part their separate ways. *Nat.Cell Biol.* 7:219-222.

Ross, J.L., M.Y. Ali, and D.M. Warshaw. 2008. Cargo transport: molecular motors navigate a complex cytoskeleton. *Curr.Opin.Cell Biol.* 20:41-47.

Rost, B., and C. Sander. 1993. Prediction of protein secondary structure at better than 70% accuracy. *J.Mol.Biol.* 232:584-599.

Ruchaud, S., M. Carmena, and W.C. Earnshaw. 2007. Chromosomal passengers: conducting cell division. *Nat.Rev.Mol.Cell Biol.* 8:798-812.

Sandblad, L., K.E. Busch, P. Tittmann, H. Gross, D. Brunner, and A. Hoenger. 2006. The Schizosaccharomyces pombe EB1 homolog Mal3p binds and stabilizes the microtubule lattice seam. *Cell.* 127:1415-1424.

Saunders, W.S., D. Koshland, D. Eshel, I.R. Gibbons, and M.A. Hoyt. 1995. Saccharomyces cerevisiae kinesin- and dynein-related proteins required for anaphase chromosome segregation. *J.Cell Biol.* 128:617-624.

Schlieker, C.D., A.G. Van der Veen, J.R. Damon, E. Spooner, and H.L. Ploegh. 2008. A functional proteomics approach links the ubiquitin-related modifier Urm1 to a tRNA modification pathway. *Proc.Natl.Acad.Sci.U.S.A.* 105:18255-18260.

Schoner, D., M. Kalisch, C. Leisner, L. Meier, M. Sohrmann, M. Faty, Y. Barral, M. Peter, W. Gruissem, and P. Buhlmann. 2008. Annotating novel genes by integrating synthetic lethals and genomic information. *BMC Syst.Biol.* 2:3.

Schroer, T.A. 2004. Dynactin. *Annu.Rev.Cell Dev.Biol.* 20:759-779.

Schroer, T.A., and M.P. Sheetz. 1991. Two activators of microtubule-based vesicle transport. *J.Cell Biol.* 115:1309-1318.

Schuyler, S.C., J.Y. Liu, and D. Pellman. 2003. The molecular function of Ase1p: evidence for a MAP-dependent midzone-specific spindle matrix. Microtubule-associated proteins. *J.Cell Biol.* 160:517-528.

Schuyler, S.C., and D. Pellman. 2002. Analysis of the size and shape of protein complexes from yeast. *Methods Enzymol.* 351:150-168.

Sharp, D.J., K.L. McDonald, H.M. Brown, H.J. Matthies, C. Walczak, R.D. Vale, T.J. Mitchison, and J.M. Scholey. 1999. The bipolar kinesin, KLP61F, cross-links microtubules within interpolar microtubule bundles of Drosophila embryonic mitotic spindles. *J.Cell Biol.* 144:125-138.

Sharp, D.J., G.C. Rogers, and J.M. Scholey. 2000. Microtubule motors in mitosis. *Nature.* 407:41-47.

Sheeman, B., P. Carvalho, I. Sagot, J. Geiser, D. Kho, M.A. Hoyt, and D. Pellman. 2003. Determinants of S. cerevisiae dynein localization and activation: implications for the mechanism of spindle positioning. *Curr.Biol.* 13:364-372.

Sherman, F. 1991. Getting started with yeast. *Methods Enzymol.* 194:3-21.

Siller, K.H., and C.Q. Doe. 2009. Spindle orientation during asymmetric cell division. *Nat.Cell Biol.* 11:365-374.

Silverman, M.A., and M.R. Leroux. 2009. Intraflagellar transport and the generation of dynamic, structurally and functionally diverse cilia. *Trends Cell Biol.* 19:306-316.

Sousa, A., R. Reis, P. Sampaio, and C.E. Sunkel. 2007. The Drosophila CLASP homologue, Mast/Orbit regulates the dynamic behaviour of interphase microtubules by promoting the pause state. *Cell Motil.Cytoskeleton.* 64:605-620.

Spencer, F., S.L. Gerring, C. Connelly, and P. Hieter. 1990. Mitotic chromosome transmission fidelity mutants in Saccharomyces cerevisiae. *Genetics.* 124:237-249.

Sproul, L.R., D.J. Anderson, A.T. Mackey, W.S. Saunders, and S.P. Gilbert. 2005. Cik1 targets the minus-end kinesin depolymerase kar3 to microtubule plus ends. *Curr.Biol.* 15:1420-1427.

Suarez-Merino, B., M. Hubank, T. Revesz, W. Harkness, R. Hayward, D. Thompson, J.L. Darling, D.G. Thomas, and T.J. Warr. 2005. Microarray analysis of pediatric ependymoma identifies a cluster of 112 candidate genes including four transcripts at 22q12.1-q13.3. *Neuro Oncol.* 7:20-31.

Suzuki, M., R. Igarashi, M. Sekiya, T. Utsugi, S. Morishita, M. Yukawa, and Y. Ohya. 2004. Dynactin is involved in a checkpoint to monitor cell wall synthesis in Saccharomyces cerevisiae. *Nat.Cell Biol.* 6:861-871.

Tanaka, K., E. Kitamura, Y. Kitamura, and T.U. Tanaka. 2007. Molecular mechanisms of microtubule-dependent kinetochore transport toward spindle poles. *J.Cell Biol.* 178:269-281.

Tanaka, K., N. Mukae, H. Dewar, M. van Breugel, E.K. James, A.R. Prescott, C. Antony, and T.U. Tanaka. 2005a. Molecular mechanisms of kinetochore capture by spindle microtubules. *Nature.* 434:987-994.

Tanaka, T.U., M.J. Stark, and K. Tanaka. 2005b. Kinetochore capture and bi-orientation on the mitotic spindle. *Nat.Rev.Mol.Cell Biol.* 6:929-942.

Tange, Y., A. Hirata, and O. Niwa. 2002. An evolutionarily conserved fission yeast protein, Ned1, implicated in normal nuclear morphology and chromosome stability, interacts with Dis3, Pim1/RCC1 and an essential nucleoporin. *J.Cell.Sci.* 115:4375-4385.

Tian, G., A. Bhamidipati, N.J. Cowan, and S.A. Lewis. 1999. Tubulin folding cofactors as GTPase-activating proteins. GTP hydrolysis and the assembly of the alpha/beta-tubulin heterodimer. *J.Biol.Chem.* 274:24054-24058.

Tian, G., Y. Huang, H. Rommelaere, J. Vandekerckhove, C. Ampe, and N.J. Cowan. 1996. Pathway leading to correctly folded beta-tubulin. *Cell.* 86:287-296.

Tirnauer, J.S., and B.E. Bierer. 2000. EB1 proteins regulate microtubule dynamics, cell polarity, and chromosome stability. *J.Cell Biol.* 149:761-766.

Tong, A.H., and C. Boone. 2006. Synthetic genetic array analysis in Saccharomyces cerevisiae. *Methods Mol.Biol.* 313:171-192.

Tong, A.H., M. Evangelista, A.B. Parsons, H. Xu, G.D. Bader, N. Page, M. Robinson, S. Raghibizadeh, C.W. Hogue, H. Bussey, B. Andrews, M. Tyers, and C. Boone. 2001. Systematic genetic analysis with ordered arrays of yeast deletion mutants. *Science.* 294:2364-2368.

Toso, A., J.R. Winter, A.J. Garrod, A.C. Amaro, P. Meraldi, and A.D. McAinsh. 2009. Kinetochore-generated pushing forces separate centrosomes during bipolar spindle assembly. *J.Cell Biol.* 184:365-372.

Tournebize, R., A. Popov, K. Kinoshita, A.J. Ashford, S. Rybina, A. Pozniakovsky, T.U. Mayer, C.E. Walczak, E. Karsenti, and A.A. Hyman. 2000. Control of microtubule dynamics by the antagonistic activities of XMAP215 and XKCM1 in Xenopus egg extracts. *Nat.Cell Biol.* 2:13-19.

Tsvetkov, A.S., A. Samsonov, A. Akhmanova, N. Galjart, and S.V. Popov. 2007. Microtubule-binding proteins CLASP1 and CLASP2 interact with actin filaments. *Cell Motil.Cytoskeleton.* 64:519-530.

Vaisberg, E.A., M.P. Koonce, and J.R. McIntosh. 1993. Cytoplasmic dynein plays a role in mammalian mitotic spindle formation. *J.Cell Biol.* 123:849-858.

Varga, V., J. Helenius, K. Tanaka, A.A. Hyman, T.U. Tanaka, and J. Howard. 2006. Yeast kinesin-8 depolymerizes microtubules in a length-dependent manner. *Nat.Cell Biol.* 8:957-962.

Walczak, C.E., and R. Heald. 2008. Mechanisms of mitotic spindle assembly and function. *Int.Rev.Cytol.* 265:111-158.

Walker, R.A., E.T. O'Brien, N.K. Pryer, M.F. Soboeiro, W.A. Voter, H.P. Erickson, and E.D. Salmon. 1988. Dynamic instability of individual microtubules analyzed by video light microscopy: rate constants and transition frequencies. *J.Cell Biol.* 107:1437-1448.

Wang, H.W., and E. Nogales. 2005. Nucleotide-dependent bending flexibility of tubulin regulates microtubule assembly. *Nature.* 435:911-915.

Watanabe, T., J. Noritake, and K. Kaibuchi. 2005. Regulation of microtubules in cell migration. *Trends Cell Biol.* 15:76-83.

Watanabe, T., J. Noritake, M. Kakeno, T. Matsui, T. Harada, S. Wang, N. Itoh, K. Sato, K. Matsuzawa, A. Iwamatsu, N. Galjart, and K. Kaibuchi. 2009. Phosphorylation of CLASP2 by GSK-3{beta} regulates its interaction with IQGAP1, EB1 and microtubules. *J.Cell.Sci.* 122:2969-2979.

Westermann, S., A. Avila-Sakar, H.W. Wang, H. Niederstrasser, J. Wong, D.G. Drubin, E. Nogales, and G. Barnes. 2005. Formation of a dynamic kinetochore- microtubule interface through assembly of the Dam1 ring complex. *Mol.Cell.* 17:277-290.

Westermann, S., D.G. Drubin, and G. Barnes. 2007. Structures and functions of yeast kinetochore complexes. *Annu.Rev.Biochem.* 76:563-591.

Winzeler, E.A., D.D. Shoemaker, A. Astromoff, H. Liang, K. Anderson, B. Andre, R. Bangham, R. Benito, J.D. Boeke, H. Bussey, A.M. Chu, C. Connelly, K. Davis, F. Dietrich, S.W. Dow, M. El Bakkoury, F. Foury, S.H. Friend, E. Gentalen, G. Giaever, J.H. Hegemann, T. Jones, M. Laub, H. Liao, N. Liebundguth, D.J. Lockhart, A. Lucau-Danila, M. Lussier, N. M'Rabet, P. Menard, M. Mittmann, C. Pai, C. Rebischung, J.L. Revuelta, L. Riles, C.J. Roberts, P. Ross-MacDonald, B. Scherens, M. Snyder, S. Sookhai-Mahadeo, R.K. Storms, S. Veronneau, M. Voet, G. Volckaert, T.R. Ward, R. Wysocki, G.S. Yen, K. Yu, K. Zimmermann, P. Philippsen, M. Johnston, and R.W. Davis. 1999. Functional characterization of the S. cerevisiae genome by gene deletion and parallel analysis. *Science.* 285:901-906.

Wittmann, T., and C.M. Waterman-Storer. 2005. Spatial regulation of CLASP affinity for microtubules by Rac1 and GSK3beta in migrating epithelial cells. *J.Cell Biol.* 169:929-939.

Witze, E.S., W.M. Old, K.A. Resing, and N.G. Ahn. 2007. Mapping protein post-translational modifications with mass spectrometry. *Nat.Methods.* 4:798-806.

Wolyniak, M.J., K. Blake-Hodek, K. Kosco, E. Hwang, L. You, and T.C. Huffaker. 2006. The regulation of microtubule dynamics in Saccharomyces cerevisiae by three interacting plus-end tracking proteins. *Mol.Biol.Cell.* 17:2789-2798.

Woodruff, J.B., D.G. Drubin, and G. Barnes. 2009. Dynein-driven mitotic spindle positioning restricted to anaphase by She1p inhibition of dynactin recruitment. *Mol.Biol.Cell.* 20:3003-3011.

Xu, H., C. Boone, and G.W. Brown. 2007. Genetic dissection of parallel sister-chromatid cohesion pathways. *Genetics.* 176:1417-1429.

Yamashita, Y.M., and M.T. Fuller. 2008. Asymmetric centrosome behavior and the mechanisms of stem cell division. *J.Cell Biol.* 180:261-266.

Ye, P., B.D. Peyser, X. Pan, J.D. Boeke, F.A. Spencer, and J.S. Bader. 2005. Gene function prediction from congruent synthetic lethal interactions in yeast. *Mol.Syst.Biol.* 1:2005.0026.

Yeh, E., R.V. Skibbens, J.W. Cheng, E.D. Salmon, and K. Bloom. 1995. Spindle dynamics and cell cycle regulation of dynein in the budding yeast, Saccharomyces cerevisiae. *J.Cell Biol.* 130:687-700.

Yin, H. 2001. Characterization of proteins required for spindle formation and orientation in Saccharomyces cerevisiae. .

Yin, H., D. Pruyne, T.C. Huffaker, and A. Bretscher. 2000. Myosin V orientates the mitotic spindle in yeast. *Nature.* 406:1013-1015.

Yin, H., L. You, D. Pasqualone, K.M. Kopski, and T.C. Huffaker. 2002. Stu1p is physically associated with beta-tubulin and is required for structural integrity of the mitotic spindle. *Mol.Biol.Cell.* 13:1881-1892.

Zhai, Y., P.J. Kronebusch, and G.G. Borisy. 1995. Kinetochore microtubule dynamics and the metaphase-anaphase transition. *J.Cell Biol.* 131:721-734.

Zhai, Y., P.J. Kronebusch, P.M. Simon, and G.G. Borisy. 1996. Microtubule dynamics at the G2/M transition: abrupt breakdown of cytoplasmic microtubules at nuclear envelope breakdown and implications for spindle morphogenesis. *J.Cell Biol.* 135:201-214.

Zhang, H., A.R. Skop, and J.G. White. 2008. Src and Wnt signaling regulate dynactin accumulation to the P2-EMS cell border in C. elegans embryos. *J.Cell.Sci.* 121:155-161.